

UNDERSTANDING HOST ANTIVIRAL SIGNALING PATHWAYS

APPROVED BY SUPERVISORY COMMITTEE

Zhijian 'James' Chen, Ph.D. (Supervisor)

Kim Orth, Ph.D. (Chair)

Richard G. W. Anderson, Ph.D.

Keith Wharton, M.D., Ph.D.

DEDICATION

To my parents, for their love, support and inspiration

UNDERSTANDING HOST ANTIVIRAL SIGNALING PATHWAYS

by

RASHU BHARGAVA

DISSERTATION

Presented to the Faculty of the Graduate School of Biomedical Sciences

The University of Texas Southwestern Medical Center at Dallas

In Partial Fulfillment of the Requirements

For the Degree of

DOCTOR OF PHILOSOPHY

The University of Texas Southwestern Medical Center at Dallas

Dallas, Texas

June, 2006

Copyright

by

Rashu Bhargava, 2006

All Rights Reserved

ACKNOWLEDGEMENTS

The best way to describe my time as a graduate student in Dr. James Chen's laboratory is 'an action packed adventure'. My rotation in James' laboratory lasted for just two weeks as opposed to the mandatory month long rotation. It took a very short time for me to appreciate the caliber of research being carried out in his lab. Along with a keen sense of observation, James has a great depth of scientific understanding that enables him to focus on important questions in a field. His enthusiasm and dedication to science are truly inspirational. Although I have learned a lot from James, I would like to specifically list three valuable lessons or 'mantras' he has passed on to me. The first lesson I learned is hard work. Troubleshooting experiments and standardizing experimental conditions are time consuming processes. James always encouraged me to work hard and invest time in performing 'clean' experiments. The second lesson I have learned is 'baby steps'. James has preached this lesson so many times that it is now imprinted in my mind. He always encouraged me to think about a problem logically, plan experiments with the proper controls and build experiments one step at a time. And the last lesson I have learned is 'believe in hitting a home run'. There have been times in the lab when my projects have hit rock bottom. James always encouraged me to stay focused, keep moving forward and believe that the whole experience will lead to a good result. So, I would like to thank my 'guru' for this wonderful opportunity to work with him and learn along the way.

I also value the support and guidance from my committee members Drs. Kim Orth, Richard Anderson and Keith Wharton. Dr. Kim Orth was always willing to share her insights on matters ranging from the future course of my projects to ideas on vacationing (I will definitely try night-time snorkeling!). With Dr. Anderson's experience and knowledge of cell biology on my side, I did not have to stain cells with Mito Tracker dye to determine the localization of MAVS in mitochondria. He took one look at the preliminary MAVS immunostaining data and told me that MAVS is a mitochondrial protein. As the chair of my qualifying examination committee, Dr. Keith Wharton provided me with help that made the whole examination process a good learning experience.

I have been very fortunate in having great lab colleagues who have made my time in the lab so memorable. Dr. Lijun Sun or 'Superman Sun' as I like to call him, is the master of multi-tasking. From providing valuable reagents to helping with key experiments, he has helped at several stages of my thesis project. Other past and present members of the Chen lab including Li, Mei, Giri, Yu-Hsin,

Zong-Ping, Meng, Chee-kwee, Hong-Hsing, Gabriel, Hon-Ren, Qin Miao, Beethoven, Wen Wen, Xiang, Vijay, Xiaomo, Xiao-Dong and Anirban, have created an open and interactive lab environment.

I have to thank several people associated with the UTSW graduate program for their help at various stages of my graduate school career. Dr. Phil Pearlman and Nancy McKinney made the transfer process from Rutgers to UTSW smooth and comfortable. Through the weekly WIPs and journal clubs, I had exciting and thought-provoking interactions with several faculty members and students of the cell regulation graduate program. I also want to acknowledge all the help and advice provided by Carla Childers.

I cannot write enough about the love and support provided to me by my friends and family. My parents, Vijay and Sarita Bhargava always encouraged me and my brother to pursue our interests. They have always put my interest before their own and have guided and supported me through some tough times. Even though I could not visit them in India for almost four years during graduate school, they were understanding and patient. My younger brother, Rishi, has always been a friend and supporter. He has been working hard on building his career in management and I am so proud of him. I could not have come so far without the blessings of all in my family. My uncle Mr. R. L. Bhargava always encouraged me to excel academically and wanted me to be the most educated person in the family. Although he is not amongst us anymore, I am sure he would be proud of me. I also want to thank my friends in Delhi, Nabanita and Meenakshi for all their love and encouragement through the years.

It is impossible to list all the contributions of my husband, Abhinav, to this work. He is a source of limitless love, support and encouragement. He also happens to be my colleague at UT Southwestern, where he is pursuing his MD/PhD degrees. Even though he had a busy schedule as a graduate student in Dr. M. Rosen's laboratory, he always found time to help me. He provided me with the Rac-CAAX box construct that I used to generate the MAVS-CAAX fusion construct. He offered all his skills and knowledge of imaging techniques to help me with generating and analyzing the confocal microscopy data described in the thesis. He proof-reads all my manuscripts and helps me prepare for presentations. He is passionate about scientific research and is always brimming with ideas for research projects. His suggestions for my projects have always been helpful. His energy and enthusiasm are like fuel for me. My parents-in-law, Suresh and Usha Seth are wonderful additions to my life. They have surrounded me with love and affection. Even though they would prefer that I spend more

time with them, they have always encouraged me to focus on my work. I am lucky to have such wonderful people in my life.

UNDERSTANDING HOST ANTIVIRAL SIGNALING PATHWAYS

Publication No. _____

Rashu Bhargava, Ph.D.

The University of Texas Southwestern Medical Center at Dallas, 2006

Supervising Professor: Zhijian 'James' Chen, Ph.D.

The innate immune response is the first line of defense against viral infections. Recent studies have revealed two immune receptor systems that detect virally-derived nucleic acids and trigger signaling pathways which lead to the activation of transcription factors like nuclear factor-kappa B (NF-kappa B), interferon regulatory factor 3 (IRF3) and interferon regulatory factor 7 (IRF7). These transcription factors regulate the synthesis of protective cytokines including type I interferons. The first detection system includes members of the toll-like

receptor family (TLR3, TLR7, TLR8 and TLR9) that reside in the endosome and signal through the associated adaptor proteins. The second pathway uses retinoic acid inducible gene – I (RIG-I) to detect cytosolic viral double-stranded RNA. RIG-I signals to NF-kappa B and IRFs through its N-terminal CARD domains. An important area of research is to identify the downstream host factors that participate in these pathways and to determine the mechanism by which they function.

Here, I describe the development of an *in vitro* biochemical assay to detect the activation of a key kinase involved in the activation of IRF3. This assay will be a valuable tool for identifying not only the specific IRF3 kinase, but also other molecular components involved in the antiviral signaling pathway.

A bioinformatics approach led to the identification of a CARD domain containing protein, termed MAVS (Mitochondrial AntiViral Signaling protein) that functions downstream of RIG-I in the antiviral signaling pathway. Besides the N-terminal CARD domain, MAVS also contains a hydrophobic C-terminal transmembrane domain that targets the protein to the outer membrane of the mitochondria. The mitochondrial localization of MAVS is essential for signaling by MAVS. The importance of mitochondrial localization of MAVS for its function is underscored by the finding that hepatitis C virus (HCV) shuts down the host innate immune system by cleaving MAVS off the mitochondria. HCV

achieves this through the action of NS3/4A, a virally encoded serine protease, which cleaves MAVS before the transmembrane domain at Cys-508.

Prior to the identification of MAVS, the focus of antiviral research was on understanding the regulation of key transcription factors by established cytosolic signaling cascades. Our findings have established an important role for mitochondria in regulating antiviral immunity and represent a new paradigm in understanding the host-pathogen relationship.

TABLE OF CONTENTS

PRIOR PUBLICATIONS	xiv
LIST OF FIGURES	xv
LIST OF ABBREVIATIONS	xviii
CHAPTER I: INTRODUCTION TO THE ANTIVIRAL IMMUNE RESPONSE	22
CHAPTER II: IDENTIFICATION AND CHARACTERIZATION OF AN IRF3 KINASE	
Introduction	48
Materials and Methods	55
Results	60
Discussion	74
CHAPTER III: IDENTIFICATION AND CHARACTERIZATION OF MAVS	
Introduction	80
Materials and Methods	83

Results	90
Discussion	106
CHAPTER IV: UNDERSTANDING THE MECHANISM BY WHICH MAVS FUNCTIONS	
Introduction	112
Materials and Methods	114
Results	116
Discussion	124
CHAPTER V: MITOCHONDRIAL LOCALIZATION OF MAVS	
Introduction	129
Materials and Methods	130
Results	133
Discussion	142
CHAPTER VI: MAVS IS TARGETED FOR CLEAVAGE BY HEPATITIS C VIRUS ENCODED NS3/4A PROTEASE	
Introduction	147
Materials and Methods	148

Results	150
Discussion	160
CHAPTER VII: CONCLUSIONS	162
Bibliography	170

PRIOR PUBLICATIONS

1. Sun Q*, Sun L*, Liu HH, Chen X, Seth RB, Forman J and Chen ZJ. The specific and essential role of MAVS in antiviral innate immune responses. *Immunity* 2006; 24 (5): 633-642.
2. Chen ZJ, Bhoj V, and Seth RB. Ubiquitin, TAK1 and IKK: is there a connection? *Cell Death and Differ.* 2006 Feb17.
3. Seth RB, Sun LJ, and Chen ZJ. Antiviral innate immunity pathways. *Cell Res* 2006 Feb; 16(2):141-147.
4. Li XD*, Sun L*, Seth RB*, Pineda G, and Chen ZJ. Hepatitis C virus protease cleaves mitochondrial antiviral signaling protein off the mitochondria to evade innate immunity. *PNAS* 2005 Dec 6; 102(49):17717-22.
5. Seth RB*, Sun L*, Ea CK, and Chen ZJ. Identification and characterization of MAVS, a mitochondrial antiviral signaling protein that activates NF-kappa B and IRF 3. *Cell* 2005 Sept 9; 122(5):669-82.
6. Kanayama A, Seth RB, Sun L, Ea CK, Hong M, Shaito A, Chiu YH, Deng L, and Chen ZJ. TAB2 and TAB3 activate the NF-kappaB pathway through binding to polyubiquitin chains. *Mol Cell.* 2004 Aug 27; 15(4):535-48.

* equal contribution.

LIST OF FIGURES

Figure 1:	Induction and downstream effects of IFN- β .	24
Figure 2:	Mechanism of activation of NF- κ B by IL-1.	29
Figure 3:	Interferon regulatory factor (IRF) family members.	33
Figure 4:	Signaling pathways triggered by TLRs.	38
Figure 5:	RIG-I mediated signaling pathway.	43
Figure 6:	IRF3 domain structure and substrate design for <i>in vitro</i> kinase assay.	49
Figure 7:	<i>In vitro</i> IRF3 kinase assay.	62
Figure 8:	Optimization of <i>in vitro</i> IRF3 kinase assay.	65
Figure 9:	IRF3 kinase activity pellets in P20 and P100 fraction.	68
Figure 10:	Fractionation of the IRF3 kinase activity on glycerol gradients.	70
Figure 11:	TBK1 and IKKi phosphorylate IRF3 group II Ser/Thr residues.	73
Figure 12:	Identification of MAVS and its sequence analysis.	91
Figure 13:	MAVS is a potent inducer of IFN- β .	93
Figure 14:	MAVS is required for IFN- β induction by Sendai virus.	96
Figure 15:	MAVS is required for the activation of IRF3 kinases and	98

	the IKK complex by Sendai virus.	
Figure 16:	MAVS is a potent antiviral protein.	100
Figure 17:	MAVS functions downstream of RIG-I and upstream of TBK1.	103
Figure 18:	MAVS expression pattern.	107
Figure 19:	Domain and sequence analysis of MAVS.	113
Figure 20:	The CARD domain is essential for MAVS signaling.	117
Figure 21:	Point mutations within CARD domain abolish MAVS function.	118
Figure 22:	The Δ CARD mutant of MAVS acts as a dominant negative inhibitor of IFN- β induction by Sendai virus.	119
Figure 23:	The transmembrane domain of MAVS is important for its function.	120
Figure 24:	The CARD and TM domain are sufficient for MAVS function.	121
Figure 25:	Intercation of MAVS with RIG-I and TRAF6.	123
Figure 26:	The transmembrane domain of MAVS is similar to the transmembrane domains of C-tail terminal anchored proteins.	130
Figure 27:	MAVS is a mitochondrial protein.	134

Figure 28:	Subcellular fractionation of MAVS.	138
Figure 29:	Mislocalization of MAVS impairs its function.	140
Figure 30:	NS3/4A blocks interferon induction by MAVS.	151
Figure 31:	MAVS is cleaved by NS3/4A.	154
Figure 32:	NS3/4A cleaves MAVS at Cys-508.	156
Figure 33:	NS3/4A co-localizes with MAVS in the mitochondria.	159
Figure 34:	Proposed model for RIG-I mediated signaling.	163

LIST OF ABBREVIATIONS

2'-5' OAS - 2'-5' Oligoadenylate synthetase

ATF-2 – Activating transcription factor-2

ATP – Adenosine triphosphate

Bcl – B cell lymphoma protein

CARD – Caspase activation and recruitment domain

cDCs – conventional dendritic cells

DBD – DNA binding domain

DNA- Deoxyribonucleic Acid

DNA-PK – DNA-dependent protein kinase

dsRNA – Double stranded RNA

E2 – Ubiquitin-conjugating enzyme

E3 – Ubiquitin ligase

ER – Endoplasmic reticulum

FADD – Fas-associated protein containing death domain

GFP – Green fluorescent protein

GST – Glutathione S-transferase

HCV – Hepatitis C virus

HMG-I – High mobility group

IAD – IRF association domain

ID – autoinhibitory domain

IFN – Interferon

IFNAR – Interferon receptor

IKKi – Inducible IKK

IL – Interleukine

IL-1R – IL-1 receptor

IL-1Racp – IL-1 receptor accessory protein

IRAK – IL-1 receptor associated kinase

IRF – Interferon regulatory factor

ISG – Interferon stimulated gene

ISGF3 – Interferon-stimulated gene factor 3

ISRE – Interferon-stimulated response element

IκB - inhibitor of NF-κB

JAK – Janus activated kinase

JNK – c Jun N-terminal kinase

LPS – lipopolysaccharide

LRR – Leucine rich repeats

MAVS – Mitochondrial antiviral signaling protein

MDA-5 – Melanoma differentiation factor

MEF – Mouse embryonic fibroblast

MyD88 – Myeloid differentiation factor

NAP1 – NAK-associated kinase 1

NDV – Newcastle disease virus

NEMO - NF- κ B essential modulator

NES – Nuclear export sequence

NF- κ B – Nuclear factor- κ B

NLS – Nuclear localization sequence

NP-40 – Nonidet P-40

NS – non-structural protein

PCR – polymerase chain reaction

pDCs – Plasmacytoid dendritic cells

PKR – Protein kinase activated by dsRNA

PRD – positive regulatory domain

PRO – Proline-rich domain

PRR – Pathogen-recognition receptor

RD – regulatory domain

RIG-I – Retinoic acid inducible gene – I

RING – Really interesting new gene

RIP1 - Receptor interacting protein kinase 1

RNA – Ribonucleic acid

RNAi – RNA interference

SH3 – Src homology 3

STAT – Signal transducer and activator of transcription

SV – Sendai virus

TAB - TAK1 associated protein

TAK 1 - TGF β activated kinase 1

TBK – TANK binding kinase

TCR – T cell receptor

TIR – Toll/IL-1R domain

TLR – Toll-like receptor

TM – Transmembrane

TNF – Tumor necrosis factor

TNFR – TNF receptor

TRAF – TNF receptor associated factor

TRIF – TIR domain containing adaptor inducing IFN

TRIKA – TRAF6-regulated IKK activator

VAMP-2 – vesicle associated membrane protein-2

VSV – Vesicular stomatitis virus

CHAPTER I: INTRODUCTION TO THE ANTIVIRAL INNATE IMMUNE RESPONSE

Viruses are highly infectious pathogens that depend on host cellular machinery for survival and replication. Most viral infections, like the common cold caused by Rhinoviruses, are efficiently resolved by the host immune system. Both branches of the immune system, the innate and adaptive immune response, contribute to antiviral immunity (Akira et al., 2006). In the early phase of an infection, the innate immune response plays an essential role in checking the progress of the virus before the later adaptive immune response develops. Cells of the innate immune system and the cytokines secreted by them are also responsible for alerting and shaping the adaptive immune response. The adaptive or acquired immune response develops in the late phase of infection and is not only involved in the elimination of a virus, but also confers immunologic memory against the pathogen. Given the importance of the innate immune response as the first line of defense against a viral infection, it is vital to understand the signaling pathways that regulate its generation. My thesis projects have focused on understanding the signaling pathways that regulate the antiviral innate immune response.

I. A. Induction and Downstream Effects of Type I Interferons (IFNs)

A viral infection triggers the host antiviral innate immune response. The pathogen-recognition receptors (PRRs) expressed by cells of the innate immune system are responsible for recognizing virus-associated nucleic acids like genomic DNA or RNA and double stranded (ds) RNA (discussed in section I.D) (Ishii and Akira, 2005). In response to a viral challenge, several cytokines including type I and type II IFNs, tumor necrosis factor- α (TNF- α), interleukin -6 (IL-6) and IL-8 are synthesized and secreted (Mogensen and Paludan, 2001). Of these, the regulation and downstream effects are best characterized for type I IFNs which include several IFN- α subtypes and a single IFN- β subtype (Honda et al., 2005c). Although, several cell types including epithelial cells, fibroblasts and macrophages are capable of synthesizing IFNs, a subset of dendritic cells - plasmacytoid dendritic cells (pDCs) have recently been identified as the major source of IFNs in response to a viral challenge (Colonna et al., 2004). Besides their role in antiviral immunity, IFN α/β also exhibit anti-proliferative and immunomodulatory effects (Honda et al., 2005c).

The expression of IFN genes is regulated at the level of transcription and has been extensively studied and is particularly well understood for the IFN- β promoter (Maniatis et al., 1998). The promoter region of IFN- β contains several cis-acting DNA elements identified as positive regulatory domains (PRDs) and are designated PRDI through PRDIV (Figure 1a). These domains serve as

Figure 1a

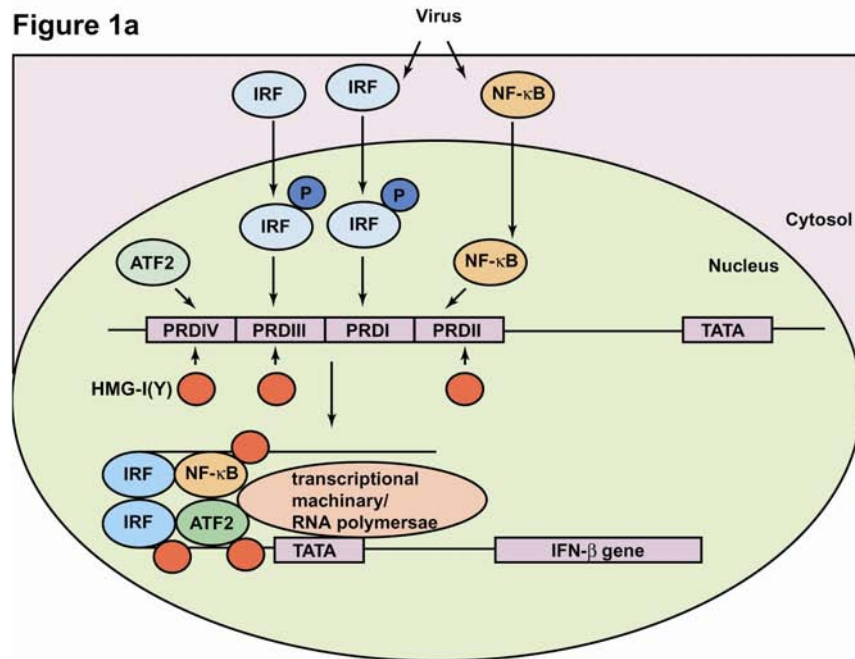


Figure 1b

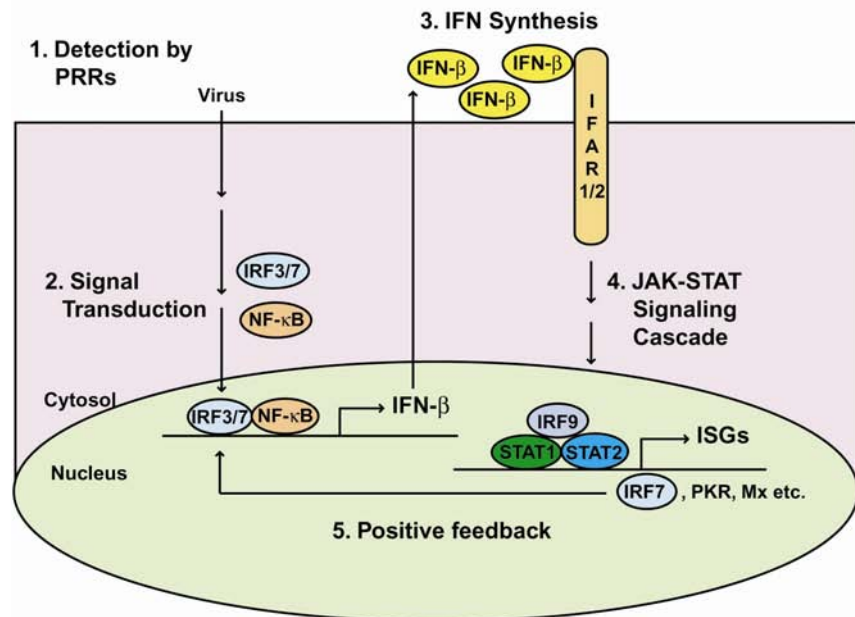


Figure 1: Induction and downstream effects of IFN- β

- (a) In response to a viral infection, three classes of transcription factors – ATF2/c-Jun, IRF and NF- κ B, are activated. These transcription factors bind to the PRD elements of the IFN- β gene in the nucleus. Together with the nuclear architectural protein HMG-I(Y), these transcription factors assemble into a stereospecific enhanceosome complex that is required for the transcriptional initiation of the IFN- β gene.
- (b) An effective innate antiviral immune response involves the following steps: 1. Detection of invading viruses by PRRs such that the receptors are activated; 2. Activation of the PRRs triggers cellular signaling cascades that lead to the activation of transcription factors like IRF3/7 and NF- κ B. Once activated these transcription factors lead to the induction of IFN- β gene; 3. The synthesized IFN- β is secreted. The secreted IFN- β acts in an autocrine or paracrine manner by binding to IFNAR1/2; 4. Activation of the IFNAR leads to the initiation of the JAK/STAT signaling pathway that leads to the activation of STAT1 and STAT2. These transcription factors associate with IRF9 to form ISGF3, which regulates the synthesis of several ISGs including IRF7, PKR, Mx proteins etc.; 5. One of the ISGs synthesized is IRF7 that induces the further expression of type I IFNs including IFN- β to form a positive feedback loop.

binding sites for at least three classes of transcription factors – ATF-2/c-Jun that binds PRD IV, nuclear factor (NF)- κ B that binds PRD II and interferon regulatory factor (IRF) family members that bind PRD I and PRD III. Together with the nuclear architectural protein HMG-I(Y), these transcription factors assemble into a stereospecific enhanceosome complex that remodels the chromatin in the promoter of IFN- β , resulting in transcriptional initiation (Thanos and Maniatis, 1992).

Synthesized IFN- β is secreted and binds to the IFN α/β receptor (IFNAR) in an autocrine and paracrine manner to initiate a positive feedback loop that

results in further production of type I IFNs (Figure 1b) (Theofilopoulos et al., 2005). The type I IFN receptors are composed of two subunits- IFNAR1 and IFNAR2. In the presence of a ligand, these receptor subunits undergo dimerization followed by autophosphorylation and activation of the associated Janus activated kinase (JAK) family members. Tyrosine kinase 2, a member of the JAK family, is associated with IFNAR1 whereas JAK1 is associated with IFNAR2. These activated kinases in turn phosphorylate and activate the signal transducer and activator of transcription 1 (STAT1) and STAT2 proteins. These transcription factors associate with a member of the IRF family of transcription factors - IRF9, to form a heterotrimeric complex, IFN-stimulated gene factor 3 (ISGF3). ISGF3 initiates the transcription of several interferon stimulated genes (ISGs) by binding to the IFN-stimulated response elements (ISRE) in their promoter regions. Extensive microarray analyses have identified several classes of proteins that constitute the ISGs (de Veer et al., 2001). Examples of ISGs include transcription factors like IRF7, kinases like PKR, RNA degrading enzymes like 2'-5'-oligoadenylate synthetase (2'-5' OAS)/RNaseL, Mx proteins that interfere with viral nucleocapsid transport, Ubiquitin-like protein ISG15 of unknown function, cytokines and chemokines like type I IFNs, IL-15 and RANTES etc. Together these ISGs inhibit various stages of the viral life cycle and induce an antiviral state in the host. The importance of the IFN- α/β signaling pathway in the antiviral innate immune response is underscored by studies in mice

with targeted disruption of the IFNAR genes (Muller et al., 1994). These mice are extremely sensitive to viral infections and exhibit increased viral replication in several tissues.

I. B. Signaling pathways that activate NF- κ B and its role in the regulation of IFN- β induction

The NF- κ B/Rel family of transcription factors regulate several physiologic processes like inflammation, immunity and apoptosis. Members of this family, which includes Rel-A (p65), Rel-B, c-Rel, p50, exist as homo- or hetero-dimers (Ghosh et al., 1998). The activity of NF- κ B is regulated at the level of subcellular localization (Silverman and Maniatis, 2001). In unstimulated cells, NF- κ B is held in the cytosol by inhibitory κ B (I κ B) family members. The activation of NF- κ B depends on the phosphorylation and subsequent degradation of the associated I κ B protein. The phosphorylation of I κ B is achieved by a multi-protein complex, termed I κ B kinase (IKK) that contains two catalytic subunits, IKK α and IKK β , and a regulatory IKK γ (also termed NF- κ B essential modulator, NEMO) subunit. Once phosphorylated, I κ B is ubiquitinated and subsequently degraded by the proteasome. Free NF- κ B translocates into the nucleus and turns on its target genes.

Several studies support the importance of NF- κ B and its interaction with the PRD II elements for the regulation of the IFN- β promoter (Lenardo et al., 1989; Thanos and Maniatis, 1992; Visvanathan and Goodbourn, 1989). In response to a challenge with viruses or dsRNA (a byproduct of viral infection), NF- κ B translocates from the cytosol to the nucleus. Direct binding between NF- κ B and PRDII elements has been demonstrated, and mutations that interfere with the binding of NF- κ B to PRD II *in vitro* severely impair IFN induction *in vivo*. Further, knock-down of the expression of NF- κ B by antisense RNA diminishes the expression of IFN- β by viruses.

Most of our understanding of the mechanism by which NF- κ B is activated has been gained by studies on signaling pathways initiated by the interleukin-1 β receptor (IL-1R), tumor necrosis factor (TNFR) or T cell receptor (TCR). Although different receptors recruit distinct signaling complexes upon activation by agonist binding, all these signals converge at the level of IKK. A paradigm for activation of IKK has emerged from studies of the IL-1 β signaling pathway (Figure 2) (Chen, 2005). When IL-1 β binds its receptor, it leads to the recruitment of IL-1R accessory protein (IL-1Racp) and forms an active receptor complex which in turn recruits an adaptor protein myeloid differentiation factor (MyD88) and kinases that include IL-1 receptor associated kinase (IRAK1) and IRAK4. IRAK1 binds to and recruits TNFR-associated factor 6 (TRAF6) that

Figure 2

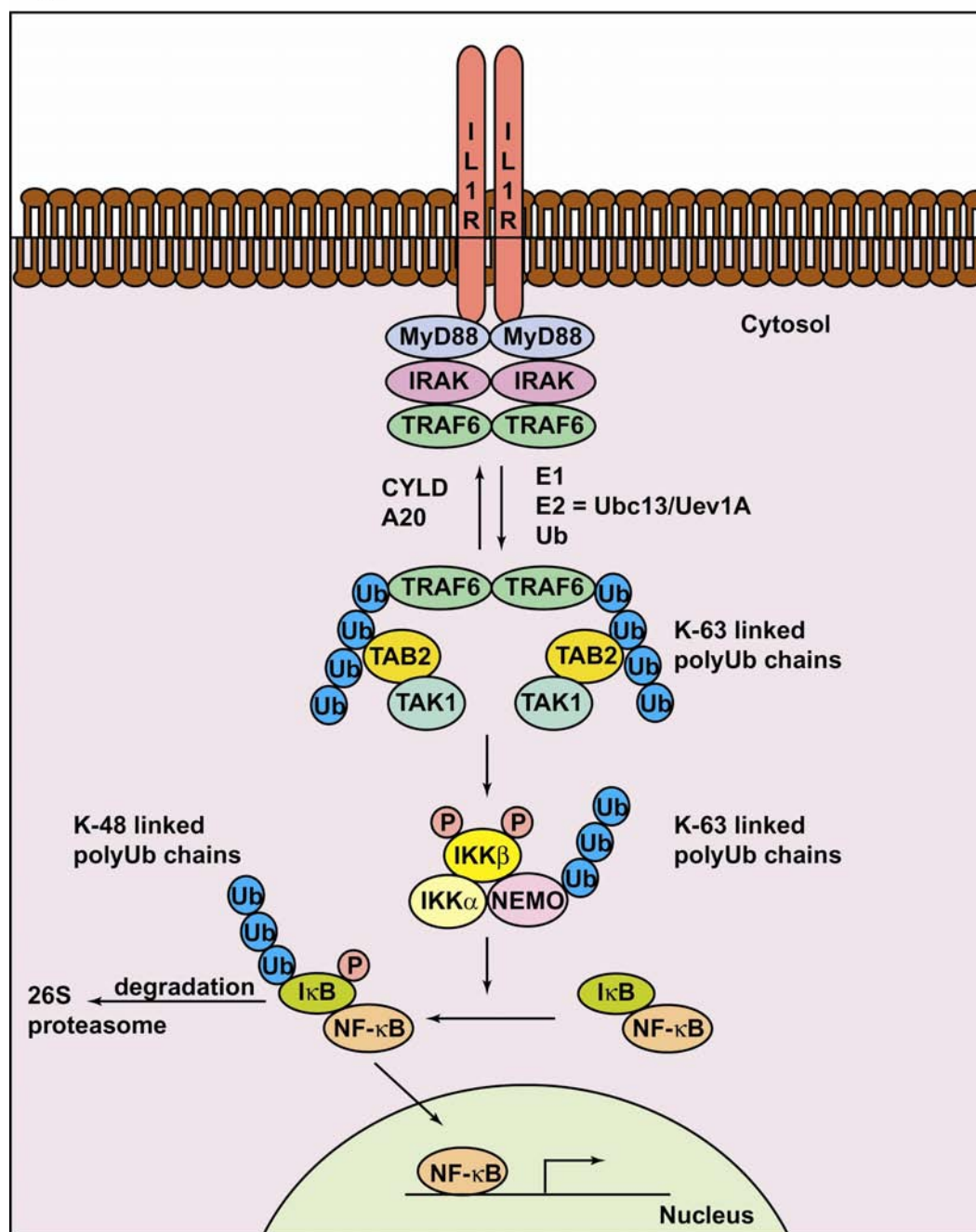


Figure 2: Mechanism of activation of NF- κ B by IL-1.

Stimulation of the IL-1R leads to the recruitment of several adaptor proteins including MyD88, IRAK and TRAF6 to the receptor. TRAF6 is an E3 ubiquitin ligase, which together with the E2 enzyme, Ubc13/Uev1A catalyzes conjugation of K-63 linked polyubiquitin chains to target protein like NEMO and TRAF6 itself. This polyubiquitination reaction can be reversed by deubiquitinating enzymes like CYLD and A20. The K-63 linked polyubiquitin chains bind to TAB2 and trigger the activation of TAK1 through an as yet unknown mechanism. Activated TAK1 phosphorylates the activation loop of $\text{IKK}\beta$, leading to IKK activation. IKK phosphorylates $\text{I}\kappa\text{B}\alpha$ protein and targets it for degradation by the 26S proteasome. NF- κ B is thus free to translocate into the nucleus where it turns on the expression of several target genes.

transmits the signal to the downstream kinases, IKK and JNK. A biochemical fractionation approach identified two intermediary protein complexes, termed TRIKA1 (TRAF6-regulated IKK activator 1) and TRIKA2, that transmit the signal from TRAF6 to IKK.

The TRIKA1 complex consists of a ubiquitin conjugating enzyme (E2) Ubc13, and a Ubc-like protein Uev1A (Deng et al., 2000). The identification of an E2 as an activator of IKK was very surprising. A better understanding of how an E2 regulates IKK was gained by studies that demonstrated that TRAF6 functions as an ubiquitin ligase (E3) in this pathway. Several family members of the TRAF family, including TRAF6, contain a highly conserved N-terminal RING domain that is found in a large family of E3 enzymes. Together with the E2 enzymes, Ubc13/Uev1A, TRAF6 catalyzes the synthesis of unique polyubiquitin chains linked through lysine-63 (K-63) of ubiquitin. K-63 linked polyubiquitin chains are different from K-48 linked polyubiquitin chains that

target a protein for degradation by the proteasome pathway. Subsequent studies have identified several targets of K-63 linked polyubiquitination, including NEMO and TRAF6 itself (Chen, 2005). Through a proteasome independent mechanism, which has not yet been well characterized, the K-63 polyubiquitinated chains of TRAF6 lead to the activation of IKK.

A trimeric protein complex of TAK1 (TGF- β activated kinase) and its associated proteins TAB1 (TAK1-binding protein) and TAB2 constitute the TRIKA2 complex (Wang et al., 2001). Biochemical assays have shown that active TAK1 directly phosphorylates IKK β within the activation loop, thereby activating the IKK complex. Further studies have shown that TAK1 is also activated by auto-polyubiquitination of TRAF6. The role of TAB1 in this pathway is not clear but TAB2 is required for the ubiquitin-dependent activation of TAK1 by TRAF6. Recent studies have shown that TAB2 and its homologue TAB3 mediate this polyubiquitination dependent activation of TAK1 (Kanayama et al., 2004). Both TAB2 and TAB3 contain a highly conserved C-terminal zinc finger domain that preferentially binds to K-63 linked polyubiquitin chains. Deletion of this domain or point mutations within this domain that impair polyubiquitin binding abolish the ability of TAB2 and TAB3 to activate TAK1 and IKK. Thus, TAB2 and TAB3 appear to activate TAK1 and IKK by binding to K-63 polyubiquitin chains of target proteins like TRAF6. The mechanism of how the activation of kinases is achieved by binding of TAB2 or TAB3 to

polyubiquitin chains is not yet understood. It has been proposed that the binding of polyubiquitinated TRAF6 to TAB2 or TAB3 facilitates the dimerization or oligomerization of TAK1 complex, thereby promoting the *trans*-autophosphorylation and activation of TAK1. Active TAK1 also phosphorylates MKK6, which activates the JNK and p38 kinase pathways.

There are seven known members of the TRAF family of ubiquitin ligases. Several members of this family have been implicated in activation of NF- κ B by diverse stimuli (Chen, 2005). TNF- α and TCR mediated activation of IKK depends on the activities of TRAF2 and TRAF6 respectively. Recent studies have also revealed a role of TRAF proteins in the activation of IRF family members (discussed in section I.D.1).

I. C. Role of IRFs in antiviral signaling pathways

Several members of the IRF family of transcription factors have important roles in regulating different aspects of the antiviral immune response including the expression of type I IFNs. There are nine known members in this family: IRF1, IRF2, IRF3, IRF4/Pip/IC-SAT, IRF5, IRF6, IRF7, IRF8 and IRF9/p48/ISGF3 γ (Figure 3) (Mamane et al., 1999). These proteins share a homology within their N-terminal DNA binding domain (DBD) that contains a repeat of five tryptophan residues spaced by 10-18 amino acids. Through this domain, the IRF family members bind similar regions of DNA including ISREs

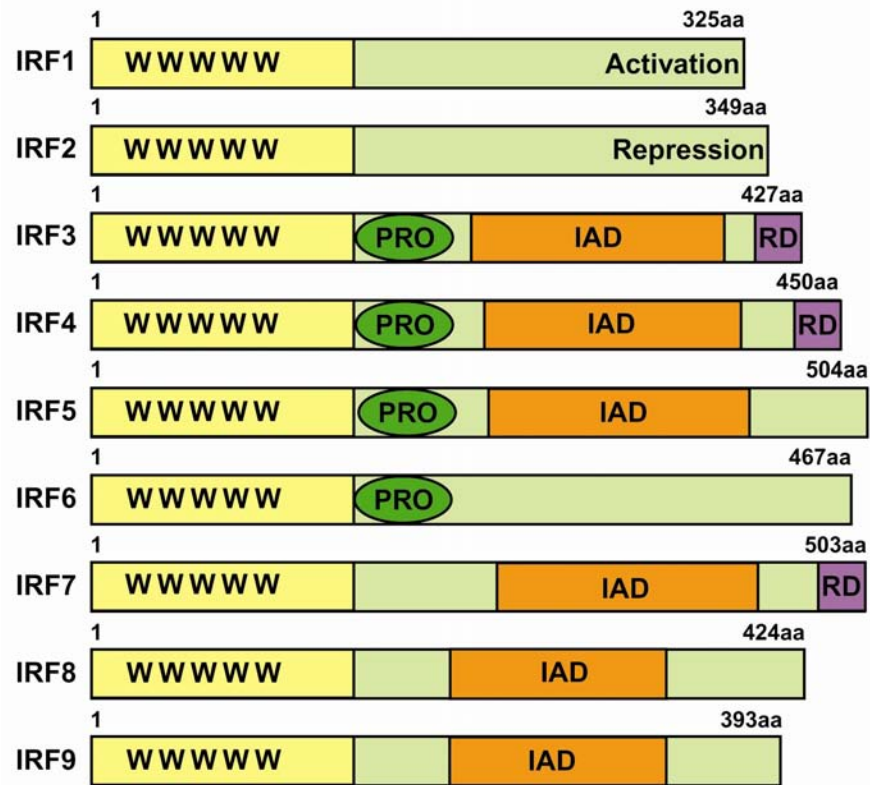
Figure 3

Figure 3: Interferon Regulatory Factor (IRF) Family Members

There are nine known members in the IRF family of transcription factors. The conserved tryptophan repeats in the DNA binding domain (DBD; yellow box) are represented as W. Certain members of the family contain a proline-rich domain (PRO), an IRF association domain (IAD) and a C-terminal regulatory domain (RD).

(found within promoter regions of several ISGs), interferon consensus sequences (ICS; found within the MHC I promoter) and interferon regulatory elements (IRF-E or PRD I and III within the IFN- β promoter).

IRF1 and IRF2 were originally identified as factors that regulated the IFN- β promoter in response to viruses and dsRNA through their interaction with the PRD I and III regions the promoter. IRF1 was identified as an activator whereas IRF2 was recognized as a repressor of IFN- β promoter induction (Harada et al., 1989). However, mouse knock-out studies revealed that IRF1 and IRF2 were dispensable for the regulation of the IFN- β promoter (Matsuyama et al., 1993). Based on primary sequence homology, a new member of the IRF family, which is ubiquitously expressed in human tissues, was identified. This factor was termed IRF3 and several studies have now confirmed that IRF3 binds the PRD I and PRD III regions within the IFN- β promoter to regulate the expression of this promoter in a virus and dsRNA- dependent manner (Sato et al., 1998; Schafer et al., 1998; Weaver et al., 1998; Yoneyama et al., 1998). Mouse embryonic fibroblasts (MEFs) derived from IRF3 knock-out mice have a defect in the production of IFN- β (Sato et al., 2000). Like NF- κ B, the activation of IRF3 is also determined by its subcellular localization. IRF3 is cytosolic in cells that have not been challenged by a viral infection. In response to such a challenge, IRF3 is phosphorylated by the IKK-like kinases TBK1 and IKKi (Fitzgerald et al., 2003; Sharma et al., 2003). Not much is understood about the regulation of these kinases by viruses. Phosphorylation of IRF3 leads to its dimerization and this

active form of IRF3 translocates into the nucleus where it binds to the IFN- β promoter.

In terms of sequence identity, IRF7 is very similar to IRF3. IRF7 homodimers regulate the transcription of the IFN- α gene and together with IRF3 bind the IFN- β promoter. An early model suggested that IRF7 is not involved in the initial phase of IFN- β induction as it is expressed at low levels in most cells in the absence of virus (Marie et al., 1998). IFN- β produced in response to a viral challenge by the IRF3-dependent pathway described above, induces transcription of IRF7. IRF7 is then activated by phosphorylation at certain key residues by TBK1/IKKi such that it binds and induces the promoter of the IFN- α gene. A recent study using IRF7 knock-out mice has suggested that transcription of IFN- β is also dependent on IRF7 (Honda et al., 2005b). IRF7^{-/-} mouse embryonic fibroblasts (MEFs) exhibited defects in the production of both IFN- α and IFN- β in response to viral infection. The revised model now suggests that IRF3 forms heterodimers with the low levels of IRF7 available in the cell to induce the initial synthesis of IFN- β . In contrast to other cell types, pDCs express constitutively high levels of IFF7. Production of IFNs by pDCs in response to TLR9 stimulation is not regulated by IRF3 function but depends completely on IRF7. Thus, IRF7 plays a central role in the induction of type I IFNs.

IRF5 is another member of the IRF family that has been suggested to regulate type I IFN expression. However, recent genetic experiments using IRF5 deficient mice showed that IRF5 is not required for type I IFN induction, but is required for the induction of proinflammatory cytokines by stimulation of TLRs (Takaoka et al., 2005).

Dendritic cells play an important role in the antiviral immune defense. IRF4 and IRF8 have recently been implicated in the development of DCs (Tailor et al., 2006). IRF8 knock-out mice have no pDCs, whereas IRF4 knock-out mice lack another subset of DCs termed CD4⁺ DCs. In DCs, IRF8 has also been implicated in the feedback phase of IFN gene induction. Further studies need to be conducted to support the role of IRF8 in the IFN pathway and to understand the mechanism by which IRF8 functions.

I. D. The two receptor systems to detect viruses

I. D. 1. The Toll-like receptor (TLR) pathway of antiviral innate immunity

The founding member of the TLRs is the Toll receptor in *Drosophila*, which was first found to instruct dorsal-ventral patterning in early embryos, and later found to also regulate anti-fungal innate immunity in adult flies (Lemaitre et al., 1996). Sequence homology search in mammalian genomes has subsequently identified 11 members of TLRs (Akira and Takeda, 2004). These receptors contain an extracellular domain characterized by leucine-rich repeats (LRRs), a

single transmembrane domain, and an intracellular signaling domain known as the Toll/IL-1R (TIR) domain. Although all TLRs share similar extracellular LRRs, they recognize very different microbial signatures (Figure 4) (Kawai and Akira, 2006b). For example, TLR3 recognizes viral double-stranded RNA, TLR4 recognizes bacterial lipopolysaccharides (LPS), whereas TLR5 is a receptor for bacterial flagellin. In most cases, however, a direct binding between a TLR and a putative microbial ligand has not been demonstrated. The intracellular TIR domain recruits signaling molecules to activate downstream signaling pathways culminating in the induction of cytokines like IFNs through NF- κ B and IRFs. Except for TLR3, all TLRs utilize MyD88 as an adaptor protein to recruit downstream signaling molecules. The TIR domains of TLR3 and TLR4 bind to another adaptor protein TRIF to activate NF- κ B and IRFs.

Among the TLRs, TLR3, 7, 8 and 9 are involved in the antiviral innate immune response (Kawai and Akira, 2006a). These receptors are differentially expressed in cells: TLR7, 8 and 9 are highly expressed in pDCs whereas TLR3 is predominantly expressed in cDCs and fibroblasts. TLR3 is the receptor for dsRNA genomes of viruses like reoviruses; TLR7 and TLR8 act as receptors for G/U-rich regions in the genomes of ssRNA viruses like vesicular stomatitis virus

Figure 4

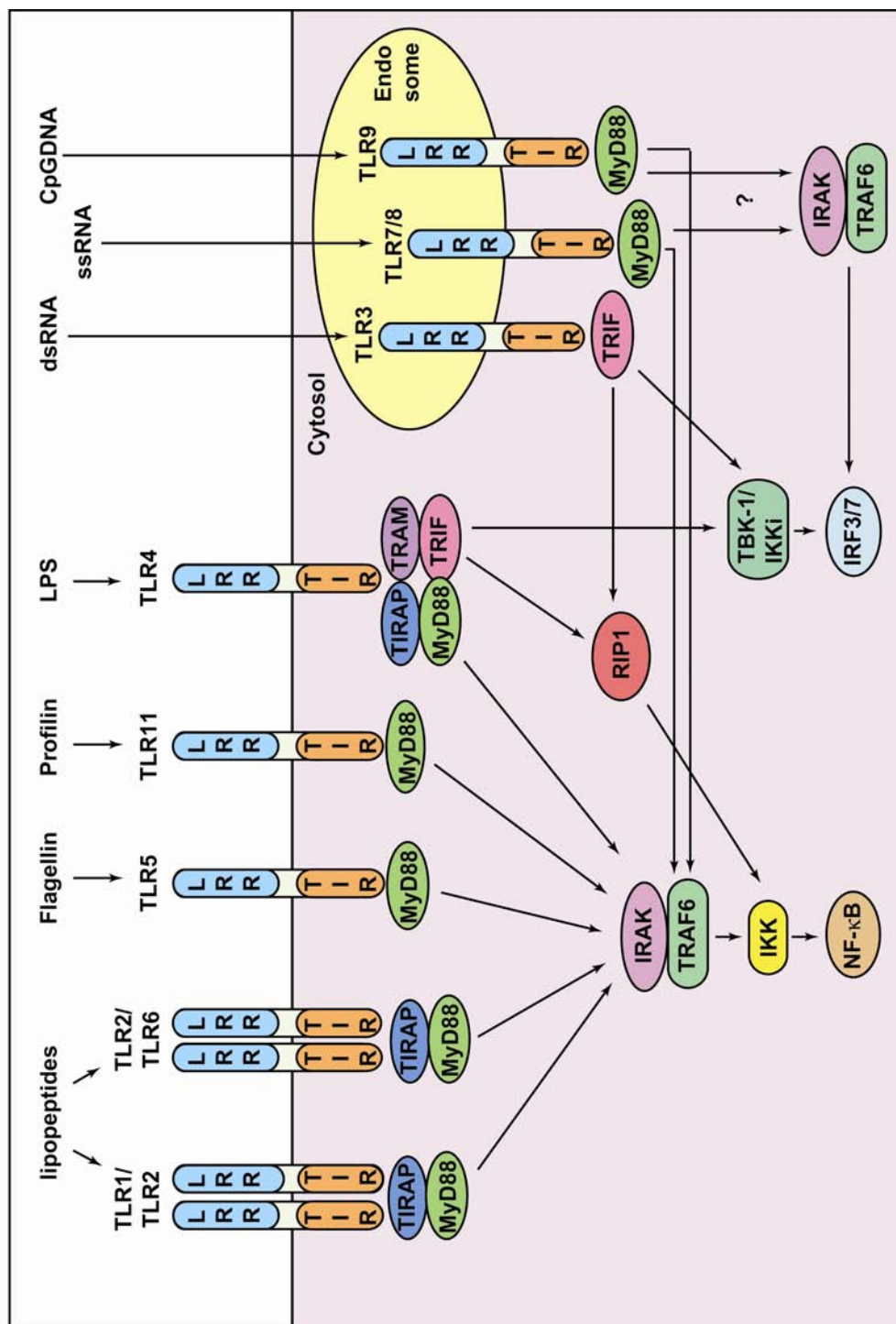


Figure 4: Signaling pathways triggered by TLRs

TLR1, TLR2, TLR4, TLR5 and TLR6 are expressed on the plasma membrane of the cell. TLRs involved in the detection of viral nucleic acids, including TLR3, TLR7/8 and TLR9, are localized in the endosomal compartment. The pathogen associated molecules recognized by the LRR domain of each receptor are indicated. The intracellular TIR domains of TLRs recruit various adaptors. TLR1/2 and TLR2/6 recruit TIRAP and MyD88; TLR5, TLR11, TLR7/8 and TLR9 recruit MyD88; TLR4 recruits four adaptors including TIRAP, MyD88, TRAM and TRIF; and TLR3 recruits TRIF. MyD88 leads to the activation of IKK by the IRAK-TRAF6 signaling module. TRIF can activate signaling pathways that lead to the induction of IFNs by activating both NF- κ B and IRF3. TRIF interacts with RIP1 to activate NF- κ B and with TBK1 to activate IRF3. TLR7 /8 and 9 can also activate IRF7 by the MyD88-IRAK-TRAF6 signaling module to induce IFN production by an as yet unknown mechanism.

(VSV) and influenza virus; TLR9 detects unmethylated CpG regions associated with genomes of DNA viruses like herpesvirus.

Mouse knock-outs for TLR7, 8 and 9 have been generated. IFN- α production by pDCs is severely compromised in TLR7-deficient mice after infection with influenza virus or VSV (Diebold et al., 2004; Lund et al., 2004). Similarly, pDCs from TLR9 knock-out mice do not produce IFNs in response to DNA viruses (Lund et al., 2003). TLR8 is phylogenetically related to TLR7. Although human TLR8, like TLR7 can signal in response to ssRNA, the response of TLR8-deficient mice to these molecules is normal, suggesting a species-specific role of TLR8.

TLR7, 8 and 9 are localized in endosomes, with the ligand binding domain facing the lumen and the TIR signaling domain positioned on the cytoplasmic side (Kawai and Akira, 2006a). Viral nucleic acids that arrive in this compartment

through endocytosis are recognized by these receptors. The endosomal localization of TLR7, 8 and 9 is essential for signaling, as disruption of the endocytic compartment by inhibitors like chloroquine abrogates signaling through these receptors (Lund et al., 2004). It has also been suggested that the ability of pDCs to induce high levels of IFNs depends on their ability to effectively retain viral RNA in the endosomes, in contrast to cDCs that rapidly transport viral RNA from endosomes to lysosomes. Further, manipulation of nucleic acids that allow them to be retained in the endosome convert them to effective TLR ligands that induce type I IFNs in cDCs (Honda et al., 2005a).

The MyD88-IRAK-TRAF6 signaling module is essential for the induction of IFNs by TLR7, 8 and 9. As mentioned previously, IRF7 is important for TLR mediated induction of IFNs. It has been shown that MyD88 and TRAF6 can bind to IRF7 directly, and recruit IRAK1 to phosphorylate IRF7, resulting in the nuclear translocation and activation of IRF7 (Kawai et al., 2004). Indeed, IRAK1-deficient mice are defective in IFN- α production in response to stimulation of TLR7 and TLR9 (Uematsu et al., 2005). Interestingly, TRAF6 appears to induce the phosphorylation of IRF7 through a mechanism that involves Ubc13-catalyzed K63 polyubiquitination. Further studies will determine if IRAK1 or another IRF7 activating kinase is activated by TRAF6 in a ubiquitin-dependent manner. The MyD88-IRAK-TRAF6 signaling module is also required for the activation of NF- κ B by IL-1 β and other TLRs such as TLR2; however,

IFNs are not induced by IL-1 β or TLR2. Thus, it is likely that TLR7, 8 and 9 recruit additional components in pDCs to activate IRF7. One such component may be TRAF3, which has recently been shown to be essential for IFN- α induction in pDCs (Hacker et al., 2006; Oganessian et al., 2006). Bone marrow-derived macrophages (BMMs) from TRAF3 knock-out mice cannot induce IFN gene by TLRs ligands like polyI:C, LPS and CpG.

As mentioned previously, TLR3 acts as a receptor for dsRNA which is produced by many viruses during replication. TLR3 signals to NF- κ B and IRF3 via the adaptor protein TRIF. The C-terminal region of TRIF interacts with RIP1, a known activator of NF- κ B (Meylan et al., 2004). This interaction is required for TLR3 mediated activation of NF- κ B as cells from RIP1-deficient mice fail to activate NF- κ B in response to dsRNA. TRIF can also bind to TBK1, which phosphorylates and activates IRF3 and IRF7 (Sato et al., 2003). Recent studies have also shown that TRIF and MyD88 can bind to TRAF3, which activates IRFs to induce type I IFNs, but inhibits NF- κ B to suppress the induction of proinflammatory cytokines (Hacker et al., 2006).

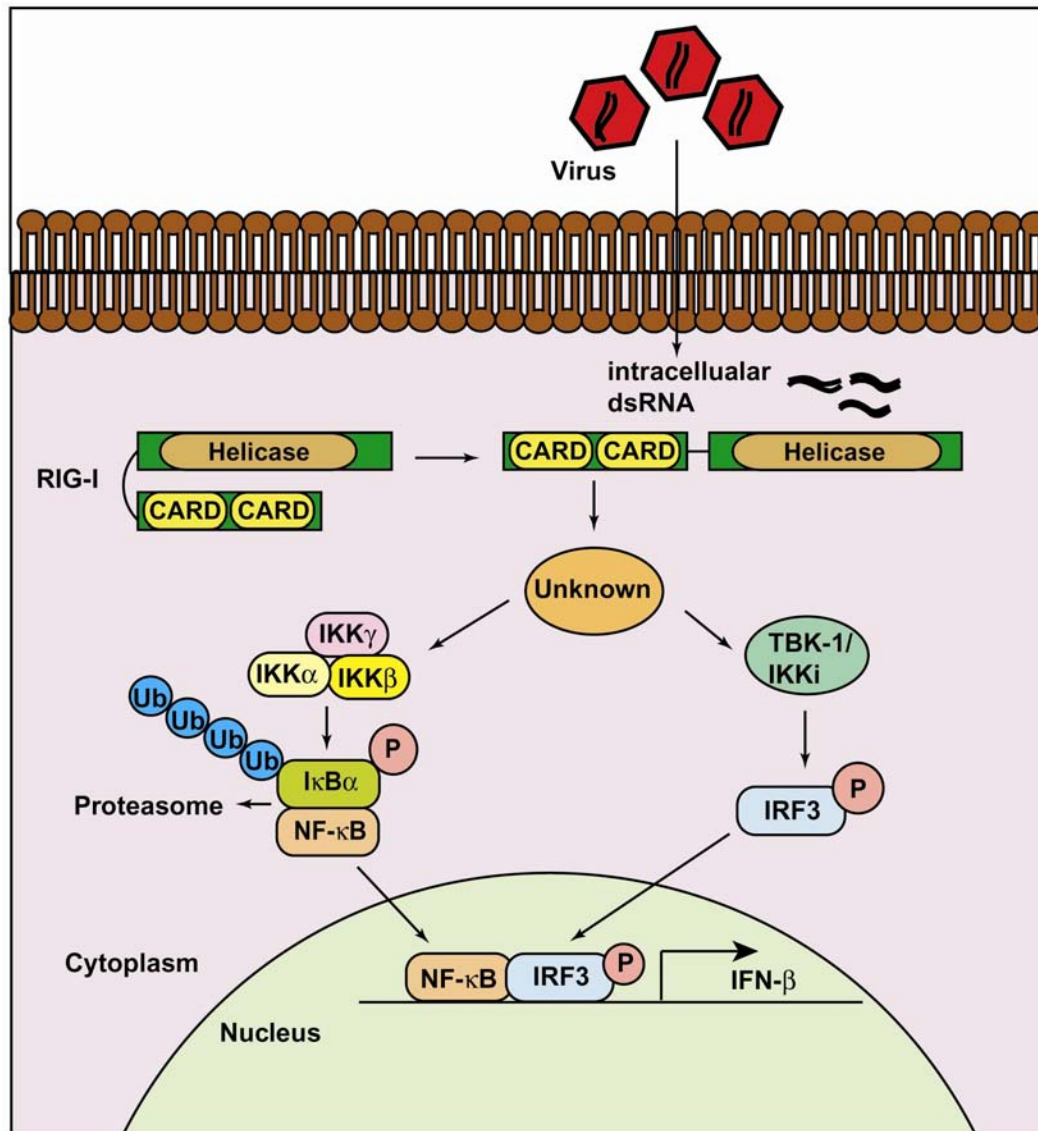
Genetic experiments demonstrate that TLR7 and TLR8 are essential for IFN induction in pDCs by RNA viruses. However, in many other cell types, including cDCs, macrophages and fibroblasts, deletion of both MyD88 and TRIF, which abolishes all TLR signaling, has no effect on viral induction of IFNs (Kato

et al., 2005). Furthermore, although human patients deficient in IRAK4 are more susceptible to bacterial infection, they have intact immune responses against viruses (Yang et al., 2005). Therefore, a TLR-independent pathway that is highly effective in providing antiviral innate immunity has been proposed.

I. D. 2. The RIG-I pathway of antiviral innate immunity

Retinoic acid inducible gene I (RIG-I) has recently been identified as an intracellular receptor for viral dsRNA (Yoneyama et al., 2004). RIG-I is a member of the DExD/H box-containing RNA helicase family of proteins that unwind dsRNA in an ATPase dependent manner. The helicase domain of RIG-I can bind both synthetic dsRNA [poly (I:C)] and viral dsRNA. Besides the C-terminal helicase domain, RIG-I also contains two tandem caspase recruitment domains (CARDs) at its N-terminus. Over-expression of the N-terminal region of RIG-I comprising the two CARD domains is sufficient to activate NF- κ B and IRF3 in the absence of a viral challenge, whereas the full-length RIG-I is activated only in the presence of dsRNA. The binding to dsRNA to the RNA helicase domain of RIG-I has been proposed to induce a conformational change that exposes the N-terminal CARD domains to recruit downstream signaling proteins (Figure 5). Further structural analysis will be required to determine the exact mechanism of how RIG-I is regulated by dsRNA binding. Another poorly understood aspect of RIG-I mediated activation of NF- κ B and IRF3 is the identity

Figure 5


Figure 5: RIG-I mediated signaling pathway

RIG-I is a receptor for intracellular dsRNA. It contains a C-terminal RNA helicase domain that binds to viral dsRNA, and two tandem CARD domains at the N-terminus. In the absence of dsRNA, RIG-I is held in an inhibited conformation such that the CARD domains cannot trigger downstream signaling. The binding of dsRNA to the helicase domain presumably induces

a conformational change that exposes the CARD domains to initiate a signaling cascade. Through an unknown signaling component, RIG-I can signal to both the NF- κ B and IRF3 signaling pathways by activating the IKK and TBK1/IKKi kinase complexes. Once activated, NF- κ B and IRF3 translocate into the nucleus and turn on the IFN- β gene promoter.

of downstream proteins that transmit the signal from the RIG-I CARD domains to the downstream IKK and TBK1/IKKi kinase complexes.

The functional significance of RIG-I in antiviral immunity was first shown by RNAi studies and confirmed by mouse knockout studies. RNAi of RIG-I in L929 cells, a mouse fibroblast cell line, not only inhibited IRF3 activation but also subsequent induction of type I IFNs in response to challenge by RNA viruses (Yoneyama et al., 2004). RIG-I knockout mouse embryos displayed severe liver degeneration and most were embryonic lethal (Kato et al., 2005). The mechanism underlying the embryonic lethal phenotype of RIG-I mutant mice is not yet understood. In RIG-I null mouse embryonic fibroblasts (MEFs) and lung fibroblasts, it was shown that the induction of IFN- β and ISGs by several RNA viruses was abolished. Pre-treatment of the fibroblasts with IFN- β increased the resistance of the RIG-I deficient fibroblasts to VSV, indicating that RIG-I is required for the induction of IFN- β and does not affect the downstream IFN- β signaling pathway.

Besides RIG-I, MDA-5 and Lpg2 have also been identified as DExD/H box RNA helicases that function in the antiviral immune response. Like RIG-I,

MDA-5 also contains two N-terminal CARD domains which can activate the IFN- β promoter (Yoneyama et al., 2005). The importance of MDA-5 as an anti-viral protein has been suggested based on the finding that paramyxovirus V protein binds MDA-5 and inhibits its function (Andrejeva et al., 2004). Lpg2 lacks the CARD domain and acts as a negative regulator of the RIG-I pathway (Andrejeva et al., 2004; Rothenfusser et al., 2005). Over-expression of Lpg2 inhibits the activation of IFN- β promoter by Sendai virus, but it does not interfere with the TLR3 signaling pathway.

The identification of the two-receptor system has raised an important question with regards to the relative importance of signaling mediated by RIG-I vs TLRs in an *in vivo* setting. This question has been addressed by comparing the IFN induction in fibroblasts and bone marrow derived dendritic cells from RIG-I^{-/-} vs MyD88^{-/-} TRIF^{-/-} mice, which lack all TLR signaling (Kato et al., 2005). The ability to induce IFN- β when challenged by NDV was severely compromised in the RIG-I^{-/-}, but not MyD88^{-/-} TRIF^{-/-}, cDCs and fibroblasts. Opposite results were observed for the pDCs, which induce IFN- β normally in the absence of RIG-I, but not in the absence of MyD88 and TRIF. Thus, RIG-I and TLR pathways are not redundant, but rather mediate antiviral signaling in different cell types.

I. E. Inhibition of antiviral signaling pathways

The mechanism of termination of the antiviral signaling pathways described above is not well understood. Some studies have suggested that a NF- κ B inducible ubiquitin-editing protein A20 is involved in negatively regulating the TLR3 and RIG-I mediated signaling pathways. A direct interaction between TRIF and A20 has been demonstrated and it has been shown that A20 degrades TRIF (Saitoh et al., 2005; Wang et al., 2004). Another study has reported that A20-mediated inhibition of the RIG-I signaling pathway is stronger than the inhibition of the TLR3-TRIF signaling pathway (Lin et al., 2006). It has been demonstrated that A20 inhibits at a step upstream of the IRF3 and IRF7 kinases, TBK1/IKKi (Lin et al., 2006). Of the two ubiquitin-editing properties exhibited by A20, N-terminal mediated de-ubiquitination and C-terminal ubiquitin ligase activity, the ligase activity is important for inhibition of the RIG-I signaling pathway (Lin et al., 2006). Further studies will be required for determining the target of A20 and the mechanism by which it checks antiviral immunity.

In addition to physiological mechanisms of silencing antiviral immunity, several viruses encode proteins that inhibit the antiviral immune pathways to support their survival. Hepatitis C virus (HCV) represents a well studied example of a virus that causes persistent host infections by suppressing the immune response. Previous studies have shown that HCV encodes a serine protease, NS3/4A which inhibits the induction of IFN- β by the RIG-I signaling pathway

(Foy et al., 2005; Foy et al., 2003). NS3/4A has been proposed to cleave an essential signaling protein in this pathway such that the target protein is rendered inactive. Thus, insights into the signaling pathways that regulate the antiviral immune response will also help us understand how viruses evade this response. The knowledge gained from these studies should lead to the development of therapeutic strategies against viral infections.

In this thesis, I will describe my efforts to understand the signaling pathways that lead to the activation of NF- κ B and IRFs following a viral infection. Chapter II describes the biochemical approach taken for identification of the kinase that phosphorylates and activates IRF3. Chapter III elaborates on the identification and characterization of a protein, termed mitochondrial antiviral signaling protein (MAVS), that functions downstream of RIG-I. Chapters IV and V will elucidate the progress we have made in understanding the mechanism by which MAVS functions. Data presented in chapter V show that MAVS is targeted by the HCV encoded protease NS3/4A such that RIG-I mediated antiviral signaling is compromised.

CHAPTER II: IDENTIFICATION AND CHARACTERIZATION OF AN IRF3 KINASE

II. A. Introduction

IRF3, a member of the IRF family of transcription factors, plays an important role in regulating the expression of type I IFNs in response to viral infections. IRF3 is a 55kDa protein consisting of 427 amino acids that resides in the cytoplasm of uninfected cells (Mamane et al., 1999). It is a multi-domain protein with a DNA binding domain (DBD), nuclear localization sequence (NLS) and nuclear export sequence (NES) at the N-terminus, a proline-rich domain and a protein interaction domain termed the IRF association domain (IAD) in the middle, and a regulatory domain (RD) at the C-terminus (Figure 6a; upper panel).

A model for the regulation of IRF3 activity in response to a viral infection has been proposed by studies conducted mostly in Dr. John Hiscott's laboratory. Extensive deletion and mutagenesis studies have identified a transactivation domain (residue 134-394) and two auto-inhibitory domains (ID) within the proline-rich domain (134-197) and the extreme C-terminal region (407-414) of IRF3 (Figure 6a) (Lin et al., 1999). It has been proposed that in the absence of virus, the interaction between the two IDs generates a closed conformation of IRF3 such that the DBD, IAD and NLS of IRF3 are masked. Thus, in the closed conformation, IRF3 cannot homodimerize, translocate into the nucleus and bind DNA. In the presence of virus, IRF3 is phosphorylated at Ser/Thr residues within

Figure 6a

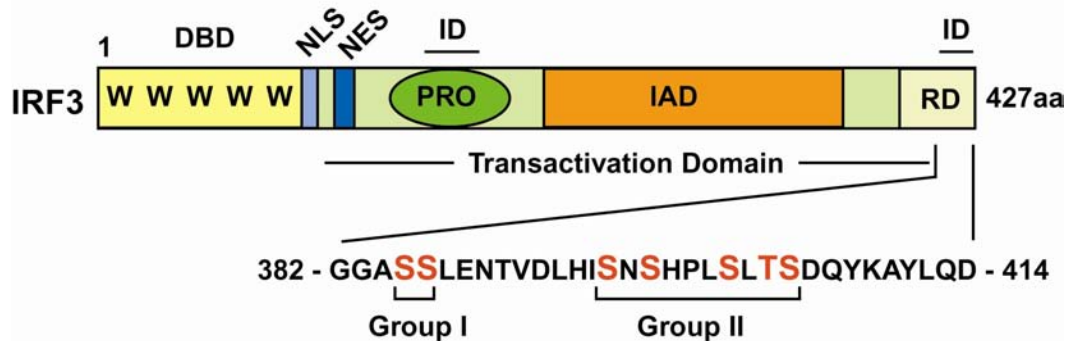


Figure 6b

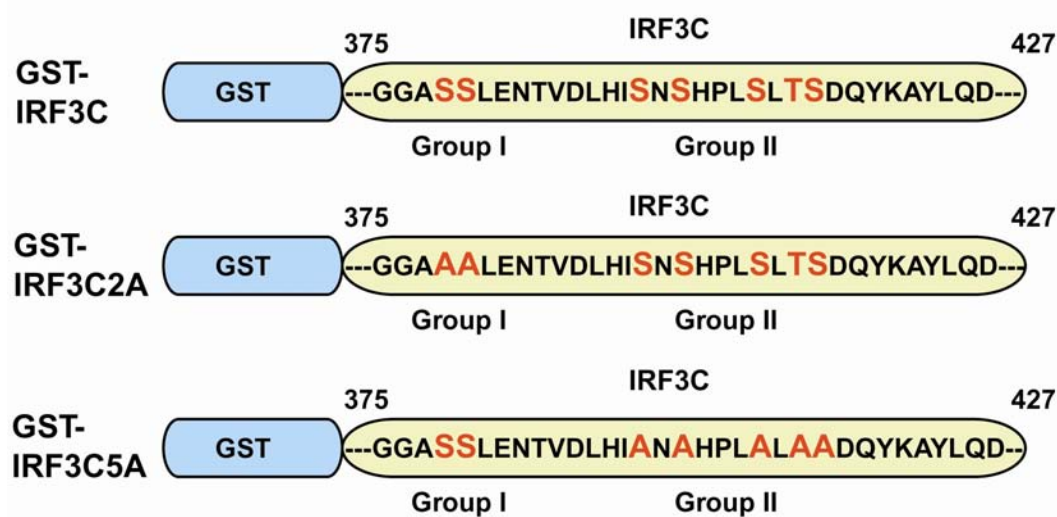


Figure 6: IRF3 domain structure and substrate design for *in vitro* kinase assay

(a) IRF3 contains an N-terminal DNA binding domain (DBD), a central proline-rich domain (PRO) and C-terminal IRF association domain (IAD) and regulatory domain (RD). The regions corresponding to the inhibitory domains (ID) that mask the activity of the DBD, NLS and transactivation

domain, are indicated. The amino acid sequence of the regulatory domain containing the group I and group II Ser/Thr residues is shown.

- (b) Recombinant protein consisting of C-terminal 52 residues of IRF3 (aa 375-427) tagged at the N-terminus with GST (GST-IRF3C) was used as substrate in the *in vitro* kinase assay. Substrates with mutations in either the group I (GST-IRF3C2A, Ser385/386 replaced with alanine) or group II residues (GST-IRF3C5A, Ser396/399/402/405 and Thr404 are replaced with alanine) were also generated.

the C-terminal RD. In this model, the C-terminal phosphorylation events not only lead to the appearance of slower migrating forms of IRF3 on SDS-PAGE, but are also predicted to lead to conformational changes that disrupt the interaction between the two IDs. This relieves the inhibition of the IADs such that IRF3 can homodimerize and translocate into the nucleus where it can associate with p300/CREB binding protein (CBP) co-activator and bind to cis-regulatory elements of its target genes.

There are seven Ser/Thr residues within the C-terminal RD of IRF3 that are phosphorylated in response to viruses - S385, S386, S396, S398, S402, T404 and S405 (Figure 6a; lower panel). The identity of the exact residues that are important for IRF3 activation is controversial. Dr. T. Fujita's group has identified S385 and S386 (referred to as group I residues in this thesis) as the key residues that regulate IRF3 activation (Suhara et al., 2000; Yoneyama et al., 1998), whereas Dr. J. Hiscott's group reported that S396, S398, S402, T404 and S405 (referred to as group II residues in this thesis) are important for activation of IRF3 (Lin et al., 1998; Lin et al., 1999). In support of group II residues as the relevant

residues for IRF3 activation, expression in 293T cells of mutant IRF3 in which these residues are replaced by alanine (this construct is referred to as IRF35A), abolishes the dimerization, cytoplasmic to nuclear translocation, association with CBP/p300, DNA binding and transcriptional activity. Further, mutation of these residues to the phosphomimetic aspartic acid (this construct is referred to as IRF35D) leads to a constitutively active form of IRF3 that can dimerize, translocate into the nucleus and associate with CBP/p300, bind to DNA and activate transcription of target genes (Lin et al., 1999). More specifically it has been shown that mutation of S396 within the group II residues to aspartic acid (this construct is referred to as IRF3S396D) is able to activate IRF3 (Servant et al., 2003).

Further studies have shown that group II residues may not be sufficient for IRF3 activation as mutations of group I residues to alanine (referred to as IRF32A) abolishes that ability of IRF3 to be activated by viruses (Suhara et al., 2000; Yoneyama et al., 1998). But mutation of group I residues to phosphomimetic aspartic acid does not generate a constitutively active form of IRF3. These studies have led to a model where group II residues are responsible for the dimerization and subsequent activation of IRF3 whereas group I residues play a regulatory role.

Dr. Fujita's group has generated an antibody that specifically recognizes phosphorylated Ser 386 (a group I residue) and shown that this residue is

phosphorylated in a virus dependent manner (Mori et al., 2004). The phosphorylated form of Ser386 is exclusively associated with the dimeric form of IRF3. Surprisingly, in studies conducted in mouse L929 fibroblast cells, it was shown that the constitutively active form of IRF3, IRF35D is phosphorylated at Ser 386. Further, mutation of group I residues to alanine in the IRF35D construct (IRF32A5D) abrogates the constitutive activity of this protein. These observations have led to the proposal that phosphorylation of group II residues leads to the sequential phosphorylation of group I residues which are important for the activity of IRF3. If this model were true, it would be expected that mutation of group II residues to alanine would abolish the phosphorylation of group I residues and subsequent dimerization and activation of IRF3. But in this study, IRF35A protein was phosphorylated at S386 at levels comparable to IRF35D protein. Further, IRF35A protein dimerizes normally in cells challenged with virus. Thus, this model might not be correct. Another explanation for the observed phosphorylation of group I residues in the IRF35A/D protein could be that the mutation of group II residues leads to some conformational changes in the protein such that the group I residues become better substrates for some unknown kinase. The observed 'normal' behavior of the IRF35A construct in this study is in contrast to the studies conducted in 293T cells, where, as discussed previously, the IRF35A construct cannot dimerize. There can be several reasons for the two groups reporting different observations. These groups have used different cell

lines in their studies and IRF3 might be regulated differently in the two cell populations. Difference in expression levels of the mutant constructs and structural or conformational perturbations as a result of extensive mutagenesis have made it difficult to interpret these results. Nonetheless, these studies support a role for group I and group II residues in the regulation of IRF3 activation.

Besides the immunoblotting based techniques used to detect the phosphorylated active forms of IRF3 in the above described studies, *in vitro* assays have been established to detect the activation of kinases that phosphorylate IRF3. In one of these studies, the *in vitro* kinase assay used a fragment of the IRF3 C-terminus (aa 375-427) fused to GST [GST-IRF3C (aa 375-427)] as a substrate and detected Newcastle disease virus (NDV) dependent phosphorylation of group I residues (Iwamura et al., 2001). Another study used a similar substrate [GST-IRF3C (aa 380-427)] to detect phosphorylation of IRF3 in response to stimulation with measles virus (tenOever et al., 2002). Virus dependent phosphorylation of this substrate occurred upon addition of whole cell extracts of measles virus stimulated cells. Mutation of group II residues to alanine resulted in a slight decrease in the signal dependent phosphorylation of the substrate. But mutation of group I residues to alanine almost completely abolished the phosphorylation of the substrate. This result shows that in addition to being phosphorylated specifically in virus infected cells, group I residues are important for the subsequent phosphorylation of group II residues. Based on these studies,

it has been proposed that phosphorylation of group I residues may be the priming step in IRF3 activation that facilitates the sequential phosphorylation of group II residues. Thus, *in vitro* kinase assays support a role of group I phosphorylation as the primary step in the activation of IRF3.

Two groups have attempted to solve the X-ray crystal structure of IRF3 to determine if the auto-inhibition model of IRF3 is relevant for its activation and to determine how phosphorylation regulates dimerization and subsequent activation of IRF3 (Qin et al., 2003; Takahashi et al., 2003). Both groups crystallized the C-terminus of IRF3 (aa173/175-427) and reported that IRF3 contains a β -sandwich core that resembles the Mad homology domain 2 (MH2) fold of the Smad protein family. Even though these groups have reported similar structures, they interpreted the data differently and proposed different mechanisms for activation of IRF3. Takahashi et. al. proposed a model where phosphorylation induces dimerization of IRF3 (Takahashi et al., 2003). They claim that the two subunits of IRF3 interact through a loop that contains group I residues of one subunit with a hydrophobic pocket on the other subunit. They suggest that rather than reversing intramolecular auto-inhibition, the phosphorylation of group I residues induces dimerization by increasing the interaction between the loop and hydrophobic pocket. On the other hand, Qin et. al. support the auto-inhibition model where phosphorylation of group I and group II residues result in conformational changes that lead to the unmasking of a hydrophobic active site that leads to the activation

of IRF3 (Qin et al., 2003). In spite of disagreement on the mechanism of activation of IRF3, both studies agreed on the accessibility of group I and group II residues for phosphorylation. Group I residues are present on the solvent-accessible turn, whereas the group II residues are packed within the structure of the protein. This observation has lent support to the possibility that phosphorylation of the accessible group I residues leads to the exposure of additional phosphorylation sites. The structure of IRF3 phosphorylated at group I and/or group II residues will provide a better understanding of the mechanism by which IRF3 is activated.

Our understanding of the regulation of IRF3 function and relative contribution of the two groups of Ser/Thr residues to this process would be vastly increased by identifying the kinase/kinases that phosphorylate group I and group II residues. Since several studies support the importance of group I residues in the activation of IRF3, we decided to use a biochemical fractionation approach to identify the kinase which phosphorylates these residues.

II. B. Materials and Methods

II. B. 1. Plasmids and antibodies

The C-terminal fragment of IRF3 (residue 375-427) was amplified using appropriate primers and cloned into the BamHI and EcoRI sites of the bacterial expression vector pGEX-4T1 such that N-terminal GST-tagged protein can be

expressed under the control of tac promoter. IRF3C2A and IRF3C5A mutants were generated by site-directed mutagenesis using the QuickChange kit (Stratagene).

Rabbit polyclonal antibody against IRF3 (SC-9082) and NEMO (SC-8330) were purchased from Santa Cruz Biotechnology. Rabbit polyclonal antibodies against IKKi and TBK1 were provided by Dr. T. Maniatis.

II. B. 2. Substrate purification

pGEX-4T1-GST-IRF3C, -IRF3C2A and -IRF3C5A constructs were transformed into E.coli BL21 pLys cells. Cultures of these cells were induced with 1mM isopropyl b-D-thiogalactoside (IPTG) and allowed to express protein for 4 hours at 37°C. Cells were harvested and after lysis by mild sonication, the bacterial lysate was cleared by centrifugation at 10,000xg for 10 minutes and applied to Glutathione Sepharose 4B (Amersham). After 3 washes, the fusion proteins were eluted with 10mM glutathione. An aliquot of purified proteins was run on SDS-PAGE gels to confirm the purity of the sample.

II. B. 3. Cell Culture and preparation of lysates

Human embryonic kidney (HEK) 293 cells were cultured in DMEM supplemented with 10% calf serum and antibiotics. Cells were infected with Sendai virus (Cantell strain; Charles River laboratories) for 20 hours at 50

hemagglutinating (HA) units/ml culture media. Briefly, cells in 10cm dishes were washed once with 1X PBS and incubated with 5 ml of Sendai virus diluted in serum free DMEM. One hour later, an equal volume of DMEM supplemented with 20% calf serum and antibiotics was added to the cells. Cells were returned to the 37°C incubator to continue culture for 17-19 hours. For the time-course study, the 21 hour time-point was started followed by the 17 hour, 12 hour and 9 hour time-points. The cell cultures corresponding to different time-point were harvested together at the end of the time-course.

P100 pellets were prepared as described previously (scheme as shown in Figure 9a). Briefly, cells that were either mock infected or infected with Sendai virus were suspended in Buffer A (20mM HEPES, pH 7.7, 1.5mM MgCl₂, 10mM KCl, 0.25M sucrose, 0.1mg/ml leupeptin, 1mM PMSF, and 1mM sodium orthovanadate). Cells were disrupted by dounce homogenizer and the homogenate was centrifuged at 1000xg for 5min in order to pellet nuclei and unbroken cells. The post-nuclear supernatant (S1) collected from the previous step was further centrifuged at 20,000xg for 10 minutes to obtain the soluble S20 and insoluble P20 fraction. To obtain the P100 pellet, the S20 fraction was centrifuged at 100,000xg for 30 min. The P100 pellet was resuspended in buffer A and disrupted by repeated pipetting or with a motor driven pellet pestle.

Detergent containing buffers used for cell lysis included – 0.2 % NP-40 lysis buffer (Buffer B: 20mM Tris-HCl, pH 7.5, 20mM β -glycerophosphate, 1mM

sodium orthovanadate, 0.5mM EGTA, 10% glycerol, 1.5mM MgCl₂, 150mM NaCl, 0.2% NP-40, 1mM PMSF, 1mM DTT, 10µg/ml leupeptin), 1% Triton X-100 lysis buffer (Buffer C: 20 mM Tris-HCl, pH 7.5, 150 mM NaCl, 10% glycerol, 1% Triton X-100, 1 mM DTT, 1 mM PMSF and 10 µg/µl leupeptin), and high salt lysis buffer (Buffer D: 20mM Tris-HCl, pH 7.5, 20mM β-glycerophosphate, 1mM sodium orthovanadate, 0.5mM EGTA, 10% glycerol, 1.5mM MgCl₂, 0.5M NaCl, 0.1% NP-40, 1mM PMSF, 1mM DTT, 10µg/ml leupeptin, 50U/ml benzonase). Soluble extracts were collected by centrifugation at 20,000xg for 15 minutes at 4°C.

II. B. 4. Kinase assays

***In vitro* IRF3 kinase assay:** S20/P100 pellets, as indicated, were used as the source of IRF3 kinase and incubated with kinase reaction buffer (Buffer E) containing GST-IRF3C/GST-IRF3C2A/GSTIRF3C5A (100 µg/ml), ATP (100 µM) and γ-³²P-ATP (5 µCi) for 30 minutes at 30°C. These reactions were subjected to SDS-PAGE and the phosphorylation of GST-substrates was analyzed by PhosphorImaging. ImageQuant software was used to quantitate the intensities of the phosphorylated bands.

IKK/TBK1 IP kinase assays: For IKK kinase assay, cells were lysed in Buffer C (20 mM Tris-HCl, pH 7.5, 150 mM NaCl, 10% glycerol, 1% Triton X-100, 1 mM DTT, 1 mM PMSF and 10 μ g/ μ l leupeptin), and the lysates cleared at 20,000xg for 15 minutes at 4°C. 500 μ g of lysate was incubated with anti-NEMO, anti-IKKi or anti-TBK1 antibody, as indicated, at 4°C for immunoprecipitation. After 1 hour, 10 μ l of protein A/G bead slurry was added. Immunoprecipitation was carried out for another hour. The beads were washed twice with buffer C and then three times with Buffer F (20 mM HEPES, pH 7.6, 50 mM NaCl, 20 mM β -glycerophosphate, 1 mM sodium orthovanadate, 10 mM $MgCl_2$ and 1 mM DTT). The beads containing the immunoprecipitated IKK complex were incubated in 10 μ l Buffer E (containing GST-IRF3C substrates or GST-I κ B α -NT, N-terminal 36 residues of I κ B α). After SDS-PAGE, the phosphorylation of the substrates was analyzed by PhosphorImaging.

II. B. 5. Glycerol gradients

P20 (600 μ g) or P100 pellets (300 μ g) were applied to a 2ml, 10-40% glycerol gradient in buffer G (20 mM Tris-HCl, pH 7.5, 150 mM NaCl). After centrifugation at 100,000xg for 3hr in a Beckman TLA-100.3 rotor at 4°C, 10 fractions of 200 μ l each were collected. These fractions were concentrated to 25 μ l

and after buffer exchange with buffer G, 1µl of each fraction was used in the IRF3 kinase assay.

II. C. Results

II. C. 1. Assay for detecting IRF3 C-terminus phosphorylation

The first step in the biochemical purification of the virus inducible IRF3 kinase involved the establishment of an *in vitro* kinase assay. This assay was used to follow the IRF3 kinase activity in lysates prepared from virus infected cells and fractionated by various methods. We set two criteria that the relevant IRF3 kinase should satisfy in the *in vitro* assay. The first criterion was inducibility, i.e. the kinase activity should be stimulated in response to viral infection. The second criteria was specificity, i.e the activity should specifically phosphorylate group I Ser residues. Our assay was based on a previously reported assay that described an *in vitro* assay to detect IRF3 kinase activity in Hela cells infected with Newcastle disease virus (NDV) (Iwamura et al., 2001). The substrate used in this assay was a GST-tagged C-terminal fragment of IRF3 (aa 375-427). Using this assay, a kinase activity, that could phosphorylate the group I Ser residues was detected in the P100 pellet. No further characterization or biochemical purification of this activity was reported.

NDV belongs to the paramyxovirus family of viruses but is not readily available commercially. Thus, to infect cells, Sendai virus, another member of

the paramyxovirus family, which can be purchased in large quantities from commercial sources, was used. Virus infection leads to the activation of IRF3 in both Hela cells and 293 cells. Since, in our laboratory, efficiency of transfection of plasmids and siRNA pairs in 293 cells is better when compared with Hela cells, 293 cell lysates were used in the *in vitro* assay.

An important step in establishing an *in vitro* assay is the choice of substrate. In *in vitro* assays, non-specific kinases, which do not phosphorylate the substrate *in vivo*, might be able to phosphorylate the substrate protein. Full length substrate protein might provide certain structural and regulatory constraints such that only a specific kinase is able to phosphorylate the protein. IRF3 has multiple phosphorylation sites at its N-terminus and C-terminus. The N-terminus of IRF3 is constitutively phosphorylated in cells such that on western blot analysis of unstimulated cells, two bands corresponding to IRF3 are observed (Servant et al., 2001). The identity of the exact IRF3 N-terminal residue that is phosphorylated has not been determined. The role of N-terminal phosphorylation for the function of IRF3 is also not clear. Further, the N-terminal phosphorylation of IRF3 in the *in vitro* assay could complicate the purification of the virus inducible group I kinase. Thus, the GST-tagged C-terminus of IRF3 (52 residues, aa 375-427, termed GST-IRF3C), which contains both the group I and group II residues, was used as a substrate in the IRF3 kinase assay (Figure 6b). Further, a previous study could detect a virus inducible IRF3 kinase activity using the same substrate.

Substrates with mutations in either the group I residues (GST-IRF3C2A, where Ser385/386 are replaced with alanine) or group II residues (GST-IRF3C5A, where Ser396/399/402/405 and Thr404 are replaced by alanine) were also generated (Figure 6b) (tenOever et al., 2002).

When Sendai virus was used to stimulate 293 cells, a virus inducible IRF3 kinase activity was detected in the P100 fraction of cells that had been infected with virus for 12 hours (Figure 7; a 3.6 fold induction over basal activity in virus stimulated P100; compare lanes 2 and 3). Thus, the activity detected by the *in vitro* assay satisfied our first criteria of being a virus-inducible.

Figure 7

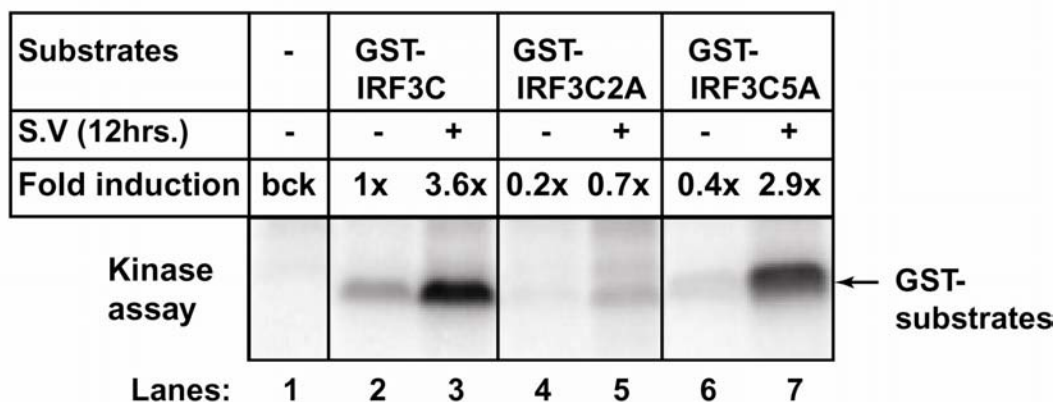


Figure 7: *In vitro* IRF3 kinase assay

Equal volumes of P100 pellets from cells that had either been mock-infected (-) or infected with Sendai virus (S.V) for 12 hours (+) were incubated with the indicated GST-IRF3C substrates and γ - 32 P-ATP. The assay reactions were subjected to SDS-PAGE and the intensities of the phosphorylated bands

were quantitated. The basal phosphorylation of GST-IRF3C substrate in mock-infected P100 reaction was quantitated (lane 2) and arbitrarily set as 1 unit. To obtain fold induction over basal activity, the band intensities of GST-IRF3C substrates were quantitated for lanes 3-7, and compared to lane 2. The values obtained are indicated. The quantitated band intensities were background (bck) corrected.

To determine the site specificity of the kinase activity, we performed *in vitro* assays with the GST-IRF3C2A and GST-IRF3C5A as substrates. The kinase activity phosphorylates the IRF3C5A substrate at levels comparable to the GST-IRF3C substrate (Figure 7). The basal activities detected with the GST-IRF3C and GST-IRF3C5A substrates are 1x and 0.4x respectively (Figure 7, compare lanes 2 and 6), and the virus stimulated activities are 3.6x and 2.9x respectively (Figure 7, compare lanes 3 and 7). IRF3C5A is probably not phosphorylated as well as the wild-type substrate because the wild-type substrate can be phosphorylated at both group I and group II residues. The IRF3C2A substrate on the other hand, is poorly phosphorylated (Figure 7). The basal activities detected with the GST-IRF3C and GST-IRF3C2A substrates are 1x and 0.2x respectively (Figure 7, compare lanes 2 and 4), and the virus stimulated activities are 3.6x and 0.7x respectively (Figure 7, compare lanes 3 and 5). Inability to detect a virus-dependent robust phosphorylation of the IRF3C2A substrate supports a model in which the group I residues are important for the subsequent phosphorylation of group II residues.

II. C. 2. Optimization of lysis conditions and time-course for the IRF3 kinase assay

The assay described above was carried out with cells disrupted by a dounce homogenizer. Detergents can also be used to efficiently disrupt the integrity of cellular membranes and to solubilize membrane proteins. In order to optimize the assay conditions, various methods of cell lysate preparation were tried. These included different detergent conditions such as 0.2% NP-40, 1.0% Triton X-100 and high salt lysis buffer (to obtain whole cell extract). A higher fold activation of virus inducible kinase activity was obtained when extracts were prepared in 0.2% NP-40 lysis buffer as compared to 1.0% Triton X-100 (Figure 8a; a 2 fold-induction over basal activity in NP-40 lysis buffer, compare lanes 1 and 2; a 1.4 fold-induction over basal activity in Triton X-100 buffer, compare lanes 5 and 6). When cells were lysed in the presence of 0.1% NP-40 and 0.5 M sodium chloride to obtain whole cell extract, a high basal activity was observed. There is no further increase in activity in virus infected lysates (Figure 8a; compare lanes 3 and 4). High salt can disrupt protein-protein interactions, therefore it is possible that the higher level of basal activation under high salt conditions is due to disruption of inhibitory interactions of the IRF3 kinase. Alternatively, it is possible that high salt conditions non-specifically activate the IRF3 kinase activity. The activity from NP-40 lysates satisfied both criteria of

Figure 8a

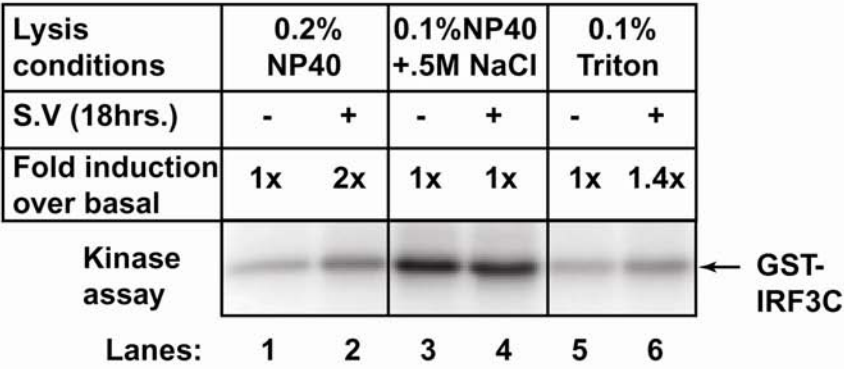


Figure 8b

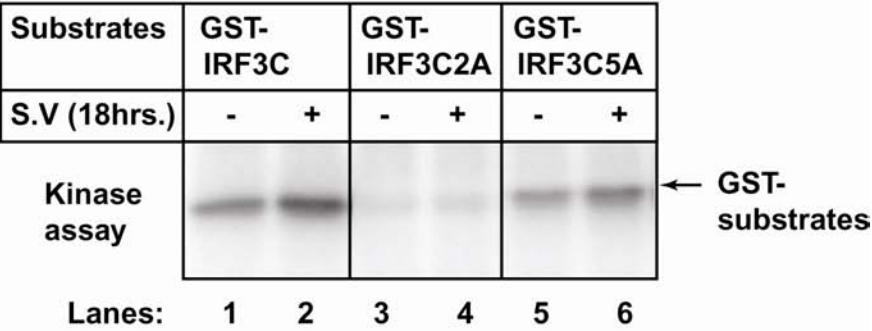


Figure 8c

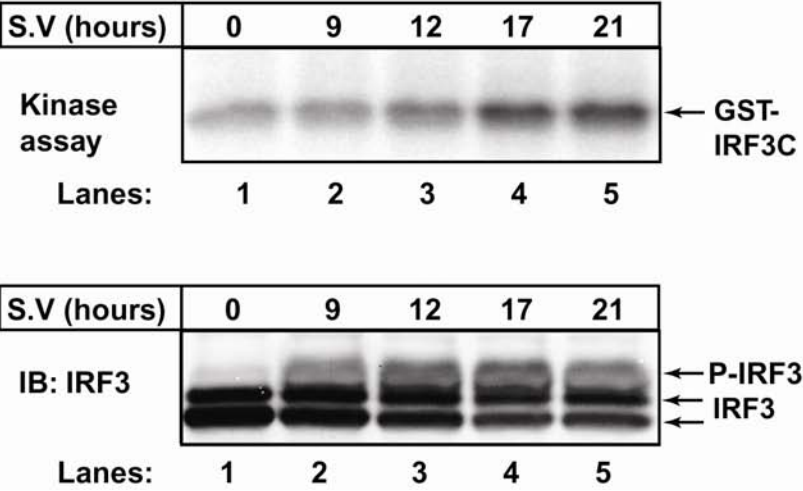


Figure 8: Optimization of *in vitro* IRF3 kinase assay

- (a) Equal number of cells were lysed in the different detergent conditions as indicated. Equal volumes of the extracts (1 μ l ~ 6-8 μ g protein) were used in the assay. For a particular detergent condition, the protein concentration of unstimulated (-) and Sendai virus (S.V) stimulated (+) extract was the same. To calculate the fold induction over basal activity, for each lysis condition, the intensity of the band corresponding to the unstimulated extract was arbitrarily set to 1, and compared to the band corresponding to the stimulated extracts. The values obtained are indicated.
- (b) Cells that were either mock-infected (-) or Sendai virus (S.V) infected, were lysed in 0.2% NP-40 containing lysis buffer. Equal amounts of lysates were incubated with GST-IRF3C substrates together with γ -³²P-ATP. The reactions were subjected to SDS-PAGE. The autoradiograph of assay reactions is shown.
- (c) *In vitro* IRF3 kinase assay was performed using lysates from cells infected with Sendai virus (S.V) for indicated time-points (upper panel). The same lysates were subjected to western blot analysis to determine the phosphorylation status of endogenous IRF3 (lower panel).

inducibility (Figure 8a) and specificity (Figure 8b), therefore this condition was used for the remainder of the project.

A time-course was performed to determine the optimum time required to detect the kinase activity. Kinase activation in *in vitro* assays was observed by 12 hours with maximal activation at 17-21 hours post-viral infection (Figure 8c, upper panel). A time-course to detect the phosphorylation of endogenous IRF3 in cells infected with virus revealed that phosphorylated forms of IRF3 could be detected as early as 9 hours (Figure 8c, lower panel) and persists for at least 21 hours. Thus, there was a delay in detection of kinase activity in the *in vitro* assay described above. One reason for the delayed detection of the kinase activity using

the *in vitro* assay could be due to lower sensitivity of the assay. Based on these results, further experiments were performed using lysates from cells that had been stimulated with virus for 18-20 hours.

II. C. 3. Fractionation of cell lysates by differential centrifugation

Next, we carried out differential centrifugation to determine the recovery of the kinase activity in P100 pellets (scheme showed in Figure 9a, upper panel). Most of the activity in the virus treated S1 fraction is retained in the S20 fraction (Figure 9a, lower panel, compare lane 2 and lane 4). When S20 is further centrifuged at 100,000xg, some of the activity remains in the soluble S100 fraction (Figure 9a, lower panel, compare lanes 4 and 8), whereas most of the activity pellets in the P100 fraction (Figure 9a, lower panel, lanes 4 and 10). Interestingly, we also detected a virus-independent IRF3 kinase activity in the P20 fraction (Figure 9a, lower panel, lanes 5 and 6). As described previously, most of the virus-inducible activity is recovered in the S20 fraction. Therefore, the P20 activity probably does not represent the observed inducible activity in S1. It is possible that a soluble inhibitory protein masks the P20 activity in the S1 fraction but the P20 activity become detectable upon the separation of soluble fraction. The activities detected in P20 and P100 could correspond either to two different kinases or to the same kinase. In the latter case, the P20 and P100 fractions could represent the same kinase which exists as two different populations with different

pelletting characteristics. Although we have not distinguished between the two possibilities, some initial characterization of these activities has been performed. Both the P20 and P100 activities are able to phosphorylate the GST-IRF3C5A substrate (Figure 9b; lanes 9-12) but poorly phosphorylate the GST-IRF3C2A

Figure 9a

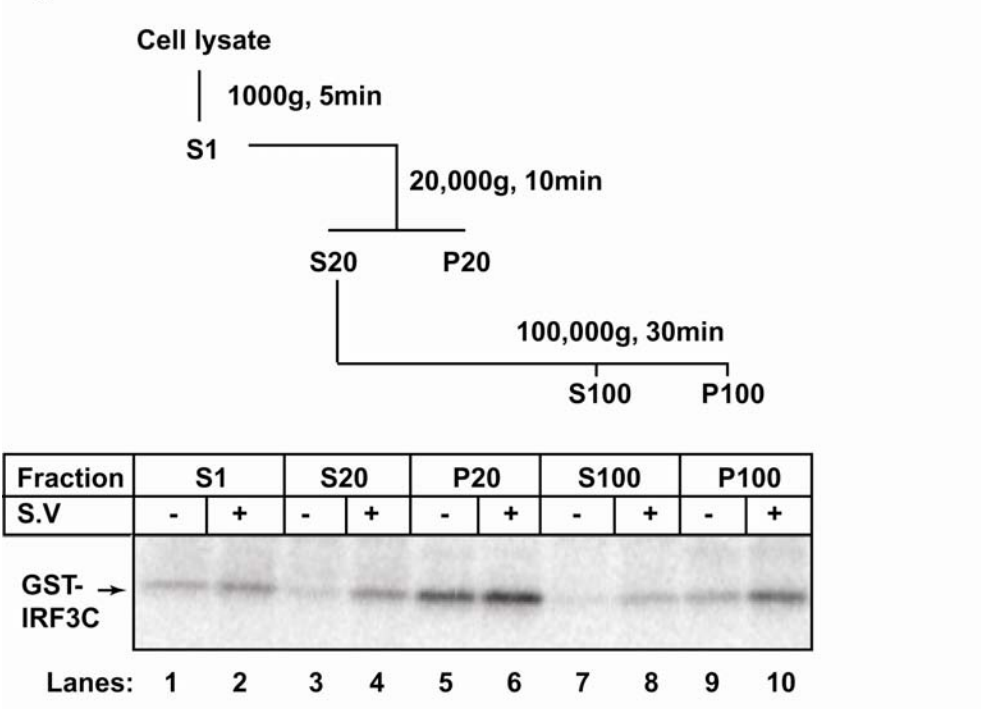


Figure 9b

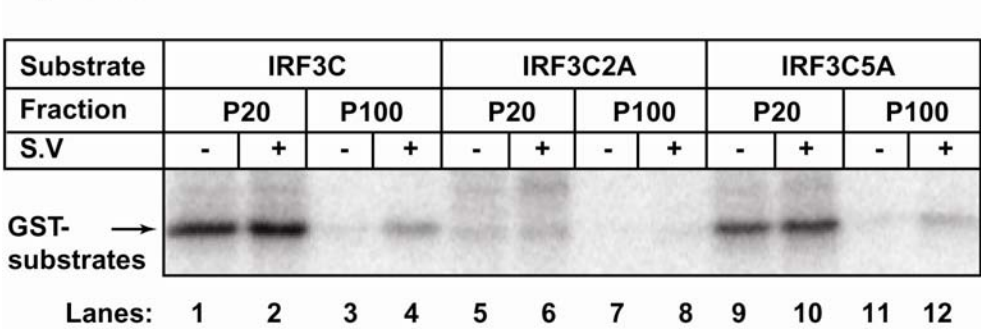


Figure 9: IRF3 kinase activity pellets in the P20 and P100 fractions

- (a) Cells that were either mock-infected (-) or Sendai virus (S.V) infected (+) were lysed in 0.2% NP-40 lysis buffer and subjected to differential centrifugation following the scheme shown in the upper panel. The volume of supernatant fractions, S1, S20 and S100 (1.1 ml) was approximately 4 times the volume in which the pellets were resuspended (0.3 ml). Therefore, to represent equivalent volume of supernatant and pellet in the assay, 4 times more volume of the supernatant (2 μ l) as compared to pellets (0.5 μ l) was used in the assay.
- (b) Equal volumes of P20 and P100 pellets from mock-infected (-) and (S.V) infected (+) cells were incubated with the indicated GST-IRF3C substrates. The reactions were subjected to SDS-PAGE. The autoradiograph of assay reactions is shown.

substrate (Figure 9b; lanes 5-8). Thus, both the fractions specifically phosphorylate the group I residues.

In order to get an idea of the size of the kinase complexes, we applied P20 and P100 pellets from mock and virus-infected cells to 10-40% glycerol gradients. The virus-independent activity in P20 is enriched in fractions 4-7 which corresponds approximately to 20-30 % glycerol (Figure 10a). P100 activity is higher in extracts from cells that were infected with virus as compared to the basal activity detected in cells that were not infected. When these extracts are applied to the glycerol gradient, the un-stimulated and stimulated kinase activities in P100 migrated in a similar fashion and enriched in fractions 5-8 which corresponds approximately to 20-30% glycerol (Figure 10b). On a 10-40% glycerol gradient, the 20S subunit of the proteasome and the 26S proteasome migrate to fraction 3

and fraction 8 respectively. Thus, the P20 and P100 activities migrate as large protein complexes with a size approximately between 20S and 26S.

Figure 10a

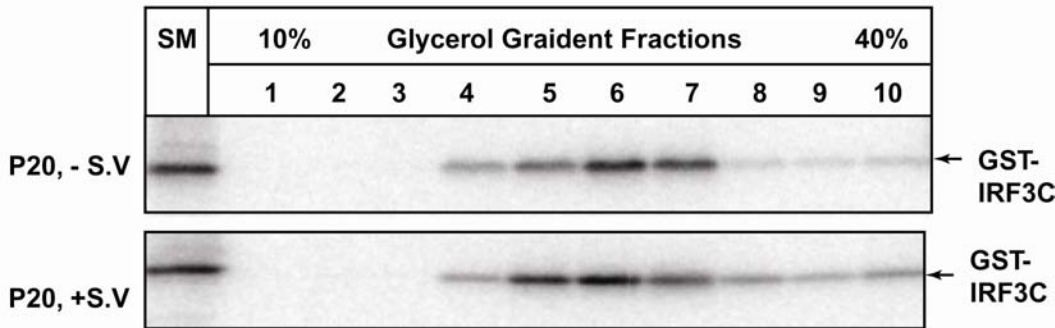


Figure 10b



Figure 10: Fractionation of the IRF3 kinase activity on glycerol gradients P20 (Figure 10a) and P100 (Figure 10b) from mock-infected (-S.V, upper panels) and Sendai virus infected (+S.V, lower panels) were applied to a 2 ml 10-40% glycerol gradients. 10 fractions were collected and the location of IRF3 kinase activity was determined in each fraction. The activity in the starting material (SM) is shown.

II. C. 4. Fractionation of P100

Since the virus-dependent IRF3 kinase activity is detected in P100, small scale fractionation of this fraction using various ion exchange and sizing columns was attempted. A major problem encountered was the generation of sufficient starting material for fractionation. For example, from one 15 cm dish of 293 cells infected with virus, we routinely obtained 400-500 μ g of total protein in the P100. To have sufficient material for mass spectrometry at the end of the fractionation protocol, at least 200mg-300mg of P100 corresponding to over 400-500 dishes was required. In the absence of sufficient starting material, attempts to fractionate P100 were suspended.

II. C. 5 TBK-1 and IKKi phosphorylate group II residues

Besides a biochemical approach to identify the kinase that phosphorylates IRF3, a candidate approach was also undertaken. It was known that viruses activate the IKK kinase complex (IKK α , IKK β and IKK γ) to stimulate the NF- κ B pathway. An attempt was made to test if IKK or its homologs, IKKi and TBK1 phosphorylate IRF3.

Purified IKK α and IKK β proteins (provided by Dr. Li Deng, Dr. James Chen's laboratory) were used in an *in vitro* assay with GST-IkB α or GST-IRF3C as substrates. Although IkB α is phosphorylated by these kinases, IRF3 C-terminus was not (Figure 11a). IKK immunoprecipitation assays were tried to

determine whether endogenously activated IKK could phosphorylate IRF3. As a control for the IKK immunoprecipitation assay, C6 cells (293T cells stably expressing IL-1 β receptor) were stimulated with IL-1 β for various time-points. As shown in Figure 11b, the IKK immunoprecipitated from these cells is able to phosphorylate the GST-I κ B α substrate (lanes 2-4). Next, the IKK complex was immunoprecipitated from 293T cells stimulated with virus for 12 to 24 hours. As shown in Figure 11b, the IKK complex immunoprecipitated from virus-stimulated cells is able to phosphorylate I κ B α (lanes 5-7) but not IRF3 (lanes 9-11). Thus, IKK complex is not the IRF3 kinase.

Antibodies provided by Dr. T. Maniatis were used to immunoprecipitate IKKi and TBK1 from virus infected cells. Although both these kinases are able to phosphorylate the IRF C-terminus, these kinases were not activated in a virus-dependent manner (Figure 11c). When immunoprecipitated IKKi is incubated with IRF3C2A and IRF3C5A substrates, it phosphorylates IRF3C2A but not IRF35A implying that IKKi is the group II residues kinase (Figure 11 d).

Soon after we performed these assays, two papers were published that established TBK1 and IKKi as the IRF3 kinases (Fitzgerald et al., 2003; Sharma et al., 2003). It has been shown that TBK1 and IKKi phosphorylate group II residues (McWhirter et al., 2004; tenOever et al., 2004). MEF cells from TBK1 knock-out mice are defective in IRF3 phosphorylation by viruses (McWhirter et al., 2004). Although these data suggest that TBK1 and IKKi may be important

for IRF3 function, the identity of the virus-inducible group I kinase is still unknown.

Figure 11a

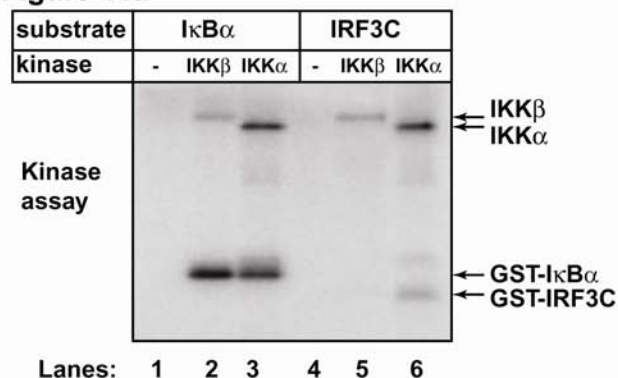


Figure 11b

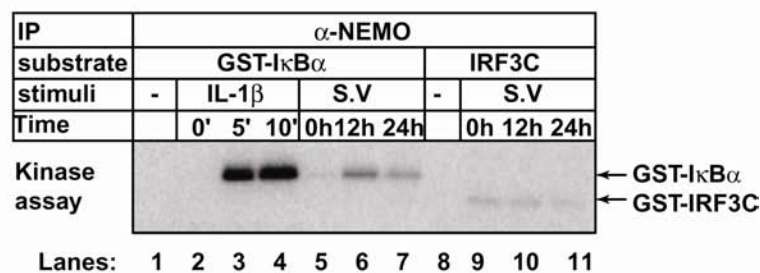


Figure 11c

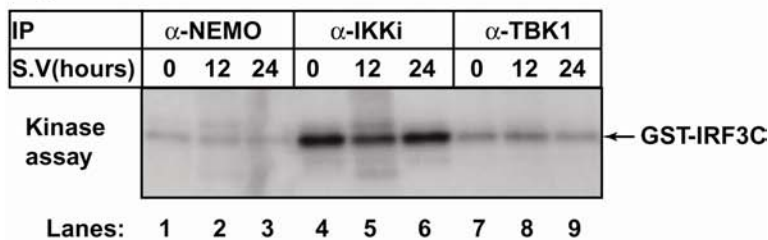


Figure 11d

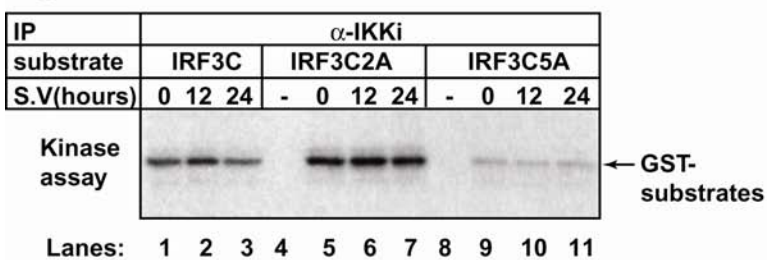


Figure 11: TBK1 and IKKi phosphorylate IRF3 group II Ser/Thr residues

- (a) Purified IKK α and IKK β kinases were incubated with GST-I κ B α (lanes 1-3) or GST-IRF3C substrates (lanes 4-6) as indicated, in an *in vitro* kinase assay. Phosphorylation of the substrates by the IKK kinases is shown.
- (b) Endogenous IKK complex was immunoprecipitated (IP) from cells that were either stimulated with IL-1 β (lanes 2-4) or with Sendai virus (S.V) (lanes 5-7 and 9-11) for different durations as indicated. The immunoprecipitated IKK complex was incubated with either GST-I κ B α (lanes 1-7) or GST-IRF3C (lanes 8-11) in an *in vitro* assay. Phosphorylation of the substrates by the IKK complex is shown.
- (c) The IKK complex (lanes 1-3), IKKi (lanes 4-6) and TBK1 (lanes 7-9) kinases were immunoprecipitated (IP) from cells challenged with Sendai virus (S.V) for different time-points and incubated with GST-IRF3C substrate in an *in vitro* kinase assay. Phosphorylation of the substrates by the kinases is shown.
- (d) IKKi was immunoprecipitated (IP) from cells challenged with Sendai virus (S.V) for different time-points and incubated with different GST-IRF3C substrates in an *in vitro* kinase assay. Phosphorylation of the substrates by the kinase is shown.

II. D. Discussion

In vitro kinase assays have been routinely used to detect the activation of endogenous kinases like IKK and MAPK in response to various stimuli (Wang et al., 2001). This chapter describes the establishment and optimization of an *in vitro* assay to detect the activation of an IRF3 kinase in Sendai virus infected 293 cells. The activity detected in this assay specifically phosphorylated the IRF3 group I serine residues. The kinetics of this activity *in vitro* was similar to the kinetics of endogenous IRF3 phosphorylation in cells challenged with Sendai virus.

The GST-tagged C-terminus of IRF3 was used as a substrate to follow the virus inducible kinase *in vitro*. Non-physiologic kinases might be able to phosphorylate the truncated form of IRF3. Thus, once the identity of the group I kinase is determined, the ability of this kinase to phosphorylate full length IRF3 should be determined. To further test the physiological importance of the identified IRF3 kinase, techniques like RNAi can be used to knock-down the expression of the kinase. In the absence of IRF3 kinase, phosphorylation of endogenous IRF3 in response to virus should be abolished.

The observation that the IRF3 kinase activity pellets in the P100 fraction of lysates centrifuged at 100,000xg is very interesting. It is not clear why the IRF3 kinase activity pellets in the P100 fraction. When cell lysates are spun at 100,000xg, plasma membrane, fragments of endoplasmic reticulum and large protein complexes including polyribosomes pellet. Therefore, it is possible that either the IRF3 kinase activity associates with some membranous compartment of cells, or it is associated with a large multiprotein complex. Several viruses including hepatitis C virus replicate in close association with membranous organelles such as the ER (Rehermann and Nascimbeni, 2005). It is possible that the IRF3 kinase localization to these membranous organelles enables rapid activation of IRF3 which in turn activates the antiviral signaling pathways. Nonetheless, separation of the kinase activity from the soluble cytosolic proteins in S100 is a good step for protein purification (Figure 9a, lower panel, 20-25 fold

purification). Besides the virus-inducible IRF3 kinase activity in P100, a virus-independent IRF3 kinase activity is detected in the P20 pellet. At 20,000xg, organelles such as the mitochondria, lysosomes and peroxisomes pellet. Since the P20 kinase activity is independent of virus stimulation, it is possible that this activity corresponds to a non-physiologic IRF3 kinase. Nonetheless, it might be informative to purify this activity as it specifically phosphorylates the group I residues. The P20 kinase activity could be the same kinase as in the P100 pellet or a distinct activity.

The purification of the IRF3 kinase activity from virus-stimulated extracts should be pursued. Difficulties were encountered in generating sufficient starting material from adherent 293 cell cultures to scale up the fractionation of the IRF3 kinase activity in P100 from virus infected cells. Since it is relatively easier to grow suspension cell cultures in large volumes, an attempt can be made to grow and virally infect 293 T cells or Hela cells in suspension cultures. Alternatively, viral infection of macrophage cell lines like THP1 and RAW cells, that grow as suspension cells can be tried.

Recently, TBK1 and IKKi have been identified as the kinases responsible for phosphorylating IRF3 in response to viruses (Fitzgerald et al., 2003; Sharma et al., 2003). Assays conducted with purified TBK1/IKKi proteins have shown that these kinases directly phosphorylate the group II residues (McWhirter et al., 2004; tenOever et al., 2004). In macrophages, both TBK1 and IKKi are expressed and

function redundantly to activate IRF3. On the other hand, in MEF cells that predominantly express TBK1, activation of IRF3 depends solely on TBK1. Thus, in TBK1 deficient MEFs, IRF3 activation and IFN production in response to virus infection are compromised.

Although we have not been able to detect a virus-induced activation of TBK1 and IKKi, a recent study has shown that immunoprecipitated TBK1 and IKKi exhibit the ability to phosphorylate the IRF3 substrate in a virus-dependent manner (tenOever et al., 2004). These experiments were carried out in a lung fibroblast cell line, A549 that were infected with vesicular stomatitis virus.

In *in vitro* experiments, immunoprecipitated TBK1 and IKKi phosphorylate the IRF3C2A substrate, implying that TBK1 and IKKi can phosphorylate group II residues independent of the phosphorylation status of group I residues. This is in contrast to the assays conducted with virus stimulated lysates which presumably contain active TBK1/IKKi, where no phosphorylation of the group II residues is observed. The reason suggested for this observation was that the group II residues cannot be phosphorylated in the absence of phosphorylation of group I residues. It is therefore surprising that in the TBK1/IKKi immunoprecipitation assays we observe robust phosphorylation of IRF3C2A substrate. Since the mechanism of regulation of TBK-1/IKKi is not understood as yet, it is possible that in lysate, these kinases are regulated such that

they phosphorylate in a group I residue dependent manner but this regulation is lost in immunoprecipitated kinases.

Although, it is clear that TBK1/IKKi are necessary for the activation of IRF3, it is not clear whether they are sufficient. It is still possible that a kinase which phosphorylates group I residues is activated in response to viruses such that group II residues become more accessible to phosphorylation by TBK1/IKKi. The phosphorylation status of group I residues in TBK1 knock-out cells has not been determined. If the kinase responsible for phosphorylating group I residues is identified, we can answer questions related to the importance of group I residue phosphorylation for IRF3 activation. The expression of group I kinase can be knocked-out by RNAi and phosphorylation status of group II residues can be determined. If the group II residues cannot be phosphorylated in the absence of the group I kinase, it will support a role of group I residues as the priming phosphorylation step that facilitates the phosphorylation of group II residues. But if TBK1 and IKKi function independently of the group I residues *in vivo*, it will imply that phosphorylation of group II residues is sufficient for the activation of IRF3.

Besides virus, polyI:C and LPS that signal through TLR3 and TLR4 respectively also regulate the activity of TBK1/IKKi (Akira and Takeda, 2004). Rapid progress has been made in the identification of molecular components of the signaling pathways induced by these receptors. Recently, NAK-associated

protein 1 (NAP1) has been identified as a subunit of the TBK1/IKKi kinase complex that is required for TLR3-TRIF mediated activation of TBK1 and subsequent activation of IRF3 (Sasai et al., 2005). Further, RIG-I has been identified as the receptor for virally derived dsRNA that leads to the activation of IRF3 in a TBK1 dependent manner (Yoneyama et al., 2004). As discussed in the next three chapters, we have identified a novel mitochondrial protein termed MAVS that functions downstream of RIG-I to activate IRF3. As TRIF, RIG-I and MAVS can regulate the activation of IRF3, an *in vitro* assay can be established to detect the activation of IRF3 kinases. It is possible that purified recombinant TRIF, RIG-I or MAVS can activate the group I kinase and TBK1/IKKi in lysates from unstimulated cells. This assay can be used for two purposes, the identification of group I kinase from unstimulated lysate, and to identify unknown factors between the upstream TRIF, RIG-I and MAVS proteins to the downstream kinases. A similar strategy has been successfully used in Dr. Chen's laboratory to identify factors that regulate the activation of IKK activity by TRAF6 (Deng et al., 2000; Wang et al., 2001). Thus, the assay described in this chapter could be a useful tool for advancing our understanding of the antiviral signaling pathway.

CHAPTER III: IDENTIFICATION AND CHARACTERIZATION OF MAVS

III. A. Introduction

Two events required to trigger an effective antiviral innate immune response are: a) detection of the invading virus by immune system receptors; and b) initiation of protein signaling cascades that regulate the synthesis of IFNs. Toll-like receptors (TLRs) 3, 7, 8 and 9 are the major antiviral PRRs that recognize distinct types of virally-derived nucleic acids located in endosomes (Kawai and Akira, 2006a). In the presence of specific ligands, these receptors can activate signaling cascades that result in the induction of type I IFNs. Recently, retinoic acid inducible gene-I (RIG-I) has been identified as the cytosolic receptor for intracellular viral dsRNA (Yoneyama et al., 2004). The molecular components of the RIG-I mediated signaling cascade, which regulate the expression of type I IFNs, are not well characterized.

RIG-I is a member of the DExD/H box-containing RNA helicase family of proteins that unwind dsRNA in an ATPase-dependent manner. Based on the presence and characteristics of conserved motifs within the primary sequence, helicase proteins are classified into five superfamilies (Cordin et al., 2006). The DExD/H box containing proteins are included in superfamily 2 and contain eight conserved motifs that possess ATPase, helicase and RNA binding ability.

RIG-I was initially identified as a gene that is induced by retinoic acid and interferon in a cell line derived from a patient with acute promyelocytic leukemia (Sun, 1997). RIG-I was also upregulated by retinoic acid in a human gastric cancer cell line (Huang et al., 2000). Since retinoic acid exhibits anti-tumor activity by inducing differentiation of tumor cells, it was suggested that RIG-I could be involved in the regulation of cellular growth and differentiation. A later study revealed that in porcine cells, the porcine reproductive and respiratory syndrome virus (PRRSV), induced the expression of the porcine homolog of RIG-I, RNA helicase induced by virus (RHIV-1) (Zhang et al., 2000). Since RIG-I contains CARD domains in addition to the helicase domain, it was suggested that RIG-I might play a signaling role in response to a viral challenge. Finally, over-expression screening for proteins that can activate IRFs identified RIG-I as an important component of the antiviral signaling pathway (Yoneyama et al., 2004).

Based on several studies, a model for the mechanism by which RIG-I functions has been developed (Sumpter et al., 2005; Yoneyama et al., 2004). Briefly, the C-terminal helicase domain is believed to bind specifically to viral dsRNA. The N-terminal CARD domains serve to activate downstream signaling cascades once a viral infection has been detected by binding of viral dsRNA to the C-terminal helicase domain. As discussed in chapter I, over-expression of an N-terminal fragment of RIG-I containing the two CARD domains is sufficient to activate NF- κ B and IRF3 in the absence of a viral infection. Besides binding to

viral dsRNA, the helicase domain of RIG-I might also play a role in regulating the activity of the CARD domains. This suggestion is based on the finding that in contrast to the constitutive activation of downstream pathways by over-expression of the N-terminal CARD domains, over-expression of full-length RIG-I cannot activate these pathways. Full-length RIG-I is activated only in the presence of dsRNA. This result indicates that in the absence of dsRNA the helicase domain interferes with the activity of the CARD domains. It has been speculated that binding of dsRNA to the helicase domain leads to conformational changes that allow the CARD domains to signal. Further structural analysis will be required to determine the exact mechanism by which this regulation is achieved.

Melanoma differentiation-associated gene 5 (MDA-5) or Helicard is a close relative of RIG-I exhibiting 23 and 35% sequence identity to the N-terminal CARD and C-terminal helicase domains, respectively (Kang et al., 2002; Kovacsovics et al., 2002). Similar to RIG-I, the helicase domain of MDA-5 can bind dsRNA and its N-terminal CARD domains can signal to NF- κ B and IRF3 (Yoneyama et al., 2005). Data from MDA-5 knock-out mice support the importance of MDA-5 as an antiviral signaling protein (Gitlin et al., 2006; Kato et al., 2006). MDA-5 and RIG-I are responsible for sensing different kinds of viruses. RIG-I is essential for the production of interferon in response to RNA viruses like paramyxoviruses, influenza virus and Japanese encephalitis virus,

whereas MDA-5 is critical for detection of picornaviruses. The molecular basis for the identification of different viruses by RIG-I and MDA-5 is not understood.

A key unresolved question regarding RIG-I function pertains to the nature and identity of proteins that function downstream of the RIG-I CARD domains to activate NF- κ B and IRF3. CARD domains were initially identified as protein-protein interaction domains involved in the cell death pathway (Bouchier-Hayes and Martin, 2002). Further studies have identified several proteins that interact through their CARD domains and participate in the activation of NF- κ B in innate and adaptive immune responses. Based on these examples, it was hypothesized that the RIG-I CARD domains function by interacting with another CARD domain containing protein. This chapter describes the identification and characterization of a CARD domain containing protein termed MAVS, that functions downstream of RIG-I.

III. B. Materials and Methods

III. B. 1. Blast search and alignments

The amino acid sequences corresponding to the two CARD domains of RIG-I and MDA-5 were blasted individually against the National center of bioinformatics (NCBI) protein database. Clustal W (<http://www.ebi.ac.uk/clustalw/>) was used to align the CARD domains of RIG-I, MDA-5 and MAVS. The amino acid sequence of human MAVS protein was

blasted against the NCBI database to identify homologs of the protein in other species.

III. B. 2. Plasmids and antibodies

MAVS sequence was amplified by PCR using the IMAGE clone 5751684 (ATCC) as a template. PCR primers were based on GenBank accession number BC044952. The open reading frame of MAVS was cloned into the XhoI and MluI sites of the mammalian expression vector pEF-IRES-Puro such that N-terminal HA-tagged MAVS can be expressed under the control of EF1 α promoter. pcDNA3-FLAG-MAVS was constructed by cloning MAVS into the XhoI and XbaI sites of pcDNA3. pcDNA3-MAVS-HA was constructed by subcloning the DNA fragment encoding MAVS-HA into the XhoI and XbaI sites of the pcDNA3 vector such that the C-terminal HA epitope was fused in frame with MAVS. pcDNA3-MAVS-Flag was constructed by subcloning the DNA fragment encoding MAVS-Flag into the XhoI and XbaI sites of the pcDNA3 vector such that the C-terminal Flag epitope was fused in frame with MAVS. pEF-BOS-FLAG-RIG-I and RIG-I(N) were kindly provided by Dr. Takashi Fujita (Tokyo Metropolitan Institute of Medical Science). The reporter gene IFN β -Luc was constructed by subcloning 110 base pairs of the IFN- β promoter into a luciferase expression vector (Dr. Giridhar R. Akkaraju, Dr. James Chen's laboratory). All constructs were verified by automated DNA sequencing.

Plasmids for p- κ B₃-TK-Luc and pCMV-LacZ have been described previously. Plasmids for Gal4-Luc, Gal4-IRF3, Flag-TRIF, Flag-TBK1 and Flag-IKK ϵ were provided by Dr. Kate Fitzgerald (University of Massachusetts at Worcester) and Dr. Tom Maniatis (Harvard).

cDNA encoding amino acids 1-242 of RIG-I was amplified by PCR and cloned into the XhoI and MluI sites of the baculoviral expression vector pFastBac (Invitrogen). For the expression of a MAVS protein fragment containing residues 131-291, the cDNA encoding this fragment was inserted into the NdeI and BamHI sites of pET14b (Novagen). These constructs were used to express recombinant proteins His₆-RIG-I (1-242) in Sf9 cells, and His₆-MAVS (131-291) in *E. coli*. The antibodies against RIG-I and MAVS were generated by immunizing rabbits with the recombinant proteins. Both antibodies were affinity purified using the respective RIG-I and MAVS antigen column. Rabbit polyclonal antibody against IRF3 (SC-9082) and NEMO (SC-8330) were purchased from Santa Cruz Biotechnology. Monoclonal antibody against IKK β (BD Bioscience), FLAG (M2; Sigma) and HA.11 (Covance) were purchased from the indicated suppliers.

III. B. 3. Cell culture and Luciferase assays

Human embryonic kidney (HEK) 293 cells were cultured in DMEM supplemented with 10% calf serum and antibiotics. Transient transfection was

carried out using the calcium phosphate precipitation method. For luciferase reporter assays, cells were seeded in 12-well plates at a cell density of 2×10^5 cells per well. On the second day, cells were co-transfected with 20 ng of a luciferase reporter gene, 20 ng of pCMV-LacZ as an internal control for transfection efficiency and the indicated expression vectors. For the IRF3 activation assay, 40 ng of Gal4-IRF3 and 40 ng of Gal4-Luc constructs were co-transfected. Each experiment was carried out in duplicates. Cells were harvested 36 hours after transfection and lysed in the passive lysis buffer (Promega). Luciferase activity was measured with a luminometer (Rosys Anthos Lucy2) using luciferin as a substrate, and β -galactosidase activity was measured with a Thermo Labsystems microplate reader at the wavelength of 405 nm using o-nitrophenyl- β -D-galactopyranoside (ONPG) as a substrate.

III. B. 4. RNAi

siRNA oligos at a final concentration of 20 nM were transfected into HEK293 cells in 12-well dish, using the calcium phosphate precipitation method. This transfection procedure was repeated on the second day to increase RNAi efficiency. On the third day, cells were transfected with indicated expression plasmids using Lipofectamine 2000 reagent (Invitrogen), and harvested 24 hours later. The sequences of the siRNA oligos are as follows (only the sense strands are shown): GFP (471-489): GCAGAAGAACGGCAUCAAG; RIG-I (2363-

2381): AAUUCAUCAGAGAUAGUCA; MAVSa (899-917):
 CCACCUUGAUGCCUGUGAA; MAVSb (1364-1382):
 CAGAGGAGAAUGAGUAUAA and TBK1 (1047-1065):
 UCAAGAACUUAUCUACGAA. These RNA oligos were synthesized at the UT
 Southwestern Center for Biomedical Invention (CBI) facility.

III. B. 5. Western Blotting and IRF3 dimerization assays

Cells were lysed in Buffer B (as in chapter II; 20mM Tris-HCl, pH 7.5, 20mM β -glycerophosphate, 1mM sodium orthovanadate, 0.5mM EGTA, 10% glycerol, 1.5mM $MgCl_2$, 150mM NaCl, 0.2% NP-40, 1mM PMSF, 1mM DTT, 10 μ g/ml leupeptin). After incubation on ice for 10 minutes, soluble extract was collected by centrifugation at 20,000xg for 15 minutes at 4°C. 20 μ g of lysate was boiled in 2X SDS sample buffer followed by SDS-PAGE. Native gel electrophoresis and IRF3 dimerization assays were carried out as described previously (Iwamura et al., 2001). Briefly, 7% gels were pre-run with 25mM and 192mM glycine, pH 8.4 with and without 1% deoxycholate (DOC) in the cathode and anode chamber, respectively, for 30 min at 40mA. 20 μ g of cell lysate in Buffer B were diluted in 2X sample buffer (125mM Tris, pH 6.8, 20% glycerol and 10 μ g/ml bromophenol blue) and applied to gel followed by electrophoresis for 45 min at 25mA. For detection of MAVS in different cell lines, cells were lysed in RIPA buffer (50mM Tris-HCl, pH 8.0, 150mM sodium chloride, 1%

Triton X-100, 0.1% SDS and 0.5% sodium deoxycholate). Lysates were cleared by centrifugation at 14,000 rpm for 15 minutes, resolved by SDS-PAGE and immunoblotted with a MAVS antibody. Immunoblotting was carried out by standard procedures and immuno-reactive proteins were visualized by colorimetric detection of an alkaline phosphatase substrate.

III. B. 6. IKK kinase assay

For IKK kinase assay, cells were lysed in Buffer C (as in chapter II; 20 mM Tris-HCl, pH 7.5, 150 mM NaCl, 10% glycerol, 1% Triton X-100, 1 mM DTT, 1 mM PMSF and 10 $\mu\text{g}/\mu\text{l}$ leupeptin), and the lysates cleared at 20,000xg for 15 minutes at 4°C. 500 μg of lysate was incubated with anti-NEMO antibody at 4°C for immunoprecipitation. After 1 hour, 10 μl of protein A/G bead slurry was added. Immunoprecipitation was carried out for another hour. The beads were washed twice with Buffer C and then three times with Buffer F (as in chapter II; 20 mM HEPES, pH 7.6, 50 mM NaCl, 20 mM β -glycerophosphate, 1 mM sodium orthovanadate, 10 mM MgCl_2 and 1 mM DTT). The beads containing the immunoprecipitated IKK complex were incubated in 20 μl of the kinase reaction buffer (Buffer E; as in chapter II) containing GST-I κ B α -NT (100 $\mu\text{g}/\text{ml}$; N-terminal 36 residues of I κ B α), ATP (100 μM) and γ - ^{32}P -ATP (5 μCi)

for 30 minutes. After SDS-PAGE, the phosphorylation of I κ B α was analyzed by PhosphorImaging.

III. B. 7. Viral infection and plaque assay

Sendai virus infection: Cells were infected with Sendai virus (Cantell strain; Charles River laboratories) for 20 hours at 50 hemagglutinating (HA) units/ml culture media. Briefly, cells in 12-well plates were washed once with 1X PBS and incubated with 0.5 ml of Sendai virus diluted in serum free DMEM. One hour later, an equal volume of DMEM supplemented with 20% calf serum and antibiotics was added to the cells. Cells were returned to the 37°C incubator to continue culture for 19 hours.

VSV infection and plaque assay: For over-expression of MAVS, HEK293 cells in 12-well plates were transfected with 0.5 μ g of pCDNA3-Flag-MAVS or empty vector. To silence the expression of MAVS, HEK293 cells were transfected with 20 nM of MAVS or GFP (control) siRNA oligos. These cells were infected with VSV (kindly provided by Dr. Michael Gale, UT Southwestern) at 0.001, 0.01, and 0.1 MOI for 24 hours. Cells were rinsed with PBS, fixed in 2% formaldehyde in PBS, and stained with 0.1% Amido Black in 10% acetic acid. For plaque assay, aliquots of culture media taken at 6, 12, 18, and 24 hours were used to infect HEK293 cells. Briefly, 293 cells in 6-well plates were infected with serial

dilutions of the recovered viruses for 1 hour. Cells were overlaid with 0.5% soft agar in DMEM and incubated for 24 hours. Plates were stained with 0.01% neutral red in DMEM for 4 hours to display plaques, which were then quantitated.

III. C. Results

III. C. 1. Search for a RIG-I CARD domain containing proteins

A bioinformatics approach was used to identify proteins that contain a CARD domain similar to those of RIG-I and its homologue MDA-5. A BLAST search with the first CARD domain of MDA-5 identified an uncharacterized protein KIAA1271 (Figure 12a, 12b). Interestingly, this protein was also identified as a putative NF- κ B activator in a large scale over-expression screening for proteins that activate an NF- κ B reporter (Matsuda et al., 2003). However, there was no further characterization of the domain structure, activity or biological function of the protein. The CARD domain of this protein is conserved from pufferfish to human (Figure 12c). Based on its biological function as an antiviral protein (discussed below) and the importance of mitochondrial localization for the function of this protein (discussed in chapter V), we termed this protein mitochondrial antiviral signaling protein (MAVS).

Figure 12a

```

MAVS 10-77      KYICRNFSN--FCNVDVVEILP-YLP-CLTARDQDRLRATCTLSGNRDTLWHLFNTLQR-
RIG-I (1) 6-78  RRSLLQAFQDYIRKTLDPITYILS-YMAPWFREEEVQYITQAEKNNKGPMEEATLFTKFLLEL
RIG-I (2) 104-176 RLLLRKRLQPEFKTRIIPDTIIS-DLSECLINQECCEILQICSTKGMMAGAEEKVECLLRS
MDA-5 (1) 12-84  RYLISCFRARVKMYIQVEPVL-D-YLT-FLPAEVKEQIQRTVATSGNMQAVELTSTLEKG
MDA-5 (2) 116-186 -QLLNLLQPTLVDKLLVRDVLDDKCMEEELTIEIDRNRIAAAENNGNESGVRELTKRIVQ-

MAVS 10-77      --RPGWVEYFIAALR
RIG-I (1) 6-78  Q-EEGWFRGFLLDALD
RIG-I (2) 104-176 D-KENWPKTLKLALE
MDA-5 (1) 12-84  VWHLGWTRBEFVEALR
MDA-5 (2) 116-186 --KENWFSAEFLNVLR

```

Figure 12b

```

1  mpfaedktyk yicrnfsnfc nvdvveilpy lpcltardqd rlratctls g nrdtlwhlfn
61  tlqrrpgwve yfiaalgce lvdladevas vyqsyqprts drppdplepp slpaerpgpp
121 tpaahsipy nscreeksy pmpvqetgap espgenseqa lqtlspraip rnpdggples
181 ssdlaalspl tssghqeqdt elgsthtaga tssltpsrgp vspsvsfqpl arstprasrl
241 pgptgsvvst gtsfsssspg lasagaaegk qgaesdqaep iicssgaeap anslpskvpt
301 tlmvpntval kvpanpasvs tvpsklptss kppgavpsna ltnpapsklp instragmvp
361 skvptsmvlt kvsastvptd gssrneetpa aptpagatgg ssawldsse nrglselsk
421 pgvlasqvds pfsgcfedla isastslgm pchgpeeney ksegtfghv aenpsiqlle
481 gnpggpadpd ggprpqadrk fqerevpchr pspgalwlvq avtgvlvvtl lvvlyrrrlh 540

```

Figure 12c

```

Human 10-77      KYICRN-----FSNFCNVDVVEILPYLPCLTARDQDRLRATCTLSGNRDTLWHLFNTLQ*
Dog 43-116      KELTDNPIYNCKLCNFGRIHVLEILPYLSCLTASDQDRLRASYQLWGNQGT LWELFNSLR
Mouse 10-77      KYIRDN-----HSKFCQVDVLEILPYLSCLTASDQDRLRASYRQIGNRDTLWGLFNNLQ
Rat 10-77       KYIRYN-----HSKFCQVDVLEILPYLSCLTASDQDRLRASYKQLCNGGT LWELFNTLQ
Chicken 10-77   NHILRN-----MSRFCDIHVASLVDSLSCLTDADRDELHTRQDMRGIRATAYK FYQHDK
Pufferfish 1-63 -----MPTIVSTVQVITQIIPYLPCLTDHRENI EAKREMYGNFDSMVL LLDCLK

***
Human 10-77      RRPGWVEYFIAALR
Dog 43-116      RRTGWVESFIKALR
Mouse 10-77      RRPGWVEVEIRALQ
Rat 10-77       RRPGWVEVEIRALR
Chicken 10-77   CRKGVVMDLINALH
Pufferfish 1-63 RRENWPEEEISALE

```

Figure 12: Identification of MAVS and its sequence analysis

- Sequence alignment of the CARD domains of MAVS, RIG-I and MDA-5, using the Clustal W program.
- The primary amino acid sequence of MAVS is shown. MAVS contains 540 amino acid residues. The CARD domain region of MAVS is highlighted in pink, the proline-rich (PRO) domain is highlighted in blue and the transmembrane (TM) domain is highlighted in yellow.
- The sequence alignment of the CARD domains of MAVS from different species based on the genome project. The asterisks (*) indicates the conserved residues that were mutated to alanine in Figure 21.

III. C. 2. Over-expression of MAVS leads to activation of IRF3 and NF- κ B

Although NF- κ B is activated by over-expression of several proteins, a much smaller number of proteins activate both NF- κ B and IRF3, which are required for the induction of IFNs. To determine if MAVS could activate NF- κ B and IRF3, a MAVS expression plasmid was transfected into 293 cells together with an IFN- β reporter in which the expression of luciferase is under the control of the IFN- β promoter. The IFN- β promoter contains enhancer elements that bind to several transcription factors including NF- κ B, IRF3 and ATF2. The coordinated activation of all of these transcription factors is required for the formation of a stereospecific enhanceosome that activates IFN- β .

Significantly, over-expression of MAVS in HEK293 cells potently activates the IFN- β promoter (Figure 13a). In control experiments, infection of the same cells with the Sendai virus, a positive strand RNA virus of the paramyxoviridae family, leads to the activation of IFN- β . Similarly, over-expression of the N-terminal CARD domains of RIG-I, but not another CARD domain protein RIP2, induced IFN- β . Consistent with the ability of MAVS to activate the assembly of the IFN- β enhanceosome, MAVS activated NF- κ B (Figure 13b) as well as IRF3 (Figure 13c). In the former case, NF- κ B activation

Figure 13a

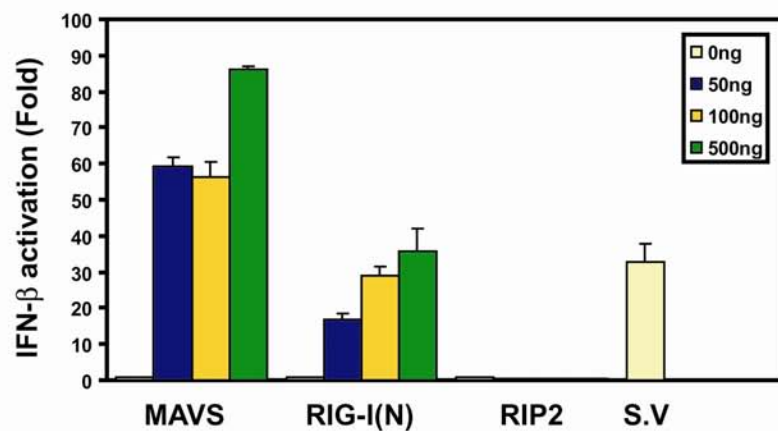


Figure 13b

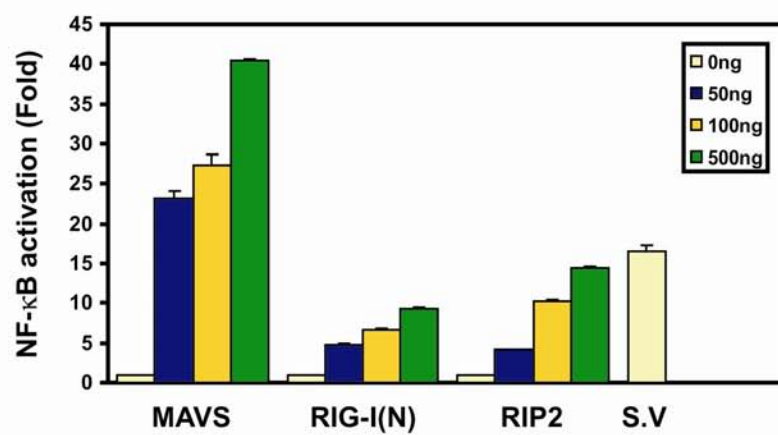


Figure 13c

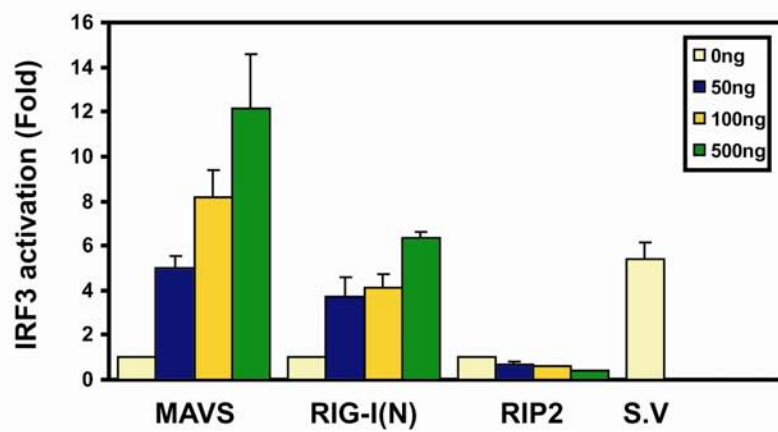
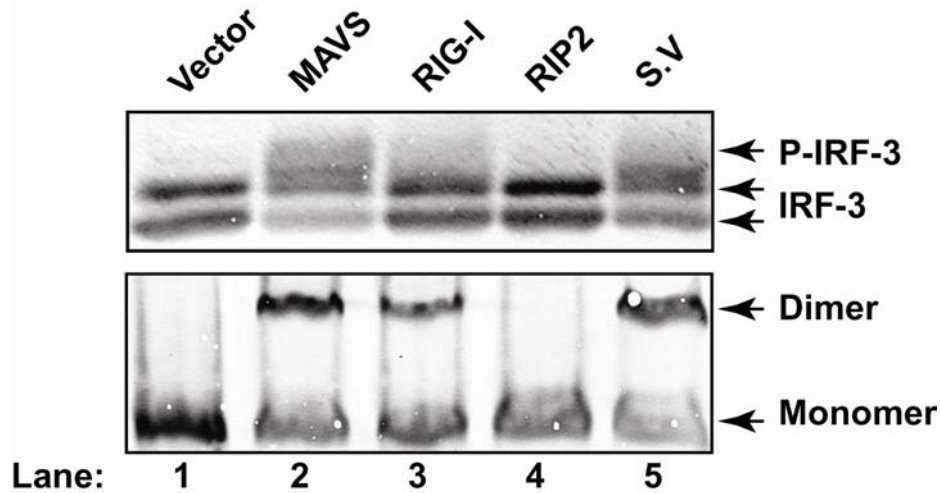


Figure 13d**Figure 13: MAVS is a potent inducer of IFN**

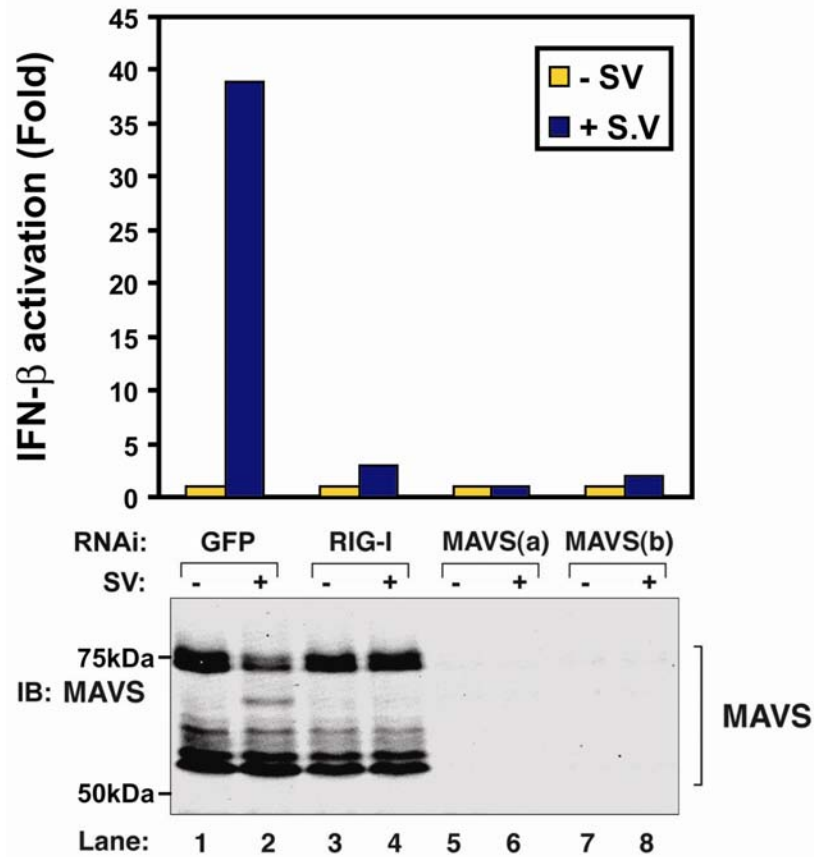
- (a) Increasing amounts of expression vectors for MAVS, RIG-I (N), and RIP2 were transfected into HEK293 cells together with an IFN β -luciferase reporter as well as pCMV-LacZ as an internal control. 36 hours after transfection, the luciferase activity was measured and normalized based on β -galactosidase activity. Each data point is obtained from duplicate experiments. S.V: cells transfected with IFN β -Luc were infected with Sendai virus for 20 hours.
- (b) Similar to (a), except that p- κ B₃-tk-Luc was transfected in lieu of IFN β -Luc.
- (c) The experiments were carried out as in (a), except that Gal4-Luc and Gal4-IRF3 plasmids were co-transfected together in lieu of IFN β -Luc.
- (d) HEK293 cells were transfected with the expression vectors for MAVS (500 ng), RIG-I(N; 200 ng), RIP2 (500 ng), the vector pcDNA3 (500 ng) or infected with Sendai virus (S.V, 50 HA units/ml). 36 hours after transfection or 20 hours after viral infection, cells were lysed to prepare protein extracts, which were then resolved by SDS-PAGE (upper panel) or native gel electrophoresis (lower panel). Phosphorylation or dimerization of IRF3 was detected by immunoblotting (IB) with an IRF3 antibody.

is measured using a luciferase reporter whose expression is driven by three copies of an NF- κ B response element. In the latter case, the activation of IRF3 is measured by the phosphorylation and dimerization of a chimeric protein consisting of IRF3 fused to the DNA binding domain of Gal4, which drives the expression of the luciferase reporter gene.

Immunoblotting experiments show that MAVS activates IRF3 by inducing its phosphorylation (Figure 13d, upper panel) and dimerization (Figure 13d, lower panel). Collectively, these results show that MAVS is a potent activator of IRF3 and NF- κ B, and its over-expression is sufficient to induce cytokines including IFN- β .

III. C. 3. MAVS is essential for antiviral signaling pathways

To determine if MAVS is required for IFN- β induction by viruses, RNAi was used to silence the expression of endogenous MAVS. Two pairs of MAVS RNAi oligos almost completely abolish IFN- β induction by Sendai virus (Figure 14). Since the sequences of these two pairs of RNA oligos are very different, it is exceedingly unlikely that they silence a common “off-target” gene responsible for IFN- β induction. As controls, RNAi of RIG-I, but not GFP, also blocks viral induction of IFN- β .

Figure 14**Figure 14: MAVS is required for IFN- β induction by Sendai virus**

To silence the expression of endogenous proteins, siRNA oligos targeting GFP (control), RIG-I, and two different regions of MAVS (a & b) were transfected into HEK293 cells. The efficiency of MAVS RNAi was confirmed by immunoblotting with a MAVS-specific antibody (bottom panel). To measure IFN β induction, the IFN β -Luc reporter plasmid was transfected into the RNAi cells, which were then infected with Sendai virus (S.V) for 20 hours followed by luciferase assays (upper panel). Each data point is obtained from duplicate experiments.

To determine if MAVS is required for the activation of IRF3 kinase, the phosphorylation and dimerization status of IRF3 was determined in response to Sendai virus in cells treated with MAVS RNAi to silence the expression of MAVS. RNAi of MAVS or RIG-I prevents the phosphorylation (Figure 15a, upper panel) and dimerization (Figure 15a, lower panel) of IRF3 induced by Sendai virus, indicating that both MAVS and RIG-I are required for IRF3 phosphorylation.

To determine if MAVS is also required for IKK activation by viruses, IKK kinase assays were performed (Figure 15b). Since the activation of IKK by Sendai virus is much slower and weaker as compared to TNF α stimulation, expression vector encoding the full-length RIG-I was transfected into HEK293 cells. The full-length RIG-I protein did not activate IKK or IRF3, but potentiated the activation of IKK (Figure 15b, lanes 3-6) such that IKK activity was detectable within 4 hours of viral infection. Importantly, RNAi of MAVS blocks IKK activation by Sendai virus, but not TNF α . Taken together, these results clearly demonstrate that MAVS is essential for the activation of IKK and IRF3 by Sendai virus.

III. C. 4. MAVS is a potent antiviral protein

Since MAVS is both necessary and sufficient for the induction of type I IFNs, we examined whether this protein could mediate immune defense against

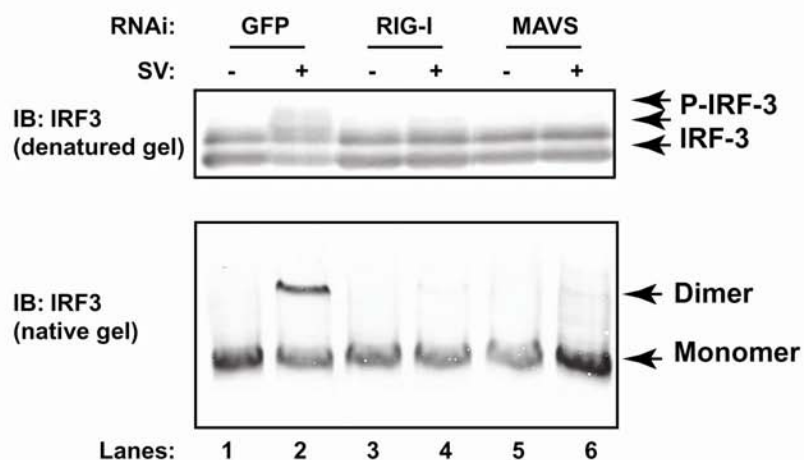
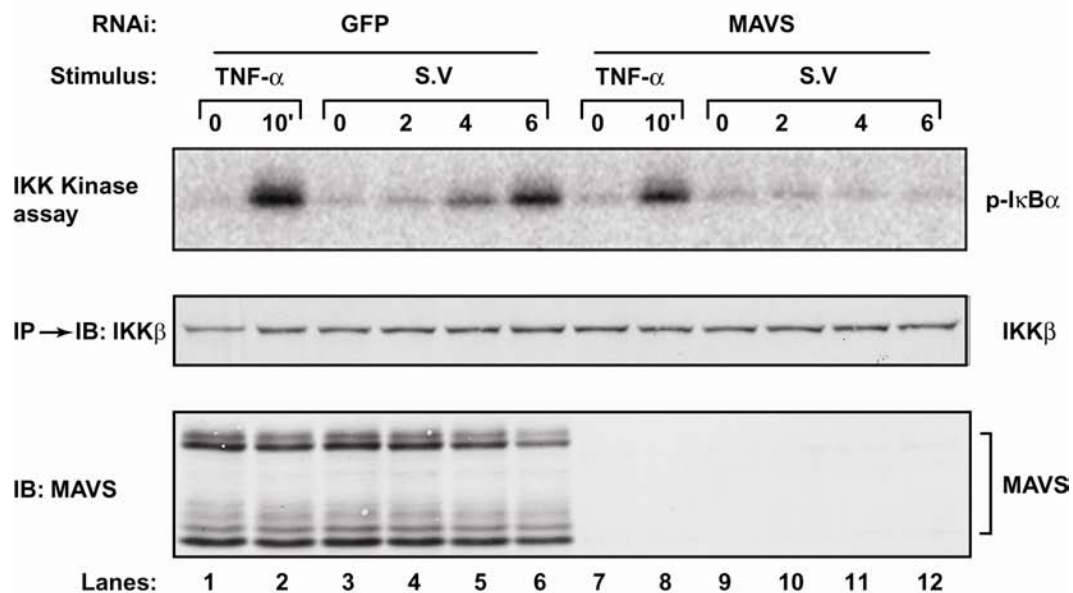
Figure 15a**Figure 15b**

Figure 15: MAVS is required for the activation of IRF3 kinases and the IKK complex by Sendai virus

(a) The siRNA transfection into HEK293 cells and viral infection were carried out as in Figure 15. Protein extracts were prepared from the cells and

- analyzed for IRF3 phosphorylation by SDS-PAGE (upper panel) or dimerization by native gel electrophoresis (lower panel).
- (b) HEK293 cells expressing the full-length RIG-I, which facilitates the activation of IKK and IRF3 by Sendai virus, were transfected with siRNA oligos for GFP or MAVS. These cells were then stimulated with TNF α (10 ng/ml) or infected with Sendai virus (50 HA units/ml) for the indicated time before cell lysates were prepared. An aliquot of the cell lysates (20 μ g) was immunoblotted with a MAVS antibody (lower panel). 500 μ g of the cell lysates were immunoprecipitated with an antibody against NEMO to isolate the IKK complex, whose activity was measured using GST-I κ B α and γ -³²P-ATP as substrates (upper panel). An aliquot of the IKK immunoprecipitate was immunoblotted with an IKK β antibody (middle panel).

the vesicular stomatitis virus (VSV), a positive strand RNA virus of the Rhodoviridae family. Infection of HEK293 cells by VSV led to nearly complete killing of the cells within 24 hours at a multiplicity of infection (MOI) of 0.01 (Figure 16a; performed by Dr. Lijun Sun, Dr. James Chen's laboratory). Transient transfection of these cells with an expression vector encoding FLAG-MAVS led to a dramatic protection of cell killing even at an MOI of 0.1. Conversely, silencing of the endogenous MAVS expression by RNAi greatly sensitizes the cell to killing by VSV at much lower MOI (0.001). Measurement of the viral titer shows that over-expression of FLAG-MAVS decreases the viral titer by more than 20 fold as compared to control cells [from 5×10^7 to 2×10^6 plaque forming unit (pfu), Figure 16b; performed by Dr. Lijun Sun, Dr. James Chen's laboratory). Conversely, RNAi of MAVS leads to an increase of viral titer by 20 fold as compared to control cells (from 5×10^7 to 10^9 pfu). These results show that

MAVS is a pivotal cellular antiviral protein whose expression level directly determines antiviral immunity.

Figure 16a

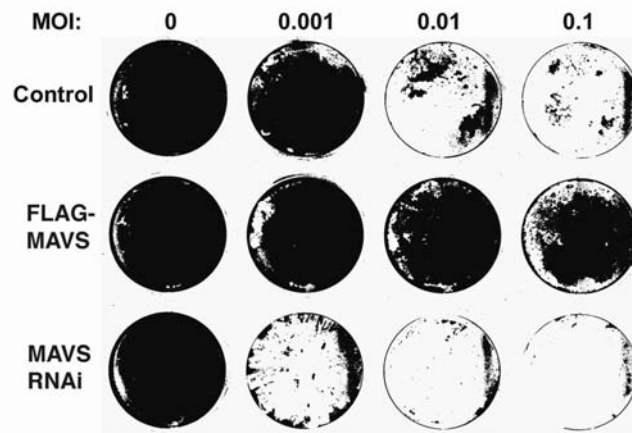


Figure 16b

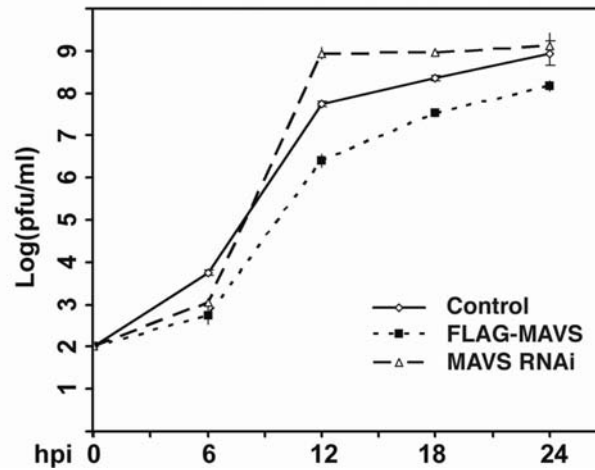


Figure 16: MAVS is a potent antiviral protein

- (a) HEK293 cells were transfected with pcDNA3-FLAG-MAVS (0.5 μ g) or siRNA oligos (20 nM) targeting MAVS. 48 hours after transfection, cells were infected with VSV at the indicated MOI for 24 hours. After fixing, cells that were not killed by the virus were stained with Amido Black.
- (b) The culture supernatant from cells infected with VSV at the MOI of 0.01 were collected at the indicated time points, and the viral titer was determined by plaque assay.

III. C. 5. Epistatic relation of MAVS with known components of the pathway

As both RIG-I and MAVS function in the antiviral signaling pathway, the epistatic relationship between these two proteins was determined. As shown in Figure 17a, RNAi of MAVS blocks the induction of IFN- β by Sendai virus, and by over-expression of the N-terminal fragment of RIG-I [designated as RIG-I (N)] as well as MAVS itself. In contrast, RNAi of RIG-I does not inhibit IFN- β induction by the over-expression of MAVS. This pair of siRNA oligos did not affect IFN- β induction by the RIG-I(N), because the sequence targeted by the RNAi oligos was located at nucleotides 2363-2381, outside the region encoding RIG-I(N). As the RIG-I siRNA oligos effectively blocked IFN- β induction by the virus, but not MAVS, it was concluded that MAVS functions downstream of RIG-I in the viral signaling pathway.

Recent studies have shown that over-expression of TRIF (Yamamoto et al., 2002), TBK1 or IKKi is sufficient to activate IFN- β , and that TBK1 and IKKi are the kinases that phosphorylate IRF3 (Fitzgerald et al., 2003; Sharma et al., 2003). We therefore investigated the relationship between MAVS and TRIF, TBK1 and IKKi. While RNAi of MAVS abolishes IFN- β induction by Sendai virus, it has no effect on the activation of IFN- β by TRIF, TBK1 or IKKi (Figure 17b). Consistent with previous reports, RNAi of RIG-I blocks the induction of IFN- β by Sendai virus but does not affect IFN- β induction by TRIF, TBK1 or

IKKi. RNAi of TBK1 only blocks IFN- β induction by itself, but has little effect on other signaling pathways. It is possible that TBK1 and IKKi function redundantly in 293 cells such that no effect of TBK1 RNAi in RIG-I and TRIF mediated signaling pathways is observed. Since it was also possible that the RNAi experiment did not result in sufficient knock-down of TBK1 protein levels, we turned to TBK1 knock-out MEF cells that are defective for IFN induction in response to stimulation with Sendai virus. As shown in Figure 17c (performed by Dr. Chee-Kwee Ea, Dr. James Chen's laboratory), over-expression of MAVS or stimulation with Sendai virus leads to an induction of IFN- α in wild-type MEF cells. The induction of IFN- α was defective in TBK1 knock-out MEF cells. Together with the data shown in Figures 17a, 17b, 17c and 15b, we propose that MAVS functions downstream of RIG-I and upstream of IKK and TBK1 (Figure 17d).

III. C. 6. Expression pattern of MAVS

Endogenous MAVS was detected with an affinity-purified MAVS antibody raised against a fragment of MAVS containing amino acids 131-291. This antibody detects two sets of bands corresponding to MAVS in crude cell lysates derived from HEK293 cells (Figure 14 and 15b). The first set of bands

Figure 17a

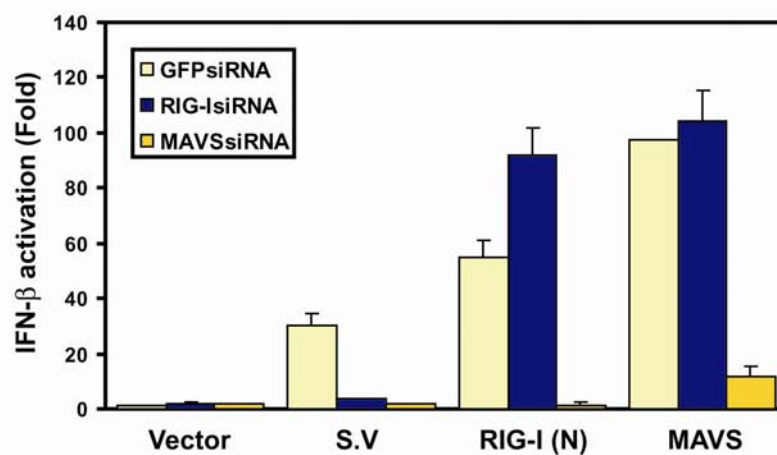


Figure 17b

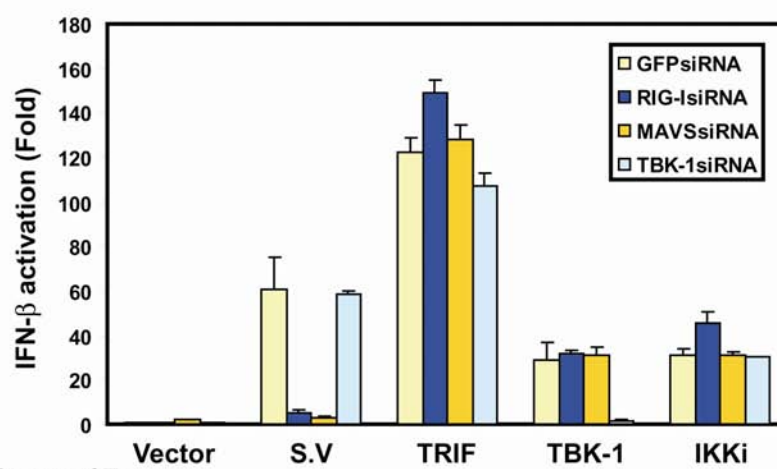


Figure 17c

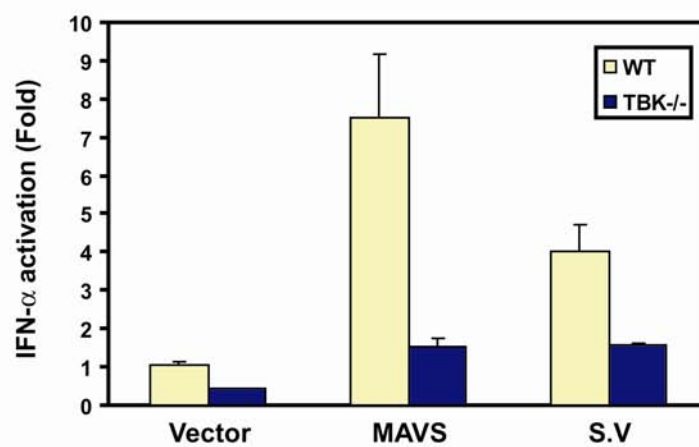
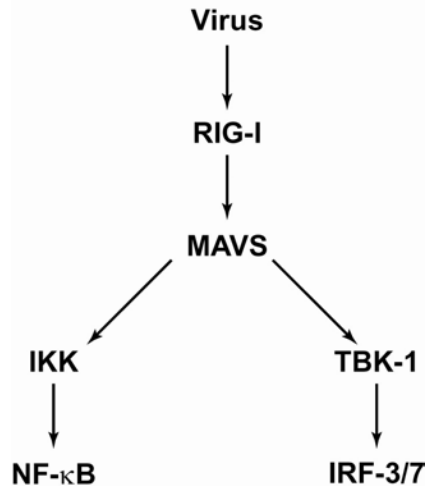


Figure 17d**Figure 17: MAVS functions downstream of RIG-I and upstream of TBK1**

- (a) HEK293 cells were transfected with siRNA oligos targeting GFP, RIG-I or MAVS. These cells were subsequently transfected with IFN β -Luc together with expression vectors (300 ng) encoding the N-terminal fragment of RIG-I [RIG-I (N)], MAVS or empty vector (pcDNA3). As a positive control, cells were infected with Sendai virus (S.V). Twenty hours after viral infection or 24 hours after transfection of the expression plasmids, cells were harvested for luciferase assays. Each data point is obtained from duplicate experiments.
- (b) HEK293 cells were transfected with siRNA oligos targeting GFP, RIG-I, MAVS or TBK1. These cells were transfected with IFN- β -Luc together with either expression vectors (300 ng) for TRIF, TBK-1 and IKKi, or with infection with Sendai virus (S.V). Twenty hours after viral infection or 24 hours after transfection of the expression plasmids, cells were harvested for luciferase assays. Each data point is obtained from duplicate experiments.
- (c) Wild-type or TBK1^{-/-} MEF cells were transfected with pIFN α 4-Luc (300 ng) and pcDNA3-FLAG-IRF7 (50 ng) together with pEF-HA-MAVS (100 ng) or control vector. For Sendai virus infection, MEF cells transfected with the luciferase reporter plasmids were infected with 50 HA units/ml of the virus. Luciferase assays were performed and data points obtained from duplicate experiments are shown.
- (d) A proposed antiviral signaling pathway. In this pathway, MAVS functions downstream of RIG-I, and upstream of IKK and TBK1.

run together with the 75kDa molecular weight marker band, whereas the lower MAVS bands correspond to a molecular weight of approximately 55kDa. MAVS contains 540 amino acid residues and has a predicted molecular weight of 56.5 kDa. The bands detected by the MAVS antibody disappear in cells transfected with two different pairs of siRNA oligos targeting distinct regions of MAVS, indicating that the bands detected by the antibody are indeed MAVS proteins (Figure 14 and 15b). It is unlikely that the multiple MAVS bands represent different spliced variants as the same expression pattern is observed when cells are transfected with MAVS cDNA. Multiple bands corresponding to MAVS are detected with an HA antibody when the HA epitope is appended to the N- or C-terminus of MAVS (Figure 18a). Surprisingly, most of the MAVS protein was present in the pellets of lysates centrifuged at 10,000xg. As will be discussed in chapter V, MAVS is a mitochondrial protein, and mitochondria pellet when lysates are spun at 10,000xg. In the lysis conditions used for this assay, MAVS could not be completely solubilized such that it pellets together with the mitochondria in the P10 pellets. Similar results were obtained with N- and C-terminal Flag-tagged MAVS (Figure 18b). It is possible that the higher bands of MAVS correspond to a modified form of MAVS. The patterns of these bands did not change when cell extracts were treated with phosphatases or glycosylase, suggesting that they are unlikely to be the phosphorylated or glycosylated forms of MAVS (data not shown). We have also been unable to obtain evidence of

MAVS modification by ubiquitin or ubiquitin-like proteins including SUMO, ISG-15 and NEDD8 (data not shown, performed by Dr. Lijun Sun, Dr. James Chen's laboratory). It is also possible that the lower bands represent a degraded or processed product of MAVS, whereas the upper band is the full-length MAVS protein. Thus, it is not clear why MAVS protein exists as multiple bands on SDS-PAGE.

We were also able to use the MAVS antibody described above to detect the expression of MAVS in different cell lines. The MAVS protein bands are detected by immunoblotting in multiple human cell lines including Jurkat (T cell), U937 (monocyte), Huh7 (hepatocyte), A549 (lung epithelial cell) and HeLa (cervical epithelial cell) (Figure 18c). Thus, MAVS is expressed in many different cell types, especially those that constitute the first line of defense against viruses, such as liver and lung cells.

III. D. Discussion

Several pathogens cross the cell membrane to replicate within the intracellular compartment of host cells. These pathogens are detected by cytosolic host cell receptors that trigger immune signaling pathways in response to an infection. Examples of cytosolic receptors include Nod1, Nod2 and IPAF that sense bacterial pathogens and RIG-I and MDA-5 that act as sensors for

Figure 18a

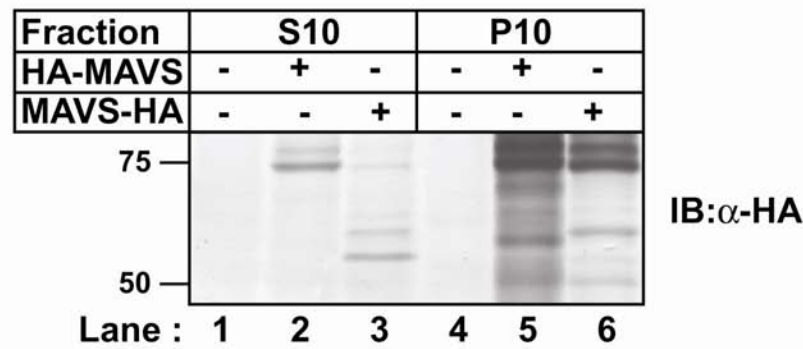


Figure 18b

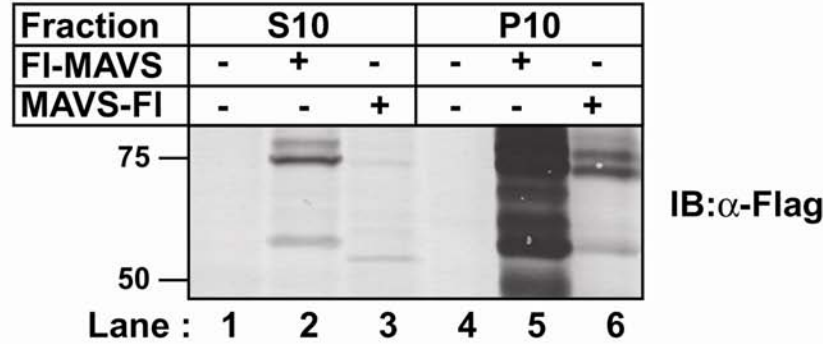


Figure 18c

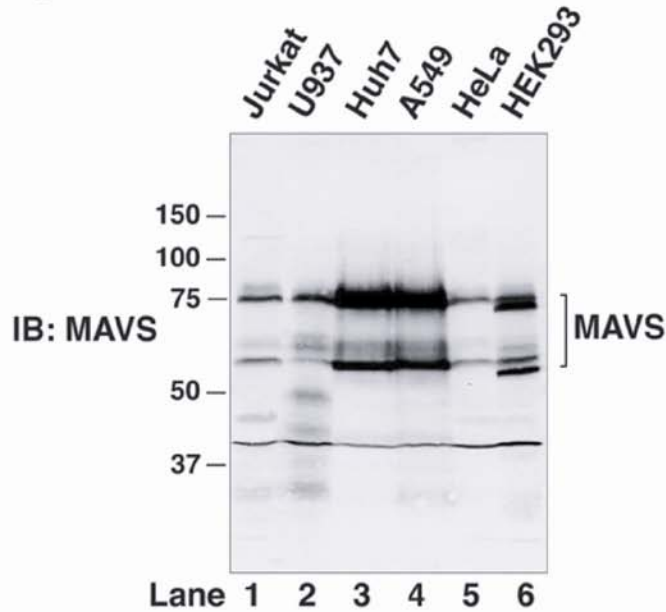


Figure 18: MAVS expression pattern

- (a) 1µg of N- and C-terminal HA-tagged MAVS constructs were transfected into HEK293 cells for 24 hours. Cell lysates were prepared and centrifuged at 10,000xg to obtain the supernatant (S10) and pellet (P10). Equal volumes of S10 and P10 were resolved on an SDS-PAGE. The expression of HA-tagged proteins was detected by immunoblotting with an HA antibody. The position of the molecular weight marker bands corresponding to 75kDa and 50kDa are shown.
- (b) Similar to (a) except Flag-tagged MAVS constructs were transfected. Flag-tagged proteins were detected by immunoblotting with a Flag antibody.
- (c) Whole cell lysates (20µg) from indicated cell lines were immunoblotted with the affinity purified MAVS antibody. Jurkat: T lymphocyte; U937: monocyte; Huh7: hepatocyte; A549: lung epithelial cell; HeLa: cervical epithelial cell; HEK293: embryonic kidney cell.

viruses (Werts et al., 2006). These intracellular receptors share a similar domain structure. They contain ligand sensing domains (LRR domain in the case of Nod 1, Nod2 and IPAF, and helicase domain in RIG-I and MDA-5), and CARD domains that signal to downstream proteins. Nod proteins signal by interacting with a CARD domain containing kinase, RIP2, which in turn activates NF-κB. Similarly, IPAF interacts with CARD domain containing protein apoptosis-associated speck-like protein (ASC) to activate caspase-1. The data presented in this chapter shows that the RIG-I mediated signaling pathway also depends on a CARD domain containing protein termed MAVS. The basis for the specific interaction between particular CARD domain containing proteins is not well understood. To understand this issue, improved primary sequence analysis

methods coupled with structural and biochemical knowledge of specific CARD-CARD interaction pairs will be required.

Ectopic expression of MAVS activates NF- κ B and IRF3 mediated pathways, which in turn lead to the transcription of antiviral cytokines and chemokines. The activation of these signaling pathways by over-expression of MAVS has a functional consequence as it can inhibit viral replication. On the other hand, the loss of MAVS expression renders cells vulnerable to virus mediated killing. These studies support a role of MAVS in the antiviral immune signaling pathway. Homologs of MAVS can be identified from humans to pufferfish, implying that this protein might have an important evolutionarily conserved function in antiviral signaling pathways.

The mechanism by which over-expression of MAVS activates the downstream pathways is currently not understood. It is possible that over-expression of MAVS simply facilitates the interaction of MAVS with other proteins in the pathway. MAVS interacting proteins might include proteins that have been previously implicated in antiviral signaling or proteins that have not been linked to this pathway as yet. Our understanding of MAVS interacting partners will be discussed in chapter IV.

Epistasis experiments suggest that MAVS functions downstream of RIG-I to regulate the activities of TBK1 and IKK. Since the RIG-I and MDA-5 CARD domains are very similar and they regulate similar signaling cascades, it is

possible that MAVS is involved in signaling downstream of MDA-5. A recent study has confirmed that MAVS is required for MDA-5 mediated activation of the IFN- β promoter (Kawai et al., 2005).

Three other groups have independently discovered MAVS and named it interferon- β promoter stimulator-1 (IPS-1) (Kawai et al., 2005) /virus-induced signaling adaptor (VISA) (Xu et al., 2005) and CARD adaptor inducing interferon (CARDIF) (Meylan et al., 2005). The data presented by these groups corroborate our data, confirming a role for MAVS in the antiviral immune response. These studies also report some conflicting data which will be discussed in more detail throughout this thesis.

As mentioned previously, the TLRs and RIG-I are the two receptor systems for detecting viral infection. TRIF is an adaptor protein required for TLR3-mediated signaling. We have shown that TRIF-dependent activation of NF- κ B and IRF3 is unaffected by the absence of MAVS. On the other hand, knock-down of MAVS protein expression by RNAi abolishes signaling by RIG-I. Therefore, we conclude that MAVS specifically signals in the RIG-I mediated signaling pathway. Two other studies support our data implying that MAVS is not required for TRIF mediated activation of IFN- β , however, Xu et.al. suggest that MAVS is essential for TRIF mediated activation of IFN- β (Xu et al., 2005). All of these studies have used RNAi to knock-down the expression of MAVS to determine if TRIF signals in a MAVS dependent manner. It is possible that the

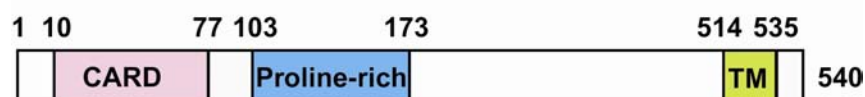
knock-down of MAVS expression was not sufficient to block signaling in studies reporting that MAVS is not required for TRIF-mediated signaling (although this level of MAVS knock-down was sufficient to block RIG-I mediated signaling). It is also possible that the siRNA pair used by Xu et. al. had some “off-target” effects that inhibit the signaling downstream of TRIF. It is important to definitively determine the role played by MAVS in the TLR3 mediated antiviral immune response. Generation of a mouse that lacks MAVS expression will be useful for determining the contribution of MAVS to the RIG-I and TLR3 mediated signaling pathways. The MAVS knock-out mouse model will also be valuable for studying the role of MAVS in antiviral immunity *in vivo*. Indeed, a MAVS deficient mouse generated in Dr. James Chen’s laboratory has definitively proved that MAVS is specifically involved in RIG-I mediated antiviral defense in multiple cell types (Sun et al., 2006). These mice are severely compromised in immune defense against viral infections supporting our conclusion that MAVS is an important component of the antiviral signaling pathways.

CHAPTER IV: UNDERSTANDING THE MECHANISM BY WHICH MAVS FUNCTIONS

IV. A. Introduction

As discussed in the previous chapter, MAVS is a novel CARD domain containing protein which functions downstream of RIG-I in the antiviral signaling pathway. The next step in the characterization of MAVS involved understanding the molecular mechanism by which MAVS functions. Towards this objective, the signaling domains encoded within MAVS were identified and characterized. Analysis of the domain structure of MAVS revealed that in addition to the N-terminal CARD domain (Figure 12), the protein also contains a central proline-rich domain (PRO) and a hydrophobic transmembrane (TM) domain at the C-terminus (Figure 19). To determine the contribution of each domain towards the function of MAVS, deletion constructs of MAVS lacking these domains were generated and tested for their ability to activate the IFN- β promoter.

The epistasis experiments described in chapter III revealed that MAVS functions downstream of RIG-I and upstream of TBK1 and IKK. To understand how MAVS functions in this signaling pathway, we took a candidate approach to determine if any of the known components of the antiviral signaling pathway interact with MAVS. The most likely candidates to interact with MAVS include the CARD domain containing proteins RIG-I and MDA-5. Non-CARD domain containing proteins including the IRF3 kinases TBK1 and IKKi, and proteins

Figure 19a**Figure 19b**

Proline-rich domain

103 PPDPLEPPSLPAERPGPPTPAAAH

127 SIPYNSCREKEPSYPMPVQETQA

150 PESPGENSEQALQTLSPRAIPRNP

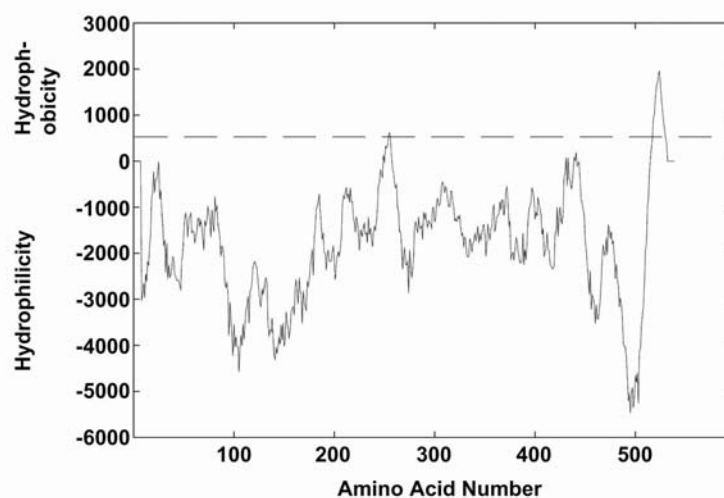
Figure 19c

Figure 19: Domain and sequence analysis of MAVS

- (a) A schematic diagram of MAVS domain organization. TM: transmembrane domain.
- (b) Amino acid sequence of the Proline-rich domain. The PxxP motifs within this domain are underlined.
- (c) Prediction of the MAVS transmembrane domain using the Tmpred server. A score of greater than 500 predicts a transmembrane region.

involved in NF- κ B activation like the IKK kinase complex and TRAF6 protein, were also tested for interaction with MAVS. Recently, it was reported that RIP1 and a death-domain containing protein FADD are involved in the virus dependent activation of IFN- β (Balachandran et al., 2004). Although the mechanism by which these proteins regulate the antiviral signaling pathway is not known, their interaction with MAVS was tested. Results from immunoprecipitation assays that were used to assess the interaction of MAVS with potential candidate proteins, are presented in this chapter.

IV. B. Materials and Methods

IV. B. 1. Identification of domains in MAVS

The amino acid sequence of MAVS was blasted against the domain database using simple modular architecture research tool (SMART; <http://smart.embl-heidelberg.de/>) to determine the domain constitution of the protein. The transmembrane domain was predicted using two different programs: TMpred (http://www.ch.embnet.org/software/TMPRED_form.html; Figure 19c), and Kyte-Doolittle hydropathy plot.

IV. B. 2. Plasmids

Truncated forms of MAVS lacking either the CARD domain (residues 10-77) or the proline-rich region (residues 103-152) were cloned using overlap

extension PCR. A similar PCR strategy was used to generate MAVS mutants lacking the intervening sequence between the CARD and TM domains (CARD-TM). Appropriate primers were used to amplify a region from residue 1–1500 to obtain the transmembrane deletion construct of MAVS. These fragments were cloned into the XhoI and XbaI sites of pcDNA3. Point mutations within the CARD domain of MAVS were introduced using the QuickChange kit (Stratagene).

IV. B. 3 Immunoprecipitation

Expression vectors encoding HA-MAVS and the indicated FLAG-tagged proteins were co-transfected into HEK293 cells. Thirty-six hours after transfection, cells were lysed in Buffer I (20 mM Tris-HCl, pH 7.5, 150 mM NaCl, 10% glycerol, 0.5% Triton X-100, 20 mM β -glycerophosphate, 1 mM sodium orthovanadate, 10 mM $MgCl_2$, 1 mM DTT, 1 mM PMSF and 10 μ g/ μ l leupeptin), and the lysates cleared at 20,000xg for 15 minutes at 4°C. 500 μ g of lysate was incubated with a polyclonal antibody against MAVS or control IgG at 4°C for immunoprecipitation. After 1 hour, 10 μ l of protein A/G bead slurry was added. Immunoprecipitation was carried out for another hour. The beads were washed three times with Buffer J (20 mM Tris-HCl, pH 7.5, 150 mM NaCl, 10% glycerol, 0.5% Triton X-100, 1 mM DTT, 1 mM PMSF and 10 μ g/ μ l leupeptin). The beads containing the

immunoprecipitated MAVS complex were resuspended in SDS sample buffer, and the eluted proteins immunoblotted with an antibody against FLAG and HA.

IV. C. Results

IV. C. 1. The CARD Domain is Essential for MAVS Signaling

To investigate the functions of MAVS CARD and proline-rich domains, expression constructs encoding MAVS mutant proteins lacking either the CARD domain (Δ CARD) or the proline-rich domain (Δ PRO; Figure 20, upper panel) were engineered. As shown in Figure 20 (lower panel), deletion of the CARD domain, but not the PRO domain, abolishes the ability of MAVS to activate IFN- β . Similar results were obtained for NF- κ B luciferase assay (data not shown).

To further test the importance of the CARD domain for MAVS function, certain conserved residues within the domain were mutated. Point mutation of a conserved threonine residue to alanine (T54A), or simultaneous mutations of three conserved residues in the CARD domain to alanine (G67A/W68A/V69A; abbreviated as AAA), severely impairs the ability of MAVS to activate IFN- β (Figure 12c and 21). These results indicate that an intact CARD domain is essential for MAVS signaling.

This conclusion was further supported by experiments depicted in Figures 22a and 22b, which show that MAVS- Δ CARD, but not MAVS- Δ PRO, functions

as a dominant negative mutant that inhibits the activation of IFN- β and NF- κ B promoters by

Figure 20

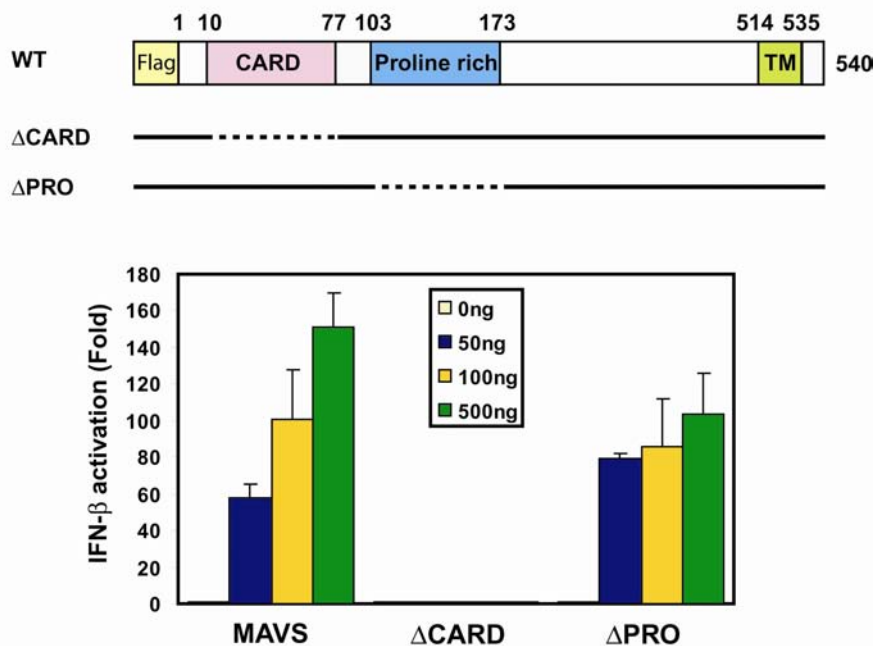
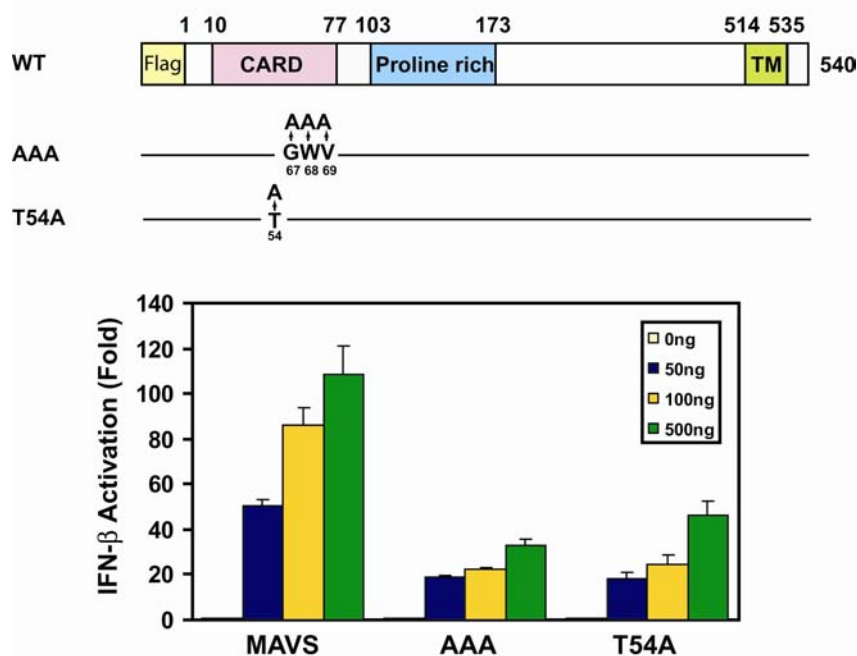


Figure 20: The CARD domain is essential for MAVS signaling

A schematic diagram illustrating the MAVS mutants is shown in the upper panel. Δ CARD: MAVS construct lacking residues 10-77; Δ PRO: MAVS construct lacking residues 103-152. HEK293 cells were transfected with IFN β -Luc together with expression vectors for MAVS and its mutants as indicated. Thirty-six hours after transfection of the expression plasmids, cells were harvested for luciferase assays. Each data point is obtained from duplicate experiments.

Sendai virus. The CARD domain alone did not function as a dominant negative mutant (data not shown), suggesting that when the CARD domain is not tethered to the rest of MAVS protein such as the transmembrane domain, it may not interact effectively with other proteins in the pathway.

Figure 21**Figure 21: Point mutations within CARD domain abolish MAVS function**

A schematic diagram illustrating the MAVS CARD domain mutants (upper panel). AAA: G67A/W68A/V69A. HEK293 cells were transfected with IFN β -Luc together with expression vectors for MAVS and its mutants as indicated. Cells were lysed 36 hours post-transfection and luciferase assays were performed. Each data point is obtained from duplicate experiments.

IV. C. 2. The C-terminal Transmembrane (TM) Domain of MAVS is Essential for its Function

The C-terminus of MAVS contains a hydrophobic domain that is predicted to be a transmembrane domain (Figure 19c). To determine the function of the putative transmembrane domain, we created a MAVS mutant protein lacking the

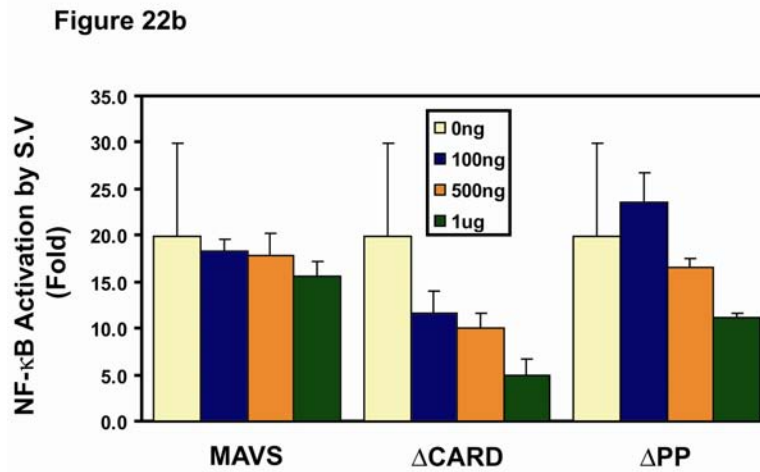
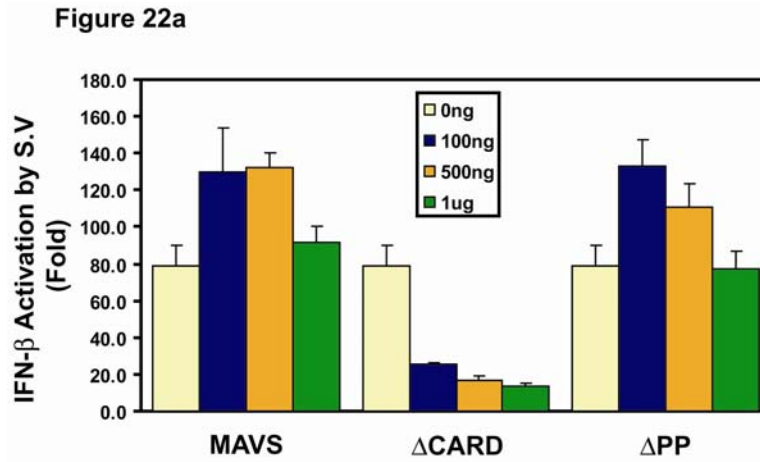


Figure 22: The DCARD mutant of MAVS acts as a dominant negative inhibitor of IFN- β induction by Sendai virus (S.V)

- (a) HEK293 cells were transfected with IFN β -Luc together with expression vectors for MAVS or its mutants. The cells were then infected with Sendai virus (S.V) for 20 hours followed by measurement of luciferase activity. Each data point is obtained from duplicate experiments.
- (b) Similar to (a), except that κ B3-Luc was used in lieu of IFN β -Luc.

C-terminal 30 residues (MAVS- Δ TM). This mutant protein completely lost its ability to activate IFN- β (Figure 23).

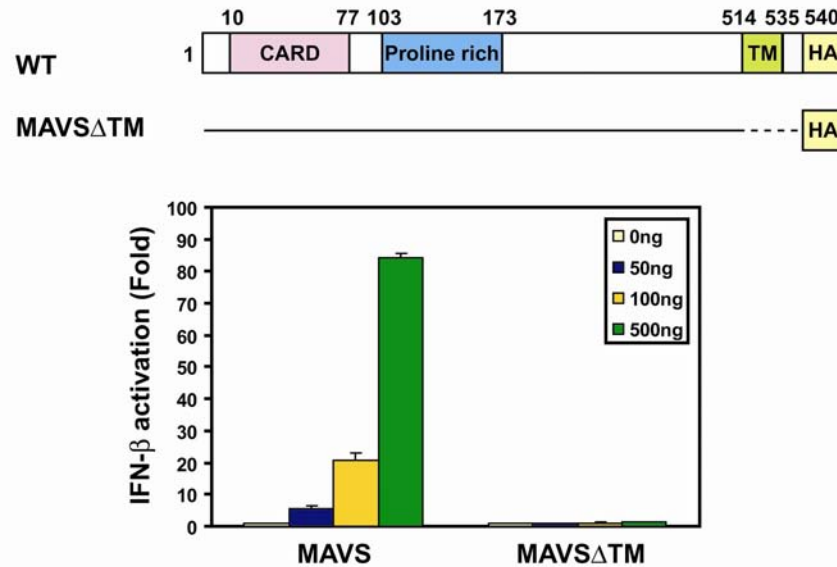
Figure 23

Figure 23: The transmembrane domain of MAVS is important for its function

The MAVS mutant lacking the C-terminal 30 residues (MAVS Δ TM) is illustrated in the upper panel. This mutant or wild type (WT) MAVS were transfected into HEK293 cells together with IFN β -Luc to measure IFN- β induction (lower panel). Cells were lysed 36 hours post-infection and luciferase assays were performed. Each data point is obtained from duplicate experiments.

IV. C. 3. The CARD and TM Domains of MAVS are Sufficient to Induce IFN- β

Since the most conserved regions of MAVS are the N-terminal CARD domain and the C-terminal TM domain, and each of these domains is necessary for MAVS signaling, we examined whether these two domains are sufficient to activate IFN- β expression. Remarkably, the MAVS mutant containing only the

CARD and TM domains (CARD-TM) is sufficient to induce IFN- β (Figure 24), whereas the mutant containing only the CARD domain is inactive. Thus, the CARD and TM domains are both necessary and sufficient for MAVS signaling.

Figure 24

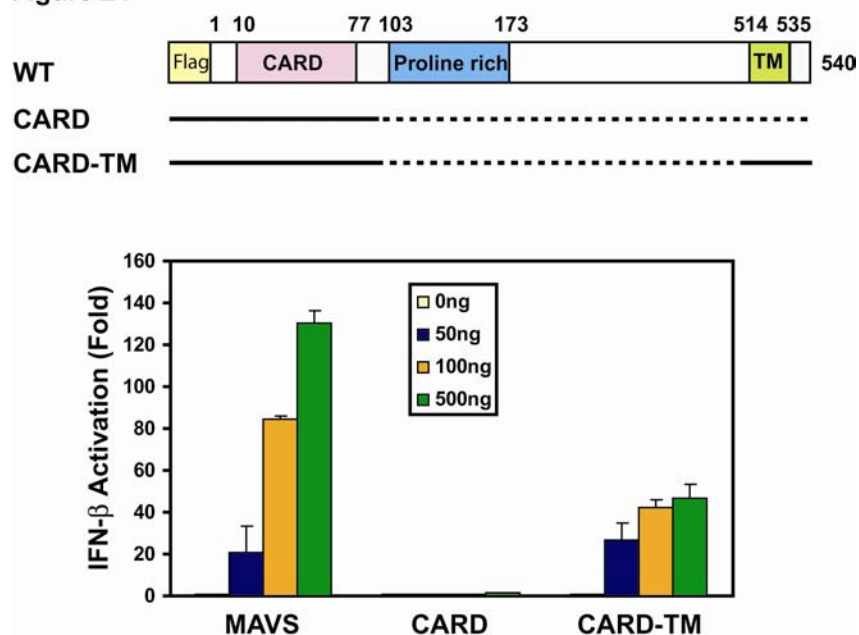


Figure 24: The CARD and TM domain are sufficient for MAVS function

A schematic diagram of a MAVS mutant containing just the CARD and TM domain is shown in the upper panel. MAVS mutants were transfected into HEK293 cells together with IFN β -Luc to measure IFN- β induction (lower panel). Each data point is obtained from duplicate experiments.

IV. C. 4. MAVS interacting partners

Co-immunoprecipitation assays were performed to determine the interaction of MAVS with candidate proteins. The candidates selected in these experiments were based on previous studies implying a role of these proteins in antiviral signaling pathways. The N-terminal CARD domain of MAVS likely mediates interaction with other CARD-containing proteins like RIG-I and MDA-5. A weak but reproducible binding between over-expressed MAVS and RIG-I in co-immunoprecipitation experiments performed at low stringency conditions could be detected (Figure 25). However, no direct interaction between endogenous MAVS and RIG-I in the presence or absence of viral infection has been detected (data not shown). Both RIG-I and MDA-5 contain two CARD domains, which may interact with each other intra-molecularly, thus preventing their interaction with other CARD domain proteins. The binding of viral RNA to the C-terminal RNA helicase domain of RIG-I may induce a conformational change that allows the tandem CARD domains of RIG-I to interact with MAVS directly or indirectly. More extensive studies are required to determine the validity and functional significance of interaction between RIG-I and MAVS.

No interaction of MAVS with the IRF3 kinases TBK1 and IKKi or IKK could be detected (data not shown). But by over-expressing MAVS together with TRAF6 in cells, an association between the two proteins could be detected by immunoprecipitation (Figure 25). This interaction occurs presumably through

two putative TRAF6-binding sequence (PXEXXAr/Ac, Ar/Ac represents an aromatic or acidic amino acid) in MAVS i) PGENSE, residues 153-158 and ii) PEENEY, residues 455- 460. However, the importance of TRAF6 for the antiviral signaling pathway is not clear as IFN- β induction by Sendai virus is not

Figure 25

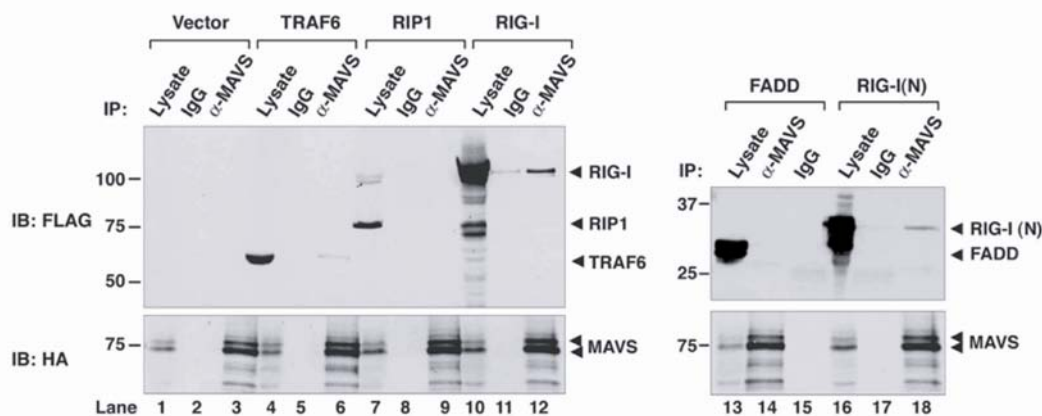


Figure 25: Interaction of MAVS with RIG-I and TRAF6

Expression vectors encoding HA-MAVS and the indicated FLAG-tagged proteins were co-transfected into HEK293 cells. 36 hours after transfection, cells were lysed in a buffer containing 0.5% Triton-X100 and 150 mM NaCl, and the proteins associated with MAVS were co-immunoprecipitated with the polyclonal antibodies against MAVS or control IgG. After washing three times with a buffer containing 0.1% Triton-X100 and 150 mM NaCl, the immunoprecipitated beads were resuspended in SDS sample buffer, and the eluted proteins immunoblotted with an antibody against FLAG or HA as indicated. Lysate represents 10% of the starting materials used for immunoprecipitation.

impaired in TRAF6-deficient MEF cells (data not shown; performed by Chee-Kwee Ea, Dr. James Chen's laboratory).

Recently, it has been shown that RIP1 and FADD are involved in viral induction of IFN- β (Balachandran et al., 2004), raising the possibility that these proteins mediate signaling by MAVS. However, no interaction between MAVS and RIP1 or FADD could be detected (Figure 25). Furthermore, the RIP1-deficient MEF cells were fully capable of producing IFN- β in response to Sendai virus infection (data not shown; performed by Chee-Kwee Ea, Dr. James Chen's laboratory). Thus, under the immunoprecipitation conditions used in these experiments, we have not been able to detect a physiologically relevant interaction of MAVS with the candidate proteins that function downstream of MAVS.

IV. D. Discussion

We have identified a novel protein termed MAVS that is involved in the antiviral signaling pathway. In order to understand the mechanism by which this protein signals, we took two approaches. In the first approach, different MAVS domains were deleted and truncated forms MAVS constructs were assessed for function. These experiments revealed that the N-terminal CARD and C-terminal transmembrane domains of MAVS are important for its function. The second approach was to detect interaction of MAVS with known signaling components of the antiviral pathway. These studies led to the identification of RIG-I and TRAF6 as MAVS binding partners.

The importance of the CARD domain of MAVS for its function is not surprising. CARD domains have been identified as protein interaction modules in several signaling pathways. We can detect an interaction between the CARD domains of MAVS and RIG-I. Thus, it is possible that RIG-I communicates with MAVS by directly interacting with its CARD domain. Besides interacting with RIG-I, an upstream component of the antiviral signaling pathway, MAVS CARD domain might also contribute to downstream signaling. As discussed in chapter III, over-expression of MAVS can activate downstream signaling independent of RIG-I. Thus, the impaired signaling by the MAVS- Δ CARD construct is probably not due to the loss of interaction with RIG-I. It is possible that the MAVS CARD domain facilitates the interaction of MAVS with another, as yet unidentified downstream protein.

The Δ CARD construct exerts a dominant negative effect on virus-induced activation of IFN- β . Thus, it is possible that regions outside the CARD domain contribute to MAVS function. A potential protein interaction domain of MAVS besides the CARD domain is the proline-rich domain. The proline-rich region of MAVS is not important for the activation of IFN- β in over-expression assays. But it is still possible that this domain is involved in the regulation of MAVS by upstream components of the RIG-I signaling pathway. The proline-rich region of MAVS contains multiple PxxP motifs. These motifs have been shown to interact with SH3 and WW domains (Cohen et al., 1995; Macias et al., 2002). As yet, no

SH3 or WW domain containing proteins have been implicated in the antiviral signaling pathway.

The C-terminus of MAVS contains a hydrophobic region that is predicted to be a transmembrane domain. Since all the known components of the RIG-I signaling pathway are cytosolic proteins, the presence of a putative transmembrane domain in MAVS is very surprising. The MAVS Δ TM construct encodes for most of the sequence of MAVS including the CARD domain, but cannot activate downstream signaling. On the other hand, even though the isolated CARD domain of MAVS is not sufficient to activate the downstream signaling, the CARD-TM fusion protein can signal. The role of the transmembrane domain for MAVS function is not clear. An interesting possibility is that the transmembrane domain contributes to the function of MAVS by targeting it to a specific location within a cell. The cellular localization of MAVS will be discussed in chapter V. Our study has not assessed the contribution of the region between the proline-rich domain and transmembrane domain towards the function of MAVS in detail.

It is critical to identify the binding partners of MAVS. Immunoprecipitation experiments performed under low stringency conditions detect a weak interaction of MAVS with RIG-I and TRAF6 when these proteins are over-expressed. Interaction between endogenous proteins could not be detected. Although we could not detect MAVS interaction with RIP1, FADD,

TBK1 or IKK complex, some studies report binding of MAVS with these proteins. Kawai et. al. report a weak interaction between over-expressed MAVS and RIP1 and FADD. But this interaction might not be required for MAVS function as the RIP1-deficient MEF cells infected with virus are fully capable of producing IFN- β . In agreement with our data, Kawai et. al. did not detect interaction of MAVS with TBK1. But Xu et. al. report binding between over-expressed MAVS and TBK1. Further, Meylan et. al. report an interaction between over-expressed MAVS and IKK complex. Thus, there is no clear consensus on MAVS interaction partners. The reason for different studies reporting different interaction partners of MAVS is not clear. It is possible that differences in the level of protein over-expression in cells and different stringency of immunoprecipitation conditions have led to differences in the observed binding. Immunoprecipitation experiments with over-expressed proteins are valuable in detecting interaction between low-affinity binding partners. But, over-expression of proteins might lead to detection of interactions that are not physiologically relevant. Thus, further studies are required to determine the physiologically relevant MAVS binding partners.

An unbiased approach to identify MAVS interacting partners needs to be performed. Since an antibody that immunoprecipitates MAVS is available, an attempt to pull-down the endogenous MAVS complex in the absence or presence

of virus should be considered. Yeast-two hybrid screening can also be used to identify MAVS interacting proteins.

CHAPTER V: MITOCHONDRIAL LOCALIZATION OF MAVS

V. A. Introduction

MAVS is an important component of the antiviral signaling pathway that signals downstream of RIG-I. MAVS contains a C-terminal hydrophobic region that is predicted to be a transmembrane domain (Figure 19c). Since components of the RIG-I signaling pathways are cytosolic proteins, the presence of a transmembrane domain in MAVS was unexpected. As shown in the previous chapter (Figure 23), the transmembrane domain is important for MAVS function.

In a class of integral membrane proteins called the tail anchored proteins, the C-terminal transmembrane domain dictates the subcellular localization of a protein (Borgese et al., 2003). Members of C-tail anchored proteins are targeted to diverse cellular membrane including endoplasmic reticulum, outer mitochondrial membrane, golgi, peroxisomes and fusion vesicles. The machinery responsible for transporting and inserting these proteins into the lipid bilayer has not been identified yet. Certain features of the C-terminal tail region that dictate the localization of these proteins been characterized. For example, proteins with shorter transmembrane regions (~20 residues) that are flanked by basic amino acids are preferentially targeted to the mitochondria (Figure 26) (Kaufmann et al., 2003) (Horie et al., 2002). Well known examples of the tail anchored proteins include the Bcl-2 family members that are targeted to the endoplasmic reticulum and mitochondria (Figure 26). Since the putative transmembrane domain of

MAVS is similar to the transmembrane domains of C-tail terminal anchored proteins, the subcellular localization of MAVS was assessed. To determine the localization of MAVS, cell biological and biochemical approaches were employed.

Figure 26

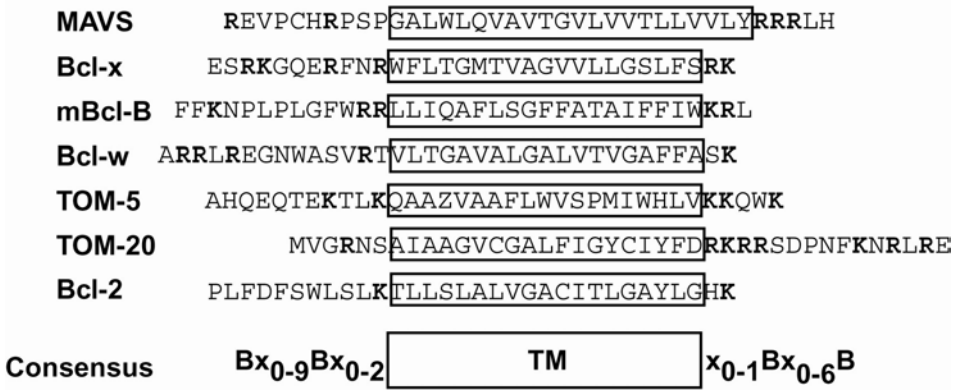


Figure 26: The transmembrane domain of MAVS is similar to the transmembrane domains of C-tail terminal anchored proteins
The alignment of the MAVS transmembrane (TM) sequence with that of transmembrane sequence from other tail anchored protein is shown. The transmembrane domains are boxed and basic residues are highlighted in dark. B: basic residue, TM: transmembrane.

V. B. Materials and Methods

V. B. 1. Plasmids and Antibodies

To replace the TM domain of MAVS with another domain that targets the fusion protein to distinct membrane locations, the following sequences were used: CAAX (residues 128-148 of Rac1); VAMP-2 (residues 84-116); Bcl-2 (residues

208- 239) and Bcl-xL (residues 202- 233). These sequences were fused to the C-terminus of MAVS (residues 1-500) using overlap extension PCR.

Antibodies against cytochrome c, cytochrome c oxidase and Bcl-xL were kindly provided by Dr. X. Wang (UT Southwestern Medical Center). Rabbit polyclonal antibody against Calnexin (Stressgen, SPA-860) and monoclonal antibody against EEA1 (BD Bioscience) were purchased from the indicated supplier.

V. B. 2. Confocal Imaging

HeLa cells were transfected with Polyfect reagent (Qiagen). 24 hours later cells were trypsinized and plated onto cover slips in 24-well plates. After allowing the cells to adhere for 12-18 hours, cells were incubated with 250 nM Mito Tracker Red (Molecular Probes) for 30 minutes at 37°C. Cells on the cover slips were then washed once with PBS and fixed in 3.7% formaldehyde in PBS for 15 minutes. Cells were permeabilized and blocked for 30 minutes at room temperature in a staining buffer containing Triton-X100 (0.2%) and BSA (3%), and then incubated with a primary antibody in the staining buffer lacking Triton-X100 for 1 hour. After washing three times in the staining buffer lacking Triton-X100, cells were incubated in secondary antibody for 1 hour. The cover slips, which were washed extensively, were dipped once in water and mounted onto slides using mounting media (VectaShield; Vector Laboratories). Imaging of the

cells was carried out using Zeiss LSM510 META laser scanning confocal microscope at the Department of Molecular Biology, UT Southwestern Medical Center.

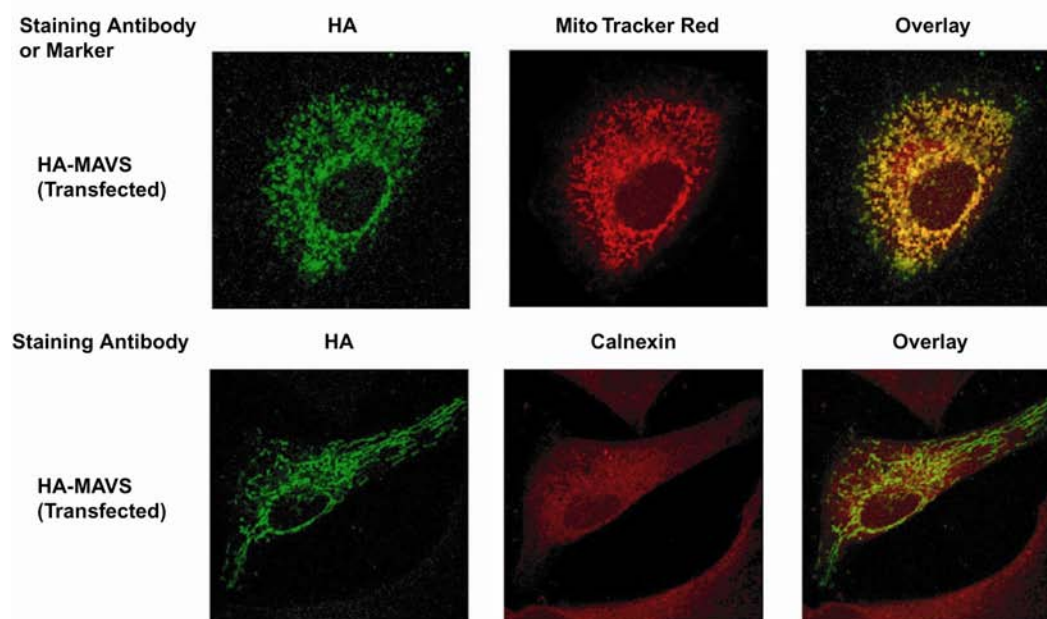
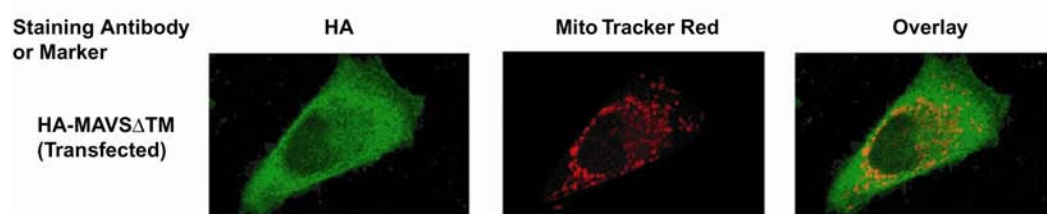
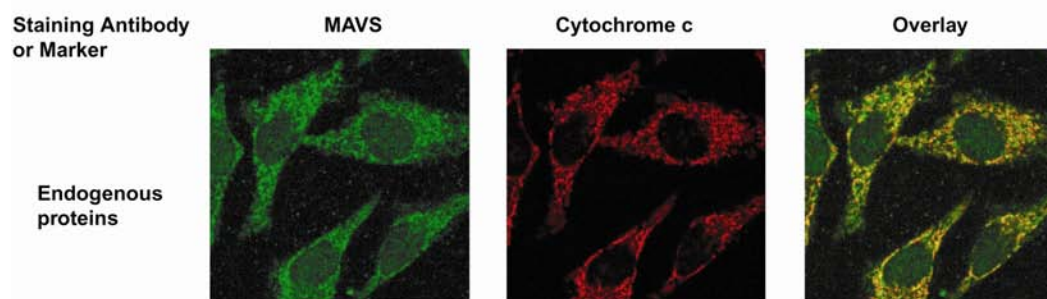
V. B. 3. Subcellular Fractionation

HEK293 cells were washed with cold PBS and lysed by douncing for 20 times in Homogenization buffer (Buffer D: 10 mM Tris-HCl, pH7.5, 2 mM MgCl₂, 10 mM KCl, 250 mM Sucrose, Protease Inhibitor cocktail, 0.5 mM DTT). The homogenate was centrifuged at 500xg for 5 minutes, and the pellet (P1) was saved as crude nuclei. The supernatant (S1) was centrifuged at 5,000xg for 10 minutes to precipitate crude mitochondria (P5). The supernatant (S5) was further centrifuged at 15,000xg for 10 minutes to generate S15 and P15. Each pellet was resuspended in Buffer D for later experiments. To further purify mitochondria, P5 was homogenized gently in Buffer D, and 800 µl of the resuspension was laid on top of a continuous sucrose gradient from 0.3-1.8M in 10 ml. After centrifugation at 100,000xg for 90 minutes in a Beckman 41Ti ultracentrifuge, 800 µl fractions were collected from the top. In some experiments (to demonstrate the membrane localization of MAVS), the mitochondrial fraction (P5) was sonicated before it was subjected to ultracentrifugation.

V. C. Results

V. C. I. MAVS is a Mitochondrial Membrane Protein

To determine the subcellular localization of MAVS, confocal microscopy to image HeLa cells transfected with an expression vector encoding HA-tagged MAVS was employed (Figure 27a). Fluorescent immunostaining with an HA-specific antibody shows a punctate pattern of MAVS localization that overlaps with the staining pattern of Mito Tracker (Figure 27a, upper panel), a fluorescent marker taken up specifically by mitochondria. As the C-terminal TM domain of MAVS is similar to that of Bcl-2, which is localized to both endoplasmic reticulum (ER) and mitochondria, we examined whether a fraction of MAVS might be localized to ER. As shown in the lower panel of Figure 27a, the staining pattern of MAVS did not overlap with that of the ER marker calnexin, indicating that MAVS is not an ER protein. Confocal microscopy also revealed that MAVS lacking the C-terminal transmembrane domain (MAVS- Δ TM) is a cytosolic protein that no longer overlaps with Mito Tracker staining (Figure 27b). To localize the endogenous MAVS protein, affinity-purified MAVS antibody was used for immunostaining (Figure 27c). Similar to the transfected HA-MAVS, the endogenous MAVS shows a punctate staining pattern that overlaps with the staining of cytochrome c, a well-known mitochondrial protein. Although the resolution of confocal microscopy did not allow for the precise localization of

Figure 27a**Figure 27b****Figure 27c**

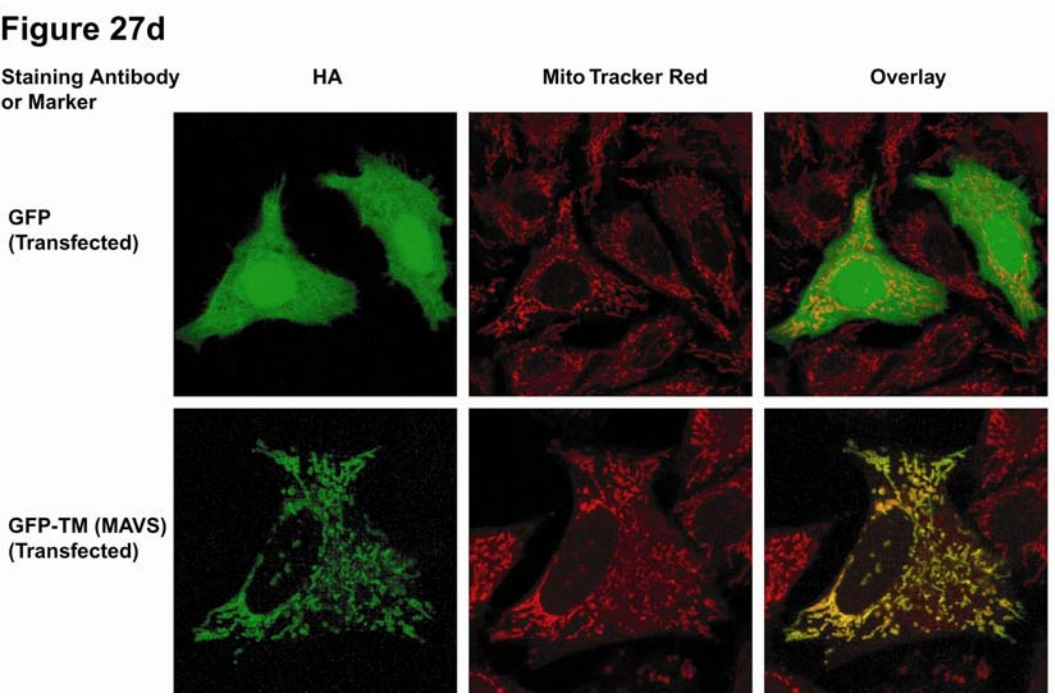


Figure 27: MAVS is a mitochondrial protein

- (a) pEF-HA-MAVS was transfected HeLa cells were fixed and stained with an HA antibody. The localization of MAVS was visualized by confocal microscopy. The mitochondria were stained with Mito Tracker. The yellow staining in the overlay image indicates co-localization of MAVS and Mito Tracker. An ER resident protein, calnexin was used to stain the ER.
- (b) Similar to (a) except pEF-HA-MAVS Δ TM was transfected into HeLa cells.
- (c) Confocal microscopy of the endogenous MAVS protein. HeLa cells were permeabilized and stained with an antibody against MAVS or cytochrome c.
- (d) Localization of over-expressed GFP and GFP-TM protein was determined by confocal microscopy. The mitochondria were stained with Mito Tracker. The yellow staining in the overlay image indicates co-localization of GFP-TM and Mito Tracker.

MAVS at the ultra-structural level within the mitochondria, these experiments clearly show that MAVS is localized to the mitochondria.

To determine if the transmembrane domain of MAVS is sufficient to target a protein to the mitochondria, the transmembrane domain of MAVS was fused to green fluorescent protein (GFP) that is localized to the cytosol and nucleus (Figure 27d, upper panel). As shown in the lower panel of Figure 27d, fusion of the transmembrane domain of MAVS to GFP is sufficient to target GFP to the mitochondria.

To further determine if MAVS is localized to the mitochondrial membrane, subcellular fractionation experiments were conducted. HEK293 cells were homogenized in an isotonic buffer that preserves mitochondria and other

organelles, and the cell lysates were subjected to differential centrifugation to separate nuclei, mitochondria, and other organelles as well as cytosol (Figure 28a; performed by Dr. Lijun Sun, Dr. James Chen's laboratory). MAVS is found in the 5,000 x g pellet (P5), together with other mitochondrial proteins including Bcl-xL and cytochrome-c oxidase (COX). Immunoblotting with an antibody against the endosomal protein EEA-1 shows that the distribution of this protein does not correlate with that of MAVS. Similarly the markers of endoplasmic reticulum (BiP) and lysosome (LAMP-1) do not co-segregate with MAVS (data not shown).

To determine whether MAVS is localized in the outer or inner mitochondrial membrane, the mitochondrial fraction (P5) was sonicated to partially rupture the outer mitochondrial membrane and then fractionated by sucrose gradient ultracentrifugation (Figure 28b; performed by Dr. Lijun Sun, Dr. James Chen's laboratory). The sonication releases cytochrome c from the intermitochondrial membrane space, and results in a small fraction of outer mitochondrial membrane floating on the top of the sucrose gradient, as indicated by immunoblotting with an antibody against Bcl-xL, which is predominantly located in the outer mitochondrial membrane. Under the same condition, the inner mitochondrial membrane protein COX remains largely in the dense fractions of the sucrose gradient. Interestingly, a small fraction of MAVS co-migrated with Bcl-xL to the lighter membrane fractions, suggesting that MAVS co-localizes

with Bcl-xL in the outer mitochondrial membrane. This conclusion was further supported by our observation that MAVS and Bcl-xL could be extracted from the mitochondrial membrane with the same concentration of Triton X-100 (0.1%), whereas the extraction of COX requires higher Triton X-100 concentration (0.2%, data not shown).

Figure 28a

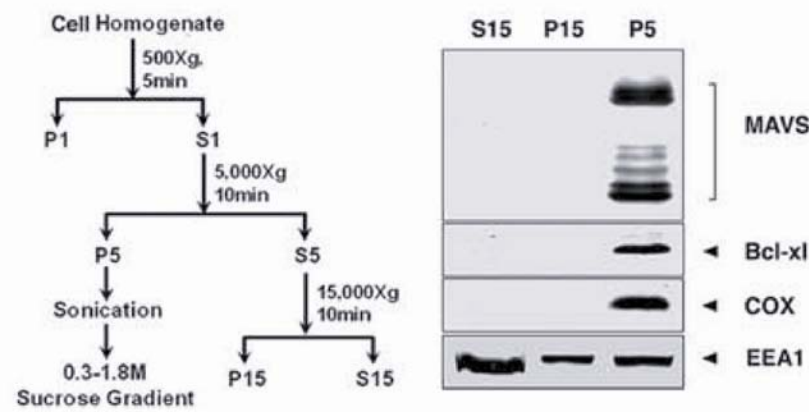


Figure 28b

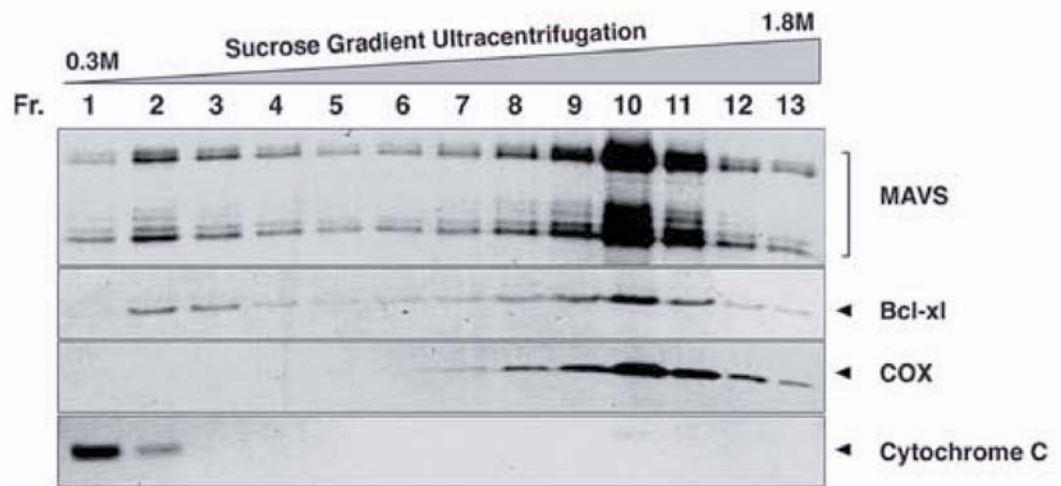


Figure 28: Subcellular fractionation of MAVS

- (a) HEK293 cells were homogenized in an isotonic buffer and then subjected to differential centrifugation according to the scheme shown in the left panel. On the right panel, different fractions as indicated were analyzed by immunoblotting with antibodies against MAVS, Bcl-xL (outer mitochondrial membrane), COX (inner mitochondrial membrane), and EEA1 (endosome marker).
- (b) The crude mitochondrial fraction (P5) was sonicated to disrupt the outer mitochondrial membrane and then fractionated by sucrose gradient ultracentrifugation. The fractions were immunoblotted with the indicated antibodies.

V. C. 2. Mislocalization of MAVS Impairs Its Function

The experiments described previously show that MAVS is predominantly localized to the mitochondrial membrane (Figure 27), and that removal of the mitochondrial targeting sequence abolishes its activity (Figure 23). To further examine the importance of mitochondrial localization for MAVS function, we replaced the C-terminal TM domain of MAVS with peptide sequences that target MAVS to different membrane locations. These sequences include the CAAX motif from Rac1 that is known to target fusion proteins predominantly to the plasma membrane (Michaelson et al., 2001); the ER targeting sequence from VAMP-2 (vesicle associated membrane protein-2), which is predominantly an ER membrane protein (Kim et al., 1999); the TM sequence from Bcl-2, which is localized in both ER and mitochondria (Kaufmann et al., 2003); and the TM sequence from Bcl-xL, which is predominantly in the mitochondrial outer membrane (Kaufmann et al., 2003). As shown in Figure 29a, replacement of the

TM domain of MAVS with the analogous domain from Bcl-2 or Bcl-xL did not impair the ability of MAVS to induce IFN- β . In contrast, the mislocalization of

Figure 29a

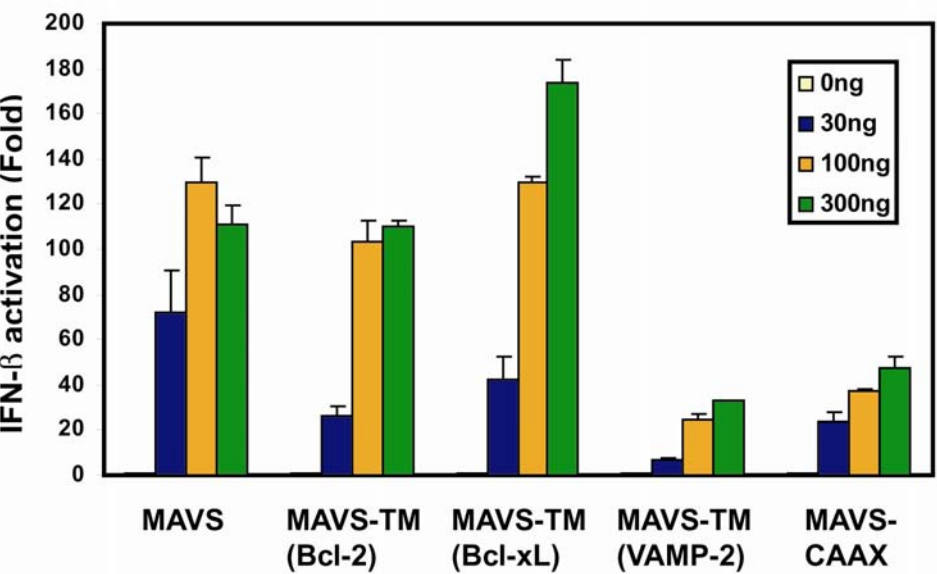
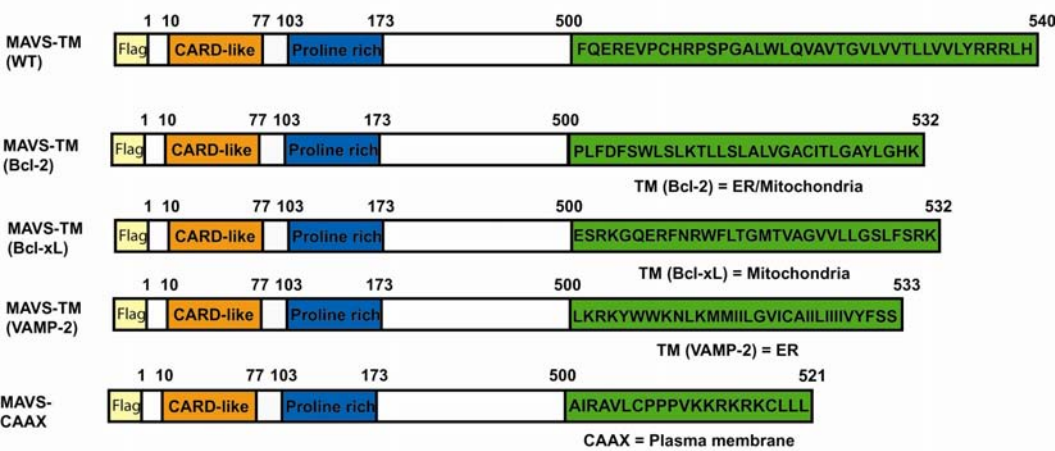


Figure 29b

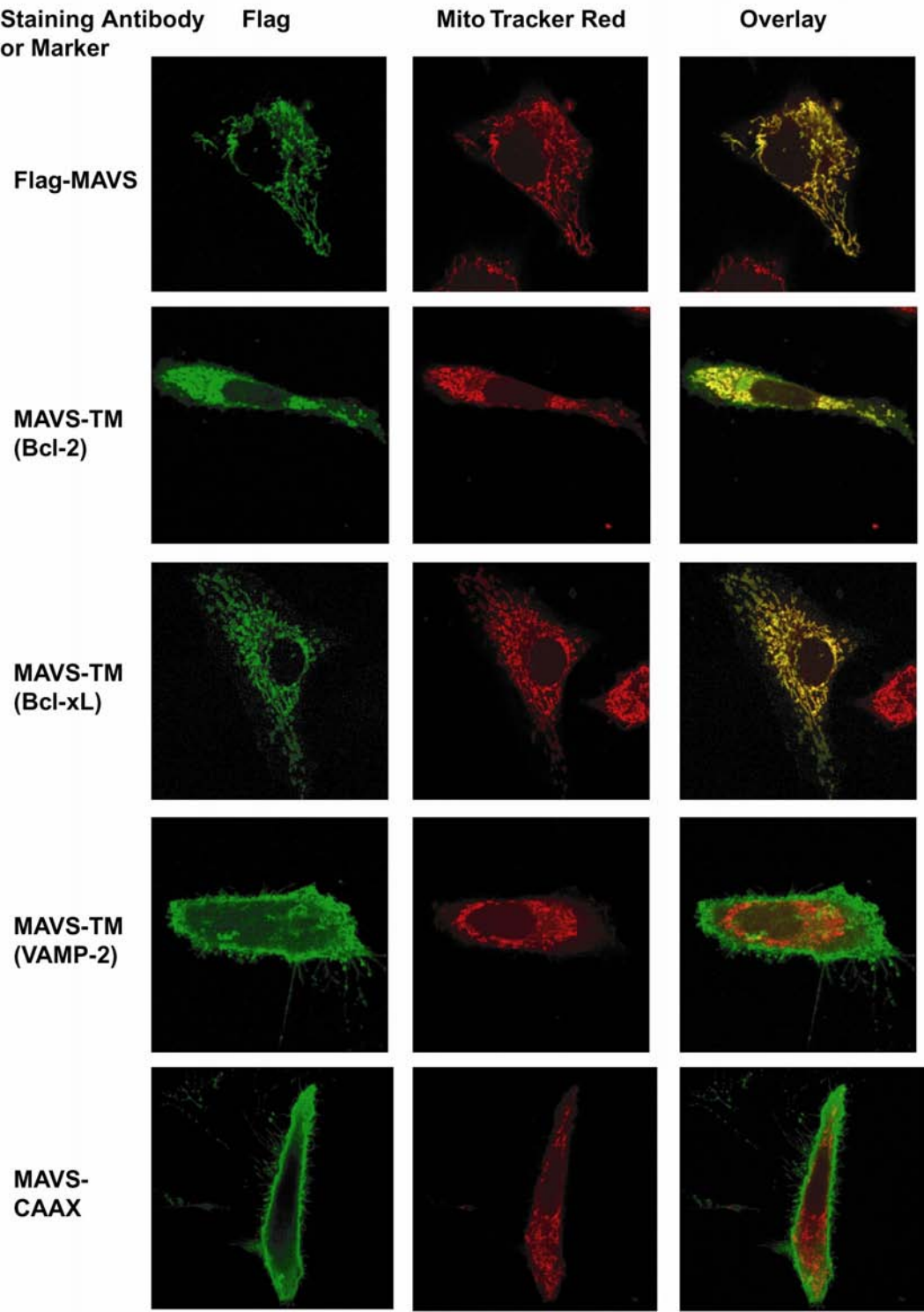


Figure 29: Mislocalization of MAVS impairs its function

- (a) Expression vectors for the MAVS fusion proteins as indicated on the top panel were transfected into HEK293 cells together with IFN β -Luc to measure IFN- β induction (lower panel).
- (b) The subcellular localization of the MAVS fusion proteins was determined by transfection of the expression vectors for the MAVS fusion proteins into Hela cells and imaging by confocal microscopy. Mito Tracker dye was used to stain the mitochondria.

MAVS to the ER (VAMP-2) or plasma membrane (CAAX) markedly reduced the activity of MAVS. Confocal microscopy experiments confirmed that the majority of MAVS fusion proteins containing the CAAX or VAMP-2 targeting sequences were no longer present in the mitochondria, whereas the fusion proteins containing the Bcl-2 or Bcl-xL targeting sequences were predominantly in the mitochondria (Figure 29b). The residual activity (20-30% of the wild type MAVS) may be due to incomplete mislocalization of the over-expressed MAVS proteins. Taken together, these results clearly demonstrate the importance of mitochondrial localization for the signaling function of MAVS.

V. D. Discussion

Data shown in this chapter supports a mitochondrial localization of MAVS (Figure 27 and 28). Similar to the transmembrane domains of other members of the tail-anchored protein family, the C-terminal hydrophobic region of MAVS is responsible for targeting MAVS to the mitochondria. Deletion of the transmembrane domain of MAVS mislocalizes the protein to the cytosol (Figure

27b). Further, fusion of the MAVS transmembrane domain to green fluorescent protein (GFP-TM) is sufficient to target GFP to the mitochondria (Figure 27d).

The transmembrane domain of MAVS is important for its function as the deletion of this domain abolishes the activity of MAVS (Figure 23). Two possibilities could explain the inability of the MAVS- Δ TM protein to signal. It is possible that the MAVS simply interacts with another component of the antiviral signaling pathway through the transmembrane domain, and loss of this interaction leads to the inability of MAVS- Δ TM to signal. In this scenario, the sequence of the transmembrane domain *per se* is important for MAVS function. A second possibility is that the mitochondrial localization of MAVS is important for its function, and the sole function of the transmembrane domain of MAVS is to target the protein to mitochondria. In this scenario, it is not the sequence of the transmembrane domain, but the ability of this domain to target MAVS to the mitochondria that is important for MAVS function. To distinguish between these possibilities, the transmembrane domain of MAVS was replaced by transmembrane domains of Bcl-2 and Bcl-xL. Bcl-2 and Bcl-xL have no known function in the antiviral immune response, but their transmembrane domains target these proteins to the mitochondria. If the sequence of the transmembrane domain is important for MAVS function, the replacement of MAVS transmembrane domain with the transmembrane domains of Bcl-2 and Bcl-xL should abolish the function of MAVS. On the other hand, if the function of

MAVS transmembrane domain of MAVS is to target the protein to the mitochondria, the fusion of MAVS to the transmembrane domain of Bcl-2 or Bcl-xL should not affect its activity. Our results show that the fusion of MAVS to the transmembrane domains of Bcl-2 or Bcl-xL does not inhibit the ability of MAVS to function. Therefore, the transmembrane domain of MAVS contributes to the function of the protein by targeting it to the mitochondria. Further, the mitochondrial localization of MAVS is important for the function of MAVS as mislocalization of MAVS to membrane compartments other than mitochondria inhibits its ability to induce the IFN- β promoter (Figure 29a).

MAVS provides the first example of a mitochondrial protein involved in the antiviral signaling pathway. Other components of the RIG-I signaling pathway including RIG-I itself, and the downstream kinases like TBK1 and IKK complex are cytosolic proteins. Mitochondria are composed of an outer and inner membrane separated by the intermembrane space. The outer mitochondrial membrane is in contact with the cytosol. Preliminary biochemical data suggest that MAVS is present on the outer mitochondrial membrane. Presumably, this localization allows MAVS to interact with other components of the antiviral signaling pathway which are cytosolic. Further studies using electron microscopy will be required to confirm the localization of MAVS to the outer mitochondrial membrane.

The orientation of MAVS within the mitochondrial outer membrane has not been determined yet. The tail-anchored proteins, including Bcl-2 family members, are inserted into the membranes such that their N-termini face the cytosol. Depending on the localization of these proteins in the endoplasmic reticulum or mitochondria, the C-terminal tail region of these proteins protrudes into the lumen of the endoplasmic reticulum or the inter-mitochondrial space respectively. Based on the topology of other tail-anchored proteins, the MAVS N-terminal CARD domain is likely to face the cytosol. Previous studies have used techniques like protease protection, glycosylation site mapping, and cysteine derivitization to define the topology of membrane bound proteins. Similar techniques can be used to confirm the orientation of MAVS.

Although no change in MAVS protein expression or modification was observed following viral infection, a change in MAVS localization was observed in the presence of virus. The majority of MAVS protein can be extracted from mitochondrial membranes of mock-infected cells with 0.5% Triton X-100. But most of the MAVS protein becomes resistant to extraction by detergent following viral infection (data not shown; performed by Dr. Lijun Sun, Dr. James Chen's laboratory). These preliminary results suggest that MAVS translocates to a detergent resistant membrane domain or protein complex following viral infection. Membrane domains termed lipid rafts are characterized by their insolubility by non-ionic detergents (Anderson and Jacobson, 2002). These

membrane domains are rich in cholesterol, sphingomyelin and glycolipids like GM1 gangliosides and have been suggested to serve as a platform for several signaling pathways including G-protein coupled receptor signaling (Chini and Parenti, 2004). Thus, it is possible that MAVS translocates to the detergent insoluble membrane domains where it serves to recruit other components of the signaling pathway. Further studies are required to determine the precise location to which MAVS emigrates, and whether this new localization is required for the function of MAVS in the antiviral immune response.

The localization of MAVS to the mitochondria provides a strategic position to detect viral replication, which often occurs in intracellular organelles such as endoplasmic reticulum. For example, the replication of hepatitis C virus (HCV) RNA occurs in a membranous web that connects the endoplasmic reticulum and mitochondria (Rehermann and Nascimbeni, 2005). The reason for why localization of MAVS to the mitochondria is important for its function is not understood. It is possible that MAVS activates NF- κ B and IRF3 by mobilizing other mitochondrial components or through direct interaction with mitochondrial proteins functioning in the antiviral signaling pathway, but either of these possibilities is unprecedented in the literature.

CHAPTER VI: MAVS IS TARGETED FOR CLEAVAGE BY HEPATITIS C VIRUS ENCODED NS3/4A PROTEASE

VI. A. Introduction

Hepatitis C virus (HCV) infects more than 170 million people in the world, and approximately 80% of the infected individuals develop persistent infection (Chisari, 2005; Lindenbach and Rice, 2005). HCV is an enveloped single-strand RNA virus belonging to the *Flaviviridae* family. It contains a 9.6-kb RNA genome that encodes a large polyprotein (over 3000 amino acids), which is cleaved into ten structural and non-structural (NS) proteins through the action of cellular peptidases as well as the viral encoded proteases including NS3/4A. NS3 contains serine protease and RNA helicase activities that require its cofactor NS4A, which tethers the holoenzyme complex to an intracellular membrane compartment. The NS3/4A protease is not only essential for generating mature viral proteins required for viral replication, but can also suppress the host antiviral immune system by cleaving putative cellular targets involved in the induction of type I IFN, such as IFN- α and IFN- β (Foy et al., 2003).

Recent studies have shown that NS3/4A inhibits interferon induction by RIG-I (Foy et al., 2005). However, RIG-I is not cleaved by NS3/4A. Although NS3/4A cleaves TRIF (Li et al., 2005a), an adaptor protein that binds to Toll-like receptors such as TLR3 and TLR4, the significance of this cleavage for antiviral immune response is not clear as TRIF is not essential for interferon induction by

viruses (Kato et al., 2005). Thus, the target of NS3/4A in the viral pathway remains to be identified.

As described in previous chapters, MAVS is a novel CARD domain involved in the antiviral signaling pathway. Since MAVS functions downstream of RIG-I, it raises the possibility that NS3/4A abolishes RIG-I mediated signaling by cleaving MAVS. This chapter describes experiments conducted to determine if MAVS is cleaved by NS3/4A such that the induction of IFN is abolished.

VI. B. Materials and Methods

VI. B. 1. Plasmids and antibodies

pcDNA3-Flag-MAVS-HA was constructed by subcloning the DNA fragment encoding MAVS-HA into the XhoI and XbaI sites of the pcDNA3-Flag vector such that the N-terminal Flag epitope was fused in frame with MAVS-HA (Dr. Lijun Sun, Dr. James Chen's laboratory). NS3/4A was amplified by RT-PCR from the RNA of HCV replicon cell line K2040, and then cloned into pcDNA3 in frame with an N-terminal Flag or Myc tag (Dr. Xiao Dong Li, Dr. James Chen's laboratory). The S139A mutant of NS3/4A and the cysteine mutant of MAVS (C508R) were generated by site-directed mutagenesis using the QuickChange kit (Stratagene). All plasmids were verified by automatic DNA sequencing.

The HCV NS3 antibody was purchased from Novocastra Laboratories Ltd. The monoclonal antibody against Myc (9E10, Santa Cruz) was purchased from the indicated suppliers.

VI. B. 2 Cell culture, transfection, and luciferase reporter assays.

HEK293 and HeLa cells were from ATCC. Transfection of HEK293 cells was carried out using the calcium phosphate precipitation method. HeLa cells were transfected using the PolyFect reagent (Qiagen). Luciferase reporter assays were performed as described previously.

VI. B. 3 Subcellular fractionation.

HEK293 cells were transfected with expression vectors for Flag-MAVS-HA or the C508R mutant together with Myc-tagged NS3/4A or its inactive mutant S139A. 36hr after transfection, cells were washed in the hypotonic buffer [10mM Tris-HCl, pH7.5, 10mM KCl, 1.5mM MgCl₂, and protease inhibitors] and then homogenized in the same buffer by douncing for 20 times. The homogenate was centrifuged at 500xg for 5 minutes to remove nuclei and unbroken cells. The supernatant was centrifuged again at 5,000xg for 10 minutes to generate membrane pellets (P; containing mostly mitochondria) and cytosolic supernatant (S).

The experimental procedures for viral infection, immunoblotting, immunoprecipitation, and confocal microscopy have been described previously.

VI. C. Results

VI. C. 1. NS3/4A blocks IFN- β induction by MAVS

To determine if NS3/4A inhibits IFN- β induction by MAVS, we transfected expression vectors encoding NS3/4A and MAVS into HEK293 cells together with a luciferase reporter driven by the IFN- β promoter (IFN β -Luc). As controls, we infected cells with Sendai virus (SV) or transfected cells with an expression vector encoding the N-terminal CARD domains of RIG-I [RIG-I(N)], which has previously been shown to induce IFN- β . In each case, NS3/4A inhibited the induction of IFN- β (Figure 30a). In contrast, the induction of IFN- β by TBK1 was not affected by NS3/4A, suggesting that NS3/4A inhibits the RIG-I pathway at the level of MAVS or at a step downstream of MAVS but upstream of TBK1. To determine if the protease activity of NS3/4A was required for this inhibition, we mutated the active site Ser-139 of NS3/4A (equivalent to Ser-1165 of the HCV polyprotein) to alanine. This mutant migrated more slowly than the wild type NS3 (Figure 30d, bottom panel), as it could no longer be cleaved at the junction between NS3 and NS4A. The protease-dead mutant completely lost its ability to inhibit IFN- β induction by Sendai virus, RIG-I(N) or MAVS. Thus, it is likely that NS3/4A inhibits interferon induction by cleaving MAVS or a target downstream of MAVS. NS3/4A also prevented the MAVS induced activation

Figure 30a

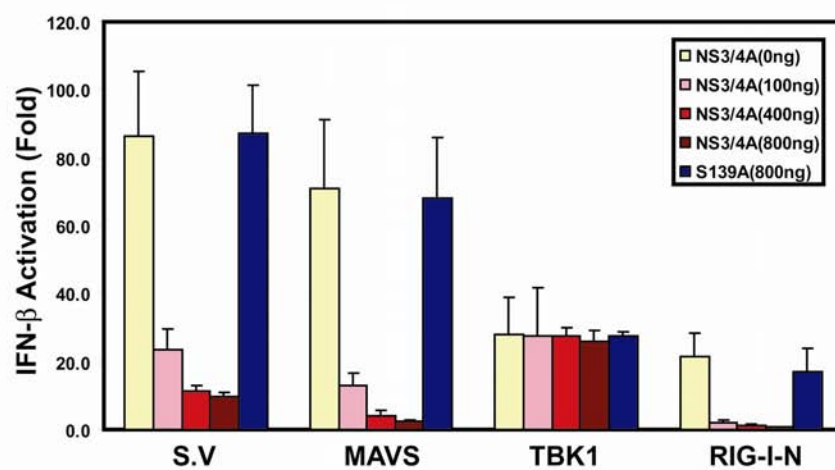


Figure 30b

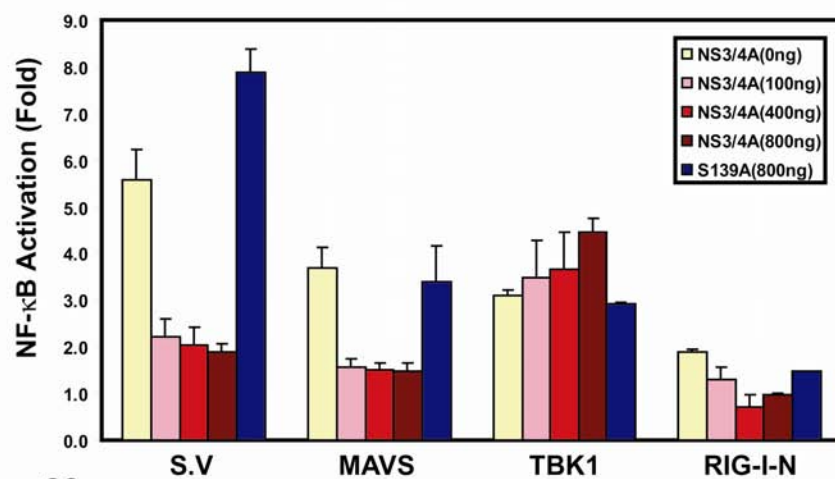


Figure 30c

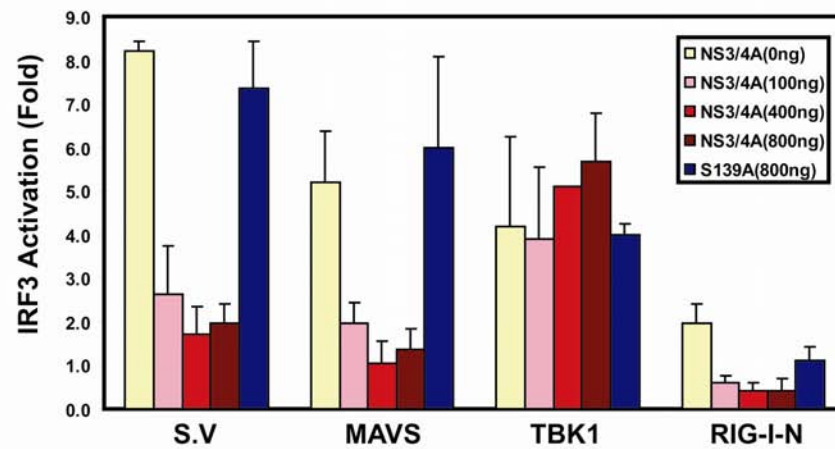
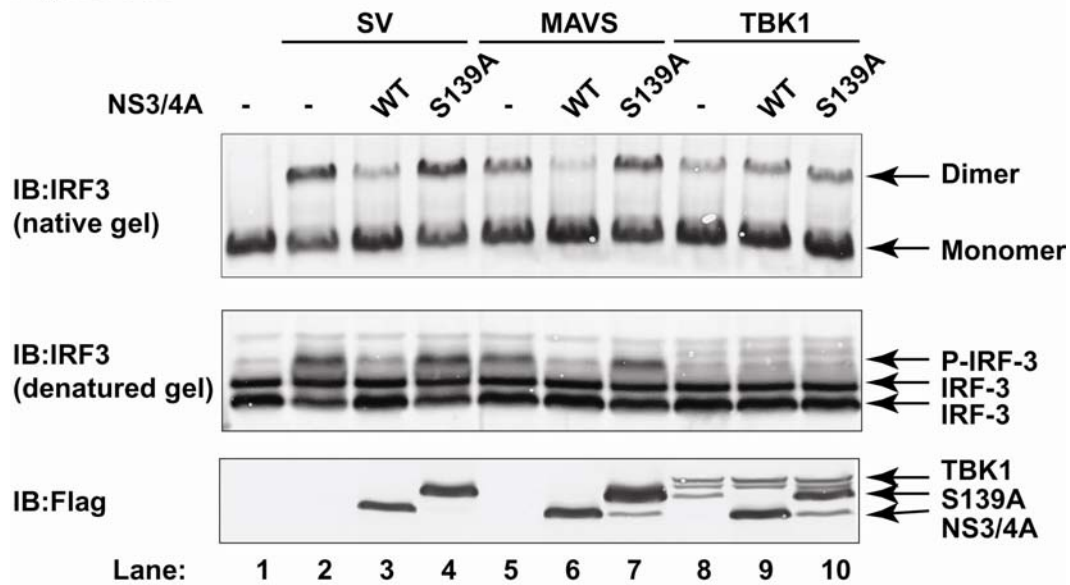


Figure 30d**Figure 30: NS3/4A blocks interferon induction by MAVS**

- (a) HEK293 cells were transfected with the IFN- β luciferase reporter construct together with the expression vector for the wild type or S139A mutant of NS3/4A. The next day, cells were transfected with expression vectors encoding MAVS, TBK1, or RIG-I(N), or infected with Sendai virus. 24 hours later, the luciferase activity was measured and normalized for transfection efficiency. The error bar represents standard deviation from the mean value of duplicated experiments.
- (b) Similar to (a), except that NF- κ B luciferase reporter was used in lieu of IFN- β -Luc.
- (c) Similar to (a), except that cells were transfected with the UAS-luciferase reporter together with the Gal4-IRF3 expression vector.
- (d) HEK293 cells were transfected with the wild type or S139A mutant of NS3/4A together with the expression vectors for MAVS (lanes 5-7) or TBK1 (lanes 8-10). In lanes 2-4, cells were infected with Sendai virus for 24 hours. Cell lysates were resolved by electrophoresis under native (upper) or denaturing condition (middle) and then immunoblotted with an antibody against IRF3. The expression of NS3/4A and TBK1 was also analyzed by immunoblotting with a Flag antibody (bottom panel).

of NF- κ B (Figure 30b) and IRF3 reporters (Figure 30c), as well as the phosphorylation and dimerization of IRF3 (Figure 30d), further supporting the notion that NS3/4A inactivates a common target required for both NF- κ B and IRF3 activation.

VI. C. 2. MAVS is the proteolytic target of NS3/4A

To determine if MAVS is the proteolytic target of NS3/4A, expression vectors encoding FLAG-NS3/4A or FLAG-NS3/4A (S139A) were transfected into HEK293 cells. As MAVS is a mitochondrial membrane protein, the cell lysates were separated into cytosolic fraction (S) and membrane pellets (P) by centrifugation, and the endogenous MAVS protein analyzed by immunoblotting with an affinity-purified MAVS antibody (Figure 31; performed by Dr. Lijun Sun, Dr. James Chen's laboratory). The expression of NS3/4A, but not the protease-dead mutant of NS3/4A, led to the generation of a faster-migrating, truncated fragment of MAVS that was approximately 3-5 kDa shorter than the full-length MAVS (Figure 31, compare lanes 3 & 4, upper panel). Interestingly, unlike the full-length MAVS that was present in the membrane pellet, the truncated fragment of MAVS was mainly present in the soluble cytosolic fraction, suggesting that the truncated fragment did not contain the C-terminal transmembrane domain. Immunoblotting experiments also showed that the

majority of NS3 is in the membrane pellet, presumably due to its association with NS4A (Figure 31, lower panel).

Figure 31

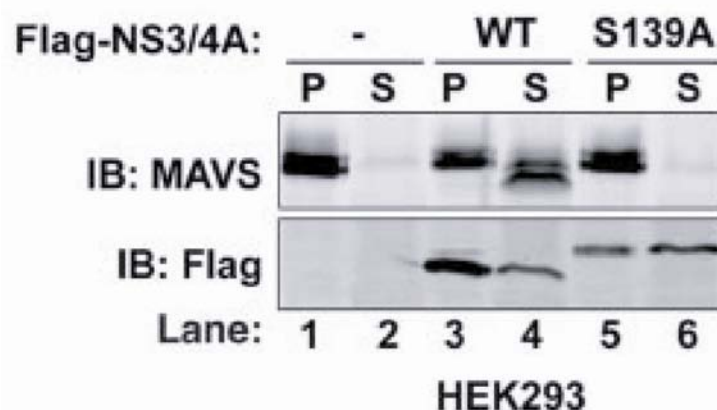


Figure 31: MAVS is cleaved by NS3/4A

HEK293 cells (lanes 1-6) cells were transfected with expression vectors for the wild type (lanes 3, 4) or S139A mutant (lanes 5, 6) NS3/4A or vector alone (lanes 1, 2). Cell lysates were separated into membrane pellet (P) or cytosolic supernatant (S), and then immunoblotted with an antibody against MAVS or Flag.

VI. C. 3. NS3/4A Cleaves MAVS at Cys-508.

NS3/4A is a serine protease that cleaves at the C-terminus of a Cys or Thr residue within a loosely defined consensus sequence [(E/D)xxxx(C/T)(S/A), where x denotes any amino acid], which is found at the junction of HCV nonstructural proteins (Figure 32a). Inspection of the MAVS amino acid sequence revealed a potential NS3/4A cleavage sequence, ⁵⁰³EREVPCH⁵⁰⁹. The potential cleavage site, Cys-508, is located 6 amino acids from the beginning of the transmembrane domain and 32 amino acids from the C-terminus of MAVS.

Cleavage at Cys-508 is predicted to generate an approximately 32-residue C-terminal fragment. Indeed, when NS3/4A is co-transfected together with an expression construct encoding a MAVS protein that is tagged with FLAG at the N-terminus and HA at the C-terminus, the MAVS protein was cleaved into a soluble FLAG-tagged N-terminal fragment that was smaller than the intact protein (Figure 32b, upper panel; compare lanes 1 & 4; performed by Dr. Lijun Sun, Dr. James Chen's laboratory). Moreover, a C-terminal fragment of approximately 7 kDa in size was detectable in both the membrane pellet and cytosolic fractions with an HA antibody (Figure 32b, middle panel; lanes 3 & 4). This cleavage product of MAVS was not detected in cells expressing the S139A mutant of NS3/4A. Although the apparent molecular mass of the C-terminal cleavage fragment was greater than the theoretical molecular mass of the fragment containing the C-terminal 32 residues of MAVS plus an HA epitope (approximately 5 kDa), this is likely due to the abnormal migration of small peptides on SDS-PAGE. Indeed, when we synthesized the C-terminal 32 residues of MAVS (residue 509 to 540) plus the HA epitope by *in vitro translation*, this fragment also migrated as an approximately 7 kDa band (data not shown, performed by Dr. Lijun Sun, Dr. James Chen's laboratory), identical to the C-terminal fragment of MAVS after cleavage by NS3/4A.

To demonstrate that Cys-508 is indeed the cleavage site, we mutated Cys-508 to Arg, which is predicted to disrupt NS3/4A cleavage based on the

Figure 32a

	-10		+10
NS3/4A	CMSADLEVV	T	STWVLVGGVL
NS4A/4B	YREFDEMEEC	A	ASHLPYIEQG
NS4B/5A	WINEDCSTPC	S	SGSWLRDVWD
NS5A/5B	EEASEDVVCC	S	SMSYTWTGAL
			↗TM
MAVS (human)	RKFQEREVPC		HRPSPGALWL
MAVS (chimpanzee)	RKFQEREVPC		HRPSPGALWL
MAVS (mouse)	QQPQEEEEHC		ASSMPWAKWL
MAVS (rat)	QQSPEEEEPC		ASSVSWAKWL
MAVS (chicken)	NNSSHAEVPT		SGDSNGPSLL
MAVS (puffer fish)	PAPQDPTKKT		SSHFLTNTK

Figure 32b

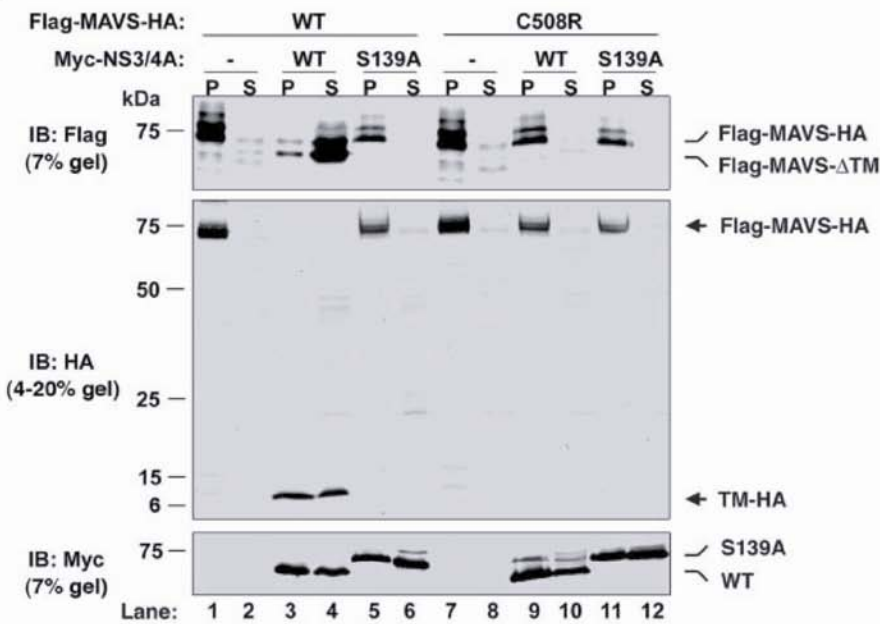


Figure 32c

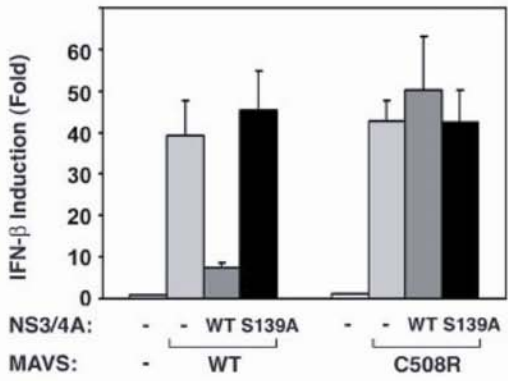


Figure 32: NS3/4A cleaves MAVS at Cys-508

- (a) Alignment of the NS3/4A cleavage site of nonstructural (NS) proteins of HCV, and the putative cleavage site at the C-terminus of MAVS from different species.
- (b) HEK293 cells were transfected with expression vectors encoding the wild type or C508R mutant of MAVS together with those encoding the wild type or S139A mutant of NS3/4A. Cell lysates were separated by differential centrifugation into the membrane pellet (P) and cytosolic supernatant (S), which were then resolved by 7% (upper panel and lower panel) or 4-20% (middle panel) SDS-PAGE, following by immunoblotting with the indicated antibody that detects the N-terminus (Flag; upper panel) or C-terminus (HA; middle panel) of MAVS, or NS3/4A (Myc; lower panel).
- (c) HEK293 cells were transfected with MAVS and NS3/4A expression vectors as in (b), except that IFN- β -Luc was also co-transfected to measure the induction of IFN- β by luciferase assay.

analysis of sequence requirement for HCV polyprotein cleavage (Kolykhalov et al., 1994). Remarkably, this single amino acid substitution completely blocked the cleavage of MAVS by NS3/4A (Figure 32b, lanes 7-12; performed by Dr. Lijun Sun, Dr. James Chen's laboratory). Furthermore, the protease-resistant mutant of MAVS was fully capable of inducing IFN- β , and this induction was no longer inhibited by NS3/4A (Figure 32c). Taken together, these results indicate that NS3/4A cleaves MAVS at Cys-508 when these proteins are co-expressed in the same cells.

VI. C. 4. NS3/4A colocalizes with MAVS in the mitochondria

It has been shown that HCV core protein and NS3/4A are localized to a mitochondrion-associated membrane structure in both cultured hepatocytes (Mottola et al., 2002; Schwer et al., 2004) and liver biopsies of chronic hepatitis C patients (Kasprzak et al., 2005). Since MAVS is a mitochondrial membrane protein, we examined whether MAVS and NS3/4A co-localize in the same membrane compartment. Expression vectors encoding Myc-NS3/4A and/or HA-MAVS were transfected into HeLa cells, which were then stained with the corresponding antibodies followed by imaging with a laser scanning confocal microscope. To stain the mitochondria, cells were incubated with Mito Tracker, a fluorescent dye taken up by the mitochondria of living cells. The staining patterns of the wild type NS3/4A overlapped with that of Mito Tracker (Figure 33a, upper panel), but not the endoplasmic reticulum resident protein calnexin (Figure 33a, lower panel), suggesting that NS3/4A is localized to the mitochondria or in a mitochondrion-associated membrane. When the wild type NS3/4A and MAVS were co-expressed, the majority of MAVS became cytosolic (presumably due to cleavage), as revealed by an antibody that detects the N-terminus of MAVS (Figure 33b, upper panel). In sharp contrast, when the wild type NS3/4A was co-expressed with MAVS-C508R, both NS3/4A and MAVS-C508R proteins co-localized in the mitochondrial membrane and showed an extensive overlapping staining pattern (Figure 33b, lower panel). These results indicate that MAVS and

Figure 33a

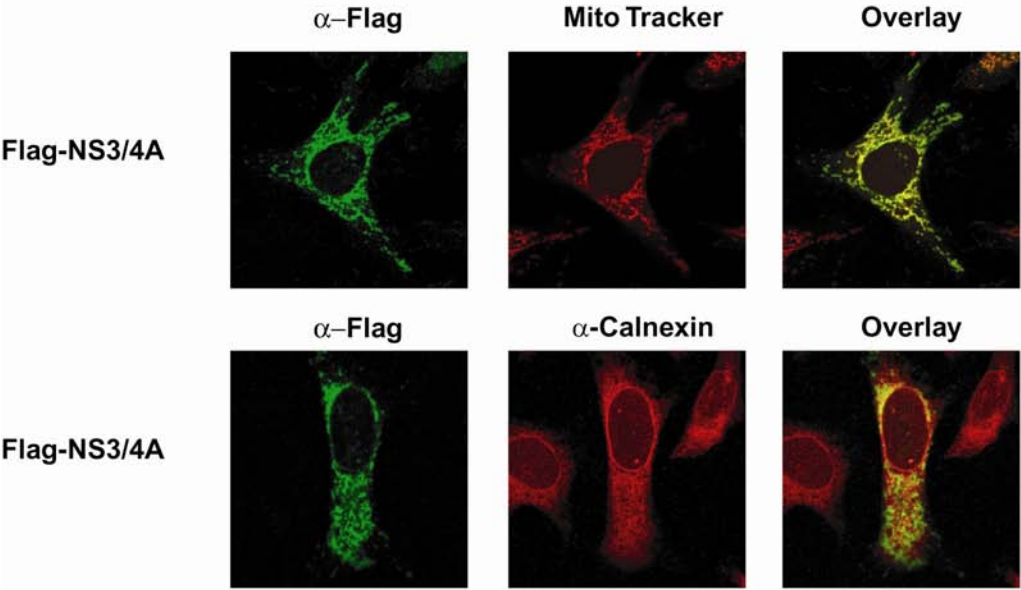


Figure 33b

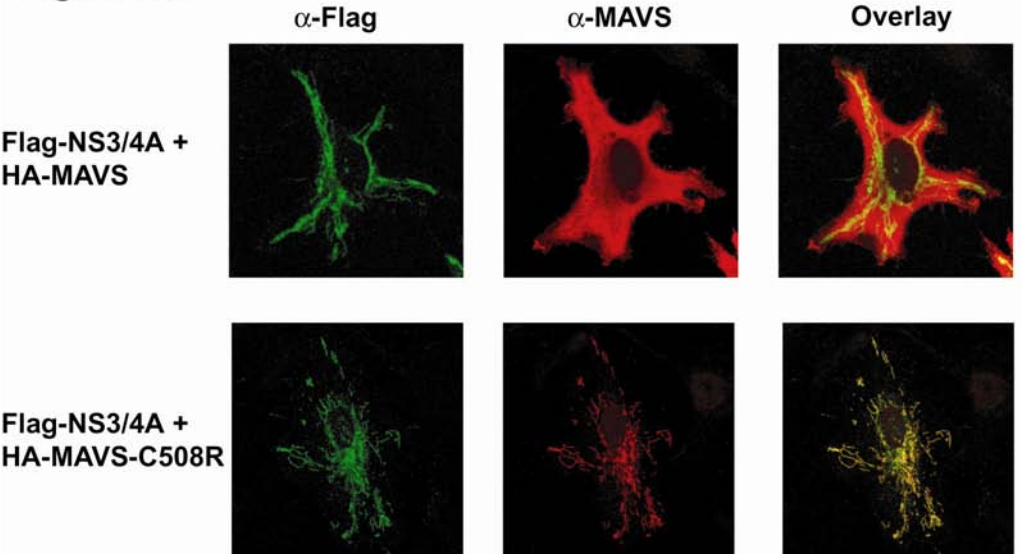


Figure 33: NS3/4A colocalizes with MAVS in the mitochondria

- (a) Expression vector for Flag-NS3/4A was transfected into HeLa cells, and the co-localization of this protein with mitochondrial (Mito Tracker; upper panel) and ER (calnexin; lower panel) markers was determined by confocal microscopy.
- (b) Expression vectors for Flag-NS3/4A and HA-MAVS or C508R mutant were transfected into HeLa cells, and the localization of these proteins was determined by staining by the indicated antibodies and visualized by confocal microscopy.

NS3/4A are co-localized in the mitochondrial membrane or are positioned in very close proximity, thus rendering MAVS vulnerable to cleavage by NS3/4A.

VI. D. Discussion

The data discussed in this chapter shows that MAVS is the proteolytic target of HCV NS3/4A protease. NS3/4A co-localizes with MAVS at the mitochondrial membrane. NS3/4A cleaves MAVS at Cys-508 such that MAVS is mislocalized from the mitochondria to the cytosol, thus preventing the induction of IFN- β .

The experiments described above were performed in cells that over-express NS3/4A. In data not shown in this chapter, Dr. Lijun Sun and Dr. X. D. Li (Dr. James Chen's laboratory) have discovered that endogenous MAVS is cleaved in HCV replicon cell culture system in which the subgenomic RNA of HCV replicates autonomously in the human hepatoma cell line Huh7 (Li et al., 2005b). The HCV subgenomic RNA encodes all the nonstructural proteins,

including the NS3/4A protease and the NS5B RNA polymerase. It has been shown previously that the HCV replicon cell lines that replicate the viral RNA efficiently suppress the host interferon induction through the proteolytic activity of NS3/4A (Foy et al., 2003). To confirm that the cleavage of MAVS is solely responsible for the failure to induce IFNs in HCV replicon cells, it was demonstrated that the expression of protease resistant MAVS (MAVS C508R) restores IFN- β induction in the replicon cells to the same level observed in the parental Huh7 cells (Li et al., 2005b).

Meylan et al. have also reported the identification of MAVS/CARDIF as the target of NS3/4A (Meylan et al., 2005). Several other groups have recently used the infectious HCV virus to demonstrate that MAVS is targeted for cleavage by NS3/4A expressed by this virus (Cheng et al., 2006; Loo et al., 2006).

Our current study not only provides the direct biochemical evidence that MAVS is the proteolytic target of NS3/4A but also underscores the importance of mitochondrial localization of MAVS in antiviral immunity. This study has important implications not only in increasing our understanding of the immune response mounted against HCV infections but also in the development of new therapies against HCV.

CHAPTER VII: CONCLUSION

VII. A. Model for function of MAVS in the RIG-I mediated antiviral signaling pathway (Figure 34)

RIG-I has recently been identified as an intracellular receptor for virally-derived dsRNA receptor. RIG-I contains two N-terminal CARD domains and a C-terminal helicase domain. The CARD domains signal to downstream components of the pathway that lead to the activation of NF- κ B and IRF3. In the absence of dsRNA, the function of RIG-I CARD domains is inhibited. It has been suggested that the binding to dsRNA to the RNA helicase domain of RIG-I induces a conformational change that exposes the N-terminal CARD domains to recruit downstream signaling proteins.

The data presented in this thesis describes the identification and characterization of a novel CARD domain containing protein that acts downstream of RIG-I. The MAVS CARD domain is important for signaling to downstream components of the pathway. Besides the CARD domain, MAVS also contains a central proline-rich domain and a C-terminal transmembrane domain. The contribution of the proline-rich domain towards MAVS function is not clear. The transmembrane domain targets MAVS to the mitochondria. Although the importance of the mitochondrial localization of MAVS for its function has been convincingly demonstrated, the role of mitochondria in the activation of IKK and TBK1 is not understood.

Figure 34

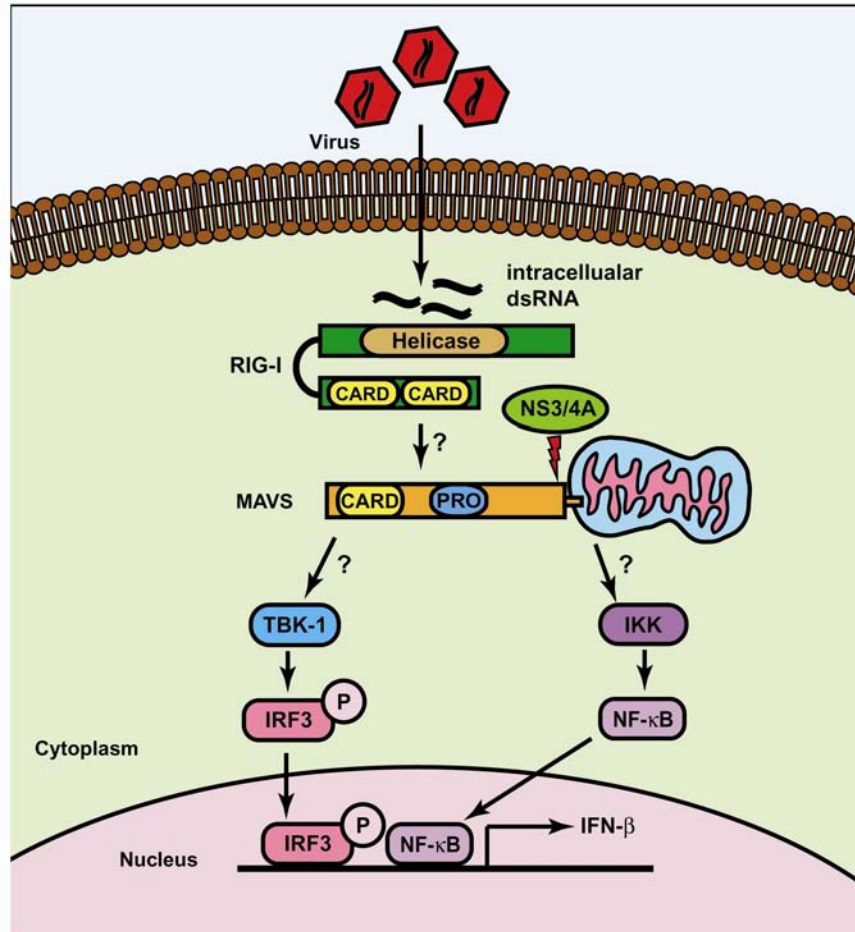


Figure 34: Proposed model for RIG-I mediated signaling

RIG-I is a receptor for intracellular dsRNA. It contains a C-terminal RNA helicase domain that binds to viral double stranded RNA, and two tandem CARD domains at the N-terminus. The binding of dsRNA to the helicase domain presumably induces a conformational change that exposes the CARD domains to initiate a signaling cascade. MAVS is a CARD domain containing mitochondrial protein that functions downstream of RIG-I. MAVS can signal to both the NF-κB and IRF3 signaling pathways by activating the IKK and TBK1/IKKi kinase complexes. Once activated, NF-κB and IRF3 translocate into the nucleus and turn on the IFN-β gene promoter. The mechanism by which MAVS activates downstream kinase pathways is not clear, although it has been shown that the mitochondrial membrane localization of MAVS is

essential for its signaling function. The importance of the mitochondrial localization of MAVS is underscored by the recent discovery that the hepatitis C virus protease NS3/4A cleaves MAVS off the mitochondria to evade the host innate immune system.

The mechanism by which MAVS is regulated by RIG-I and how MAVS signals to downstream kinases warrants further investigation. Although MAVS interacts with RIG-I in over-expression experiments, the physiologic relevance of this interaction in transmission of signal from RIG-I to MAVS remains to be verified. The signaling mechanism of MAVS is also a subject of debate at present. MAVS interacts with TRAF6 through two TRAF6 binding motifs. However, as discussed in chapter IV, the MAVS mutant (CARD-TM) that lacks all TRAF-binding sites is still capable of inducing IFN- β . Furthermore, TRAF6-deficient cells have normal induction of IFN- β following viral infection. Interaction of MAVS with RIP-1 and FADD has been proposed as a mechanism by which MAVS signals to IKK (Kawai et al., 2005). However, RIP1-deficient MEF cells are also fully capable of inducing IFN- β following viral challenges. Meylan et al. report that MAVS directly binds to IKK α and IKK β (Meylan et al., 2005), but other studies have not been able to detect this interaction. Thus, there is no consensus mechanism that emerges from these independent studies. Further studies are clearly required to elucidate the mechanism of MAVS signaling.

The discovery of MAVS has also provided a breakthrough in the field of hepatitis C virus (HCV) research. MAVS is the long-sought target of HCV

encoded NS3/4A protease. NS3/4A cleaves MAVS at Cys-508, which is located a few residues before the mitochondrial targeting domain of MAVS. As a result of the proteolytic cleavage, MAVS is dislodged from the mitochondria and becomes an inactive cytosolic fragment. This observation further underscores the importance of mitochondrial localization for MAVS function.

VII. B. Contribution of mitochondria in antiviral signaling pathway

The demonstration that the obligatory localization of MAVS to the mitochondria is essential for its function, points to a role of mitochondria in the antiviral signaling pathway. The mechanistic understanding of the contribution of mitochondria for MAVS-mediated signaling is unclear.

Mitochondria have emerged as major sensors of extracellular and intracellular stress. The role of mitochondria in regulating apoptosis in stress signals has been well characterized (Wang, 2001). Several apoptotic and anti-apoptotic proteins are localized to the mitochondria. The first mitochondrial protein known to be involved in apoptosis is the proto-oncogene Bcl-2, which has a C-terminal mitochondrial transmembrane domain similar to that of MAVS. In normal cells, the Bcl-2 family of proteins prevents the release of pro-apoptotic molecules such as cytochrome c and SMAC/DIABLO from the mitochondria to the cytoplasm. In response to an apoptotic stimulus such as DNA damage, cytochrome c and SMAC are released to the cytosol to initiate a caspase cascade

leading to cell death. It is therefore plausible that MAVS activates NF- κ B and IRF3 by mobilizing other mitochondrial components.

It is possible that there are other, as yet unidentified mitochondrial proteins that are involved in antiviral signaling. MAVS might depend on interaction with other mitochondrial proteins to trigger downstream signaling. In this regard, the pelleting of a virus inducible IRF3 kinase activity, described in chapter II of this thesis, in the P20 and P100 fractions is very intriguing. It is possible that this kinase is associated with certain cellular membranes. The presence of the IRF3 kinase activity in purified membrane fractions, like mitochondria, endoplasmic reticulum etc. can be detected by the *in vitro* assay described in chapter II. Therefore, mitochondria could simply act as a platform that aids in the assembly of a signaling competent protein complex.

The role for a mitochondrial protein in the RIG-I mediated antiviral signaling pathway described in this thesis, may be applicable to other immunity pathways as well. Several pathways can activate both NF- κ B and IRF3 in response to various pathogenic stimuli. These include the signaling cascade initiated by TLR3 (Kawai and Akira, 2006a) and the signaling cascade activated in response to bacterial pathogens like *Listeria monocytogenes* (Stetson and Medzhitov, 2006). Although we have shown that the TLR3-TRIF mediated induction of IFN- β is independent of MAVS, it is possible that another, as yet unidentified mitochondrial protein contributes to signaling in this pathway.

Listeria monocytogenes induces the synthesis of IFN- β by releasing bacterial DNA into the cytoplasm. The molecular components of the signaling pathway that detects bacterial DNA to trigger the activation of NF- κ B and IRF3 have not been identified as yet. But it is plausible that the anti-bacterial immunity pathway also depends on the function of a mitochondrial protein.

Prior to the identification of MAVS, the focus of antiviral research was on understanding the regulation of key transcription factors by established cytosolic signaling cascades. Our findings have established an important role for mitochondria in regulating antiviral immunity and represent a new paradigm in understanding the host-pathogen relationship.

VII. C. MAVS and disease

We have shown that higher expression of MAVS endows cells with stronger immunity to viral infection, whereas the loss of MAVS expression renders cells vulnerable to viral killing. These results raise the possibility that variations in the expression levels of MAVS may endow different individuals with differential immunity against viral diseases.

We have also shown that MAVS is required to induce a strong immune defense against HCV; however, HCV counterattacks by utilizing the NS3/4A protease to cleave MAVS, thereby evading the immune response. Since a point mutation at Cys-508 of MAVS completely prevents its cleavage by NS3/4A and

restores its antiviral activity, it would be interesting to determine whether there are sequence variations of MAVS in human population that confer differential sensitivity to NS3/4A, hence differential immunity to HCV. Our understanding of the MAVS-HCV interaction can be exploited to fight against HCV infections. For example, the cleavage of MAVS from the mitochondrial membrane may be a diagnostic marker for an established HCV infection. We have reported a good antibody to detect MAVS and this antibody can be used to determine localization of MAVS in patient samples. Indeed this antibody has recently been used to detect mislocalization of MAVS to the cytosol in liver tissues of patients chronically infected with HCV (Loo et al., 2006). Furthermore, blocking the cleavage of MAVS by NS3/4A may be effective in the prevention and treatment of HCV.

HCV may not be the only pathogen that targets MAVS to evade the host immune system. Although the mitochondrial localization of MAVS may allow the host immune system to detect many viruses that replicate in intracellular membrane locations proximal to the mitochondria, it may also render MAVS vulnerable to viral attack. For example, it has recently been shown that the hepatitis A virus (HAV) inhibits interferon response at a step downstream of RIG-I but upstream of TBK1/IKKi, raising the possibility that MAVS may be a target of an HAV protein. Future studies should uncover more examples of host-

pathogen interaction that where the functional status of MAVS determine the outcome of the disease.

Bibliography

- Akira, S., and Takeda, K. (2004). Toll-like receptor signalling. *Nat Rev Immunol* 4, 499-511.
- Akira, S., Uematsu, S., and Takeuchi, O. (2006). Pathogen recognition and innate immunity. *Cell* 124, 783-801.
- Anderson, R. G., and Jacobson, K. (2002). A role for lipid shells in targeting proteins to caveolae, rafts, and other lipid domains. *Science* 296, 1821-1825.
- Andrejeva, J., Childs, K. S., Young, D. F., Carlos, T. S., Stock, N., Goodbourn, S., and Randall, R. E. (2004). The V proteins of paramyxoviruses bind the IFN-inducible RNA helicase, mda-5, and inhibit its activation of the IFN-beta promoter. *Proc Natl Acad Sci U S A* 101, 17264-17269.
- Balachandran, S., Thomas, E., and Barber, G. N. (2004). A FADD-dependent innate immune mechanism in mammalian cells. *Nature* 432, 401-405.
- Borgese, N., Colombo, S., and Pedrazzini, E. (2003). The tale of tail-anchored proteins: coming from the cytosol and looking for a membrane. *J Cell Biol* 161, 1013-1019.
- Bouchier-Hayes, L., and Martin, S. J. (2002). CARD games in apoptosis and immunity. *EMBO Rep* 3, 616-621.
- Chen, Z. J. (2005). Ubiquitin signalling in the NF-kappaB pathway. *Nat Cell Biol* 7, 758-765.
- Cheng, G., Zhong, J., and Chisari, F. V. (2006). Inhibition of dsRNA-induced signaling in hepatitis C virus-infected cells by NS3 protease-dependent and -independent mechanisms. *Proc Natl Acad Sci U S A*.
- Chini, B., and Parenti, M. (2004). G-protein coupled receptors in lipid rafts and caveolae: how, when and why do they go there? *J Mol Endocrinol* 32, 325-338.
- Chisari, F. V. (2005). Unscrambling hepatitis C virus-host interactions. *Nature* 436, 930-932.
- Cohen, G. B., Ren, R., and Baltimore, D. (1995). Modular binding domains in signal transduction proteins. *Cell* 80, 237-248.

- Colonna, M., Trinchieri, G., and Liu, Y. J. (2004). Plasmacytoid dendritic cells in immunity. *Nat Immunol* 5, 1219-1226.
- Cordin, O., Banroques, J., Tanner, N. K., and Linder, P. (2006). The DEAD-box protein family of RNA helicases. *Gene* 367, 17-37.
- de Veer, M. J., Holko, M., Frevel, M., Walker, E., Der, S., Paranjape, J. M., Silverman, R. H., and Williams, B. R. (2001). Functional classification of interferon-stimulated genes identified using microarrays. *J Leukoc Biol* 69, 912-920.
- Deng, L., Wang, C., Spencer, E., Yang, L., Braun, A., You, J., Slaughter, C., Pickart, C., and Chen, Z. J. (2000). Activation of the IkappaB kinase complex by TRAF6 requires a dimeric ubiquitin-conjugating enzyme complex and a unique polyubiquitin chain. *Cell* 103, 351-361.
- Diebold, S. S., Kaisho, T., Hemmi, H., Akira, S., and Reis e Sousa, C. (2004). Innate antiviral responses by means of TLR7-mediated recognition of single-stranded RNA. *Science* 303, 1529-1531.
- Fitzgerald, K. A., McWhirter, S. M., Faia, K. L., Rowe, D. C., Latz, E., Golenbock, D. T., Coyle, A. J., Liao, S. M., and Maniatis, T. (2003). IKKepsilon and TBK1 are essential components of the IRF3 signaling pathway. *Nat Immunol* 4, 491-496.
- Foy, E., Li, K., Sumpter, R., Jr., Loo, Y. M., Johnson, C. L., Wang, C., Fish, P. M., Yoneyama, M., Fujita, T., Lemon, S. M., and Gale, M., Jr. (2005). Control of antiviral defenses through hepatitis C virus disruption of retinoic acid-inducible gene-I signaling. *Proc Natl Acad Sci U S A* 102, 2986-2991.
- Foy, E., Li, K., Wang, C., Sumpter, R., Jr., Ikeda, M., Lemon, S. M., and Gale, M., Jr. (2003). Regulation of interferon regulatory factor-3 by the hepatitis C virus serine protease. *Science* 300, 1145-1148.
- Ghosh, S., May, M. J., and Kopp, E. B. (1998). NF-kappa B and Rel proteins: evolutionarily conserved mediators of immune responses. *Annu Rev Immunol* 16, 225-260.
- Gitlin, L., Barchet, W., Gilfillan, S., Cella, M., Beutler, B., Flavell, R. A., Diamond, M. S., and Colonna, M. (2006). Essential role of mda-5 in type I IFN responses to polyriboinosinic:polyribocytidylic acid and encephalomyocarditis picornavirus. *Proc Natl Acad Sci U S A*.

Hacker, H., Redecke, V., Blagoev, B., Kratchmarova, I., Hsu, L. C., Wang, G. G., Kamps, M. P., Raz, E., Wagner, H., Hacker, G., *et al.* (2006). Specificity in Toll-like receptor signalling through distinct effector functions of TRAF3 and TRAF6. *Nature* *439*, 204-207.

Harada, H., Fujita, T., Miyamoto, M., Kimura, Y., Maruyama, M., Furia, A., Miyata, T., and Taniguchi, T. (1989). Structurally similar but functionally distinct factors, IRF-1 and IRF-2, bind to the same regulatory elements of IFN and IFN-inducible genes. *Cell* *58*, 729-739.

Honda, K., Ohba, Y., Yanai, H., Negishi, H., Mizutani, T., Takaoka, A., Taya, C., and Taniguchi, T. (2005a). Spatiotemporal regulation of MyD88-IRF-7 signalling for robust type-I interferon induction. *Nature* *434*, 1035-1040.

Honda, K., Yanai, H., Negishi, H., Asagiri, M., Sato, M., Mizutani, T., Shimada, N., Ohba, Y., Takaoka, A., Yoshida, N., and Taniguchi, T. (2005b). IRF-7 is the master regulator of type-I interferon-dependent immune responses. *Nature* *434*, 772-777.

Honda, K., Yanai, H., Takaoka, A., and Taniguchi, T. (2005c). Regulation of the type I IFN induction: a current view. *Int Immunol* *17*, 1367-1378.

Horie, C., Suzuki, H., Sakaguchi, M., and Mihara, K. (2002). Characterization of signal that directs C-tail-anchored proteins to mammalian mitochondrial outer membrane. *Mol Biol Cell* *13*, 1615-1625.

Huang, S. L., Shyu, R. Y., Yeh, M. Y., and Jiang, S. Y. (2000). Cloning and characterization of a novel retinoid-inducible gene 1(RIG1) deriving from human gastric cancer cells. *Mol Cell Endocrinol* *159*, 15-24.

Ishii, K. J., and Akira, S. (2005). Innate immune recognition of nucleic acids: beyond toll-like receptors. *Int J Cancer* *117*, 517-523.

Iwamura, T., Yoneyama, M., Yamaguchi, K., Suhara, W., Mori, W., Shiota, K., Okabe, Y., Namiki, H., and Fujita, T. (2001). Induction of IRF-3/-7 kinase and NF-kappaB in response to double-stranded RNA and virus infection: common and unique pathways. *Genes Cells* *6*, 375-388.

Kanayama, A., Seth, R. B., Sun, L., Ea, C. K., Hong, M., Shaito, A., Chiu, Y. H., Deng, L., and Chen, Z. J. (2004). TAB2 and TAB3 activate the NF-kappaB pathway through binding to polyubiquitin chains. *Mol Cell* *15*, 535-548.

Kang, D. C., Gopalkrishnan, R. V., Wu, Q., Jankowsky, E., Pyle, A. M., and Fisher, P. B. (2002). mda-5: An interferon-inducible putative RNA helicase with double-stranded RNA-dependent ATPase activity and melanoma growth-suppressive properties. *Proc Natl Acad Sci U S A* 99, 637-642.

Kasprzak, A., Seidel, J., Biczysko, W., Wysocki, J., Spachacz, R., and Zabel, M. (2005). Intracellular localization of NS3 and C proteins in chronic hepatitis C. *Liver Int* 25, 896-903.

Kato, H., Sato, S., Yoneyama, M., Yamamoto, M., Uematsu, S., Matsui, K., Tsujimura, T., Takeda, K., Fujita, T., Takeuchi, O., and Akira, S. (2005). Cell type-specific involvement of RIG-I in antiviral response. *Immunity* 23, 19-28.

Kato, H., Takeuchi, O., Sato, S., Yoneyama, M., Yamamoto, M., Matsui, K., Uematsu, S., Jung, A., Kawai, T., Ishii, K. J., *et al.* (2006). Differential roles of MDA5 and RIG-I helicases in the recognition of RNA viruses. *Nature* 441, 101-105.

Kaufmann, T., Schlipf, S., Sanz, J., Neubert, K., Stein, R., and Borner, C. (2003). Characterization of the signal that directs Bcl-x(L), but not Bcl-2, to the mitochondrial outer membrane. *J Cell Biol* 160, 53-64.

Kawai, T., and Akira, S. (2006a). Innate immune recognition of viral infection. *Nat Immunol* 7, 131-137.

Kawai, T., and Akira, S. (2006b). TLR signaling. *Cell Death Differ* 13, 816-825.

Kawai, T., Sato, S., Ishii, K. J., Coban, C., Hemmi, H., Yamamoto, M., Terai, K., Matsuda, M., Inoue, J., Uematsu, S., *et al.* (2004). Interferon-alpha induction through Toll-like receptors involves a direct interaction of IRF7 with MyD88 and TRAF6. *Nat Immunol* 5, 1061-1068.

Kawai, T., Takahashi, K., Sato, S., Coban, C., Kumar, H., Kato, H., Ishii, K. J., Takeuchi, O., and Akira, S. (2005). IPS-1, an adaptor triggering RIG-I- and Mda5-mediated type I interferon induction. *Nat Immunol* 6, 981-988.

Kim, P. K., Hollerbach, C., Trimble, W. S., Leber, B., and Andrews, D. W. (1999). Identification of the endoplasmic reticulum targeting signal in vesicle-associated membrane proteins. *J Biol Chem* 274, 36876-36882.

Kolykhalov, A. A., Agapov, E. V., and Rice, C. M. (1994). Specificity of the hepatitis C virus NS3 serine protease: effects of substitutions at the 3/4A, 4A/4B,

4B/5A, and 5A/5B cleavage sites on polyprotein processing. *J Virol* 68, 7525-7533.

Kovacsovics, M., Martinon, F., Micheau, O., Bodmer, J. L., Hofmann, K., and Tschopp, J. (2002). Overexpression of Helicard, a CARD-containing helicase cleaved during apoptosis, accelerates DNA degradation. *Curr Biol* 12, 838-843.

Lemaitre, B., Nicolas, E., Michaut, L., Reichhart, J. M., and Hoffmann, J. A. (1996). The dorsoventral regulatory gene cassette spatzle/Toll/cactus controls the potent antifungal response in *Drosophila* adults. *Cell* 86, 973-983.

Lenardo, M. J., Fan, C. M., Maniatis, T., and Baltimore, D. (1989). The involvement of NF-kappa B in beta-interferon gene regulation reveals its role as widely inducible mediator of signal transduction. *Cell* 57, 287-294.

Li, K., Foy, E., Ferreon, J. C., Nakamura, M., Ferreon, A. C., Ikeda, M., Ray, S. C., Gale, M., Jr., and Lemon, S. M. (2005a). Immune evasion by hepatitis C virus NS3/4A protease-mediated cleavage of the Toll-like receptor 3 adaptor protein TRIF. *Proc Natl Acad Sci U S A* 102, 2992-2997.

Li, X. D., Sun, L., Seth, R. B., Pineda, G., and Chen, Z. J. (2005b). Hepatitis C virus protease NS3/4A cleaves mitochondrial antiviral signaling protein off the mitochondria to evade innate immunity. *Proc Natl Acad Sci U S A* 102, 17717-17722.

Lin, R., Heylbroeck, C., Pitha, P. M., and Hiscott, J. (1998). Virus-dependent phosphorylation of the IRF-3 transcription factor regulates nuclear translocation, transactivation potential, and proteasome-mediated degradation. *Mol Cell Biol* 18, 2986-2996.

Lin, R., Mamane, Y., and Hiscott, J. (1999). Structural and functional analysis of interferon regulatory factor 3: localization of the transactivation and autoinhibitory domains. *Mol Cell Biol* 19, 2465-2474.

Lin, R., Yang, L., Nakhaei, P., Sun, Q., Sharif-Askari, E., Julkunen, I., and Hiscott, J. (2006). Negative regulation of the retinoic acid-inducible gene I-induced antiviral state by the ubiquitin-editing protein A20. *J Biol Chem* 281, 2095-2103.

Lindenbach, B. D., and Rice, C. M. (2005). Unravelling hepatitis C virus replication from genome to function. *Nature* 436, 933-938.

Loo, Y. M., Owen, D. M., Li, K., Erickson, A. K., Johnson, C. L., Fish, P. M., Carney, D. S., Wang, T., Ishida, H., Yoneyama, M., *et al.* (2006). Viral and therapeutic control of IFN-beta promoter stimulator 1 during hepatitis C virus infection. *Proc Natl Acad Sci U S A* *103*, 6001-6006.

Lund, J., Sato, A., Akira, S., Medzhitov, R., and Iwasaki, A. (2003). Toll-like receptor 9-mediated recognition of Herpes simplex virus-2 by plasmacytoid dendritic cells. *J Exp Med* *198*, 513-520.

Lund, J. M., Alexopoulou, L., Sato, A., Karow, M., Adams, N. C., Gale, N. W., Iwasaki, A., and Flavell, R. A. (2004). Recognition of single-stranded RNA viruses by Toll-like receptor 7. *Proc Natl Acad Sci U S A* *101*, 5598-5603.

Macias, M. J., Wiesner, S., and Sudol, M. (2002). WW and SH3 domains, two different scaffolds to recognize proline-rich ligands. *FEBS Lett* *513*, 30-37.

Mamane, Y., Heylbroeck, C., Genin, P., Algarte, M., Servant, M. J., LePage, C., DeLuca, C., Kwon, H., Lin, R., and Hiscott, J. (1999). Interferon regulatory factors: the next generation. *Gene* *237*, 1-14.

Maniatis, T., Falvo, J. V., Kim, T. H., Kim, T. K., Lin, C. H., Parekh, B. S., and Wathlet, M. G. (1998). Structure and function of the interferon-beta enhanceosome. *Cold Spring Harb Symp Quant Biol* *63*, 609-620.

Marie, I., Durbin, J. E., and Levy, D. E. (1998). Differential viral induction of distinct interferon-alpha genes by positive feedback through interferon regulatory factor-7. *Embo J* *17*, 6660-6669.

Matsuda, A., Suzuki, Y., Honda, G., Muramatsu, S., Matsuzaki, O., Nagano, Y., Doi, T., Shimotohno, K., Harada, T., Nishida, E., *et al.* (2003). Large-scale identification and characterization of human genes that activate NF-kappaB and MAPK signaling pathways. *Oncogene* *22*, 3307-3318.

Matsuyama, T., Kimura, T., Kitagawa, M., Pfeffer, K., Kawakami, T., Watanabe, N., Kundig, T. M., Amakawa, R., Kishihara, K., Wakeham, A., and *et al.* (1993). Targeted disruption of IRF-1 or IRF-2 results in abnormal type I IFN gene induction and aberrant lymphocyte development. *Cell* *75*, 83-97.

McWhirter, S. M., Fitzgerald, K. A., Rosains, J., Rowe, D. C., Golenbock, D. T., and Maniatis, T. (2004). IFN-regulatory factor 3-dependent gene expression is defective in Tbk1-deficient mouse embryonic fibroblasts. *Proc Natl Acad Sci U S A* *101*, 233-238.

Meylan, E., Burns, K., Hofmann, K., Blancheteau, V., Martinon, F., Kelliher, M., and Tschoop, J. (2004). RIP1 is an essential mediator of Toll-like receptor 3-induced NF-kappa B activation. *Nat Immunol* 5, 503-507.

Meylan, E., Curran, J., Hofmann, K., Moradpour, D., Binder, M., Bartenschlager, R., and Tschoop, J. (2005). Cardif is an adaptor protein in the RIG-I antiviral pathway and is targeted by hepatitis C virus. *Nature* 437, 1167-1172.

Michaelson, D., Silletti, J., Murphy, G., D'Eustachio, P., Rush, M., and Philips, M. R. (2001). Differential localization of Rho GTPases in live cells: regulation by hypervariable regions and RhoGDI binding. *J Cell Biol* 152, 111-126.

Mogensen, T. H., and Paludan, S. R. (2001). Molecular pathways in virus-induced cytokine production. *Microbiol Mol Biol Rev* 65, 131-150.

Mori, M., Yoneyama, M., Ito, T., Takahashi, K., Inagaki, F., and Fujita, T. (2004). Identification of Ser-386 of interferon regulatory factor 3 as critical target for inducible phosphorylation that determines activation. *J Biol Chem* 279, 9698-9702.

Mottola, G., Cardinali, G., Ceccacci, A., Trozzi, C., Bartholomew, L., Torrisi, M. R., Pedrazzini, E., Bonatti, S., and Migliaccio, G. (2002). Hepatitis C virus nonstructural proteins are localized in a modified endoplasmic reticulum of cells expressing viral subgenomic replicons. *Virology* 293, 31-43.

Muller, U., Steinhoff, U., Reis, L. F., Hemmi, S., Pavlovic, J., Zinkernagel, R. M., and Aguet, M. (1994). Functional role of type I and type II interferons in antiviral defense. *Science* 264, 1918-1921.

Oganesyan, G., Saha, S. K., Guo, B., He, J. Q., Shahangian, A., Zarnegar, B., Perry, A., and Cheng, G. (2006). Critical role of TRAF3 in the Toll-like receptor-dependent and -independent antiviral response. *Nature* 439, 208-211.

Qin, B. Y., Liu, C., Lam, S. S., Srinath, H., Delston, R., Correia, J. J., Derynck, R., and Lin, K. (2003). Crystal structure of IRF-3 reveals mechanism of autoinhibition and virus-induced phosphoactivation. *Nat Struct Biol* 10, 913-921.

Rehermann, B., and Nascimbeni, M. (2005). Immunology of hepatitis B virus and hepatitis C virus infection. *Nat Rev Immunol* 5, 215-229.

Rothenfusser, S., Goutagny, N., DiPerna, G., Gong, M., Monks, B. G., Schoenemeyer, A., Yamamoto, M., Akira, S., and Fitzgerald, K. A. (2005). The

RNA helicase Lgp2 inhibits TLR-independent sensing of viral replication by retinoic acid-inducible gene-I. *J Immunol* 175, 5260-5268.

Saitoh, T., Yamamoto, M., Miyagishi, M., Taira, K., Nakanishi, M., Fujita, T., Akira, S., Yamamoto, N., and Yamaoka, S. (2005). A20 is a negative regulator of IFN regulatory factor 3 signaling. *J Immunol* 174, 1507-1512.

Sasai, M., Oshiumi, H., Matsumoto, M., Inoue, N., Fujita, F., Nakanishi, M., and Seya, T. (2005). Cutting Edge: NF-kappaB-activating kinase-associated protein 1 participates in TLR3/Toll-IL-1 homology domain-containing adapter molecule-1-mediated IFN regulatory factor 3 activation. *J Immunol* 174, 27-30.

Sato, M., Suemori, H., Hata, N., Asagiri, M., Ogasawara, K., Nakao, K., Nakaya, T., Katsuki, M., Noguchi, S., Tanaka, N., and Taniguchi, T. (2000). Distinct and essential roles of transcription factors IRF-3 and IRF-7 in response to viruses for IFN-alpha/beta gene induction. *Immunity* 13, 539-548.

Sato, M., Tanaka, N., Hata, N., Oda, E., and Taniguchi, T. (1998). Involvement of the IRF family transcription factor IRF-3 in virus-induced activation of the IFN-beta gene. *FEBS Lett* 425, 112-116.

Sato, S., Sugiyama, M., Yamamoto, M., Watanabe, Y., Kawai, T., Takeda, K., and Akira, S. (2003). Toll/IL-1 receptor domain-containing adaptor inducing IFN-beta (TRIF) associates with TNF receptor-associated factor 6 and TANK-binding kinase 1, and activates two distinct transcription factors, NF-kappa B and IFN-regulatory factor-3, in the Toll-like receptor signaling. *J Immunol* 171, 4304-4310.

Schafer, S. L., Lin, R., Moore, P. A., Hiscott, J., and Pitha, P. M. (1998). Regulation of type I interferon gene expression by interferon regulatory factor-3. *J Biol Chem* 273, 2714-2720.

Schwer, B., Ren, S., Pietschmann, T., Kartenbeck, J., Kaehlcke, K., Bartenschlager, R., Yen, T. S., and Ott, M. (2004). Targeting of hepatitis C virus core protein to mitochondria through a novel C-terminal localization motif. *J Virol* 78, 7958-7968.

Servant, M. J., Grandvaux, N., tenOever, B. R., Duguay, D., Lin, R., and Hiscott, J. (2003). Identification of the minimal phosphoacceptor site required for in vivo activation of interferon regulatory factor 3 in response to virus and double-stranded RNA. *J Biol Chem* 278, 9441-9447.

Servant, M. J., ten Oever, B., LePage, C., Conti, L., Gessani, S., Julkunen, I., Lin, R., and Hiscott, J. (2001). Identification of distinct signaling pathways leading to the phosphorylation of interferon regulatory factor 3. *J Biol Chem* 276, 355-363.

Sharma, S., tenOever, B. R., Grandvaux, N., Zhou, G. P., Lin, R., and Hiscott, J. (2003). Triggering the interferon antiviral response through an IKK-related pathway. *Science* 300, 1148-1151.

Silverman, N., and Maniatis, T. (2001). NF-kappaB signaling pathways in mammalian and insect innate immunity. *Genes Dev* 15, 2321-2342.

Stetson, D. B., and Medzhitov, R. (2006). Recognition of cytosolic DNA activates an IRF3-dependent innate immune response. *Immunity* 24, 93-103.

Suhara, W., Yoneyama, M., Iwamura, T., Yoshimura, S., Tamura, K., Namiki, H., Aimoto, S., and Fujita, T. (2000). Analyses of virus-induced homomeric and heteromeric protein associations between IRF-3 and coactivator CBP/p300. *J Biochem (Tokyo)* 128, 301-307.

Sumpter, R., Jr., Loo, Y. M., Foy, E., Li, K., Yoneyama, M., Fujita, T., Lemon, S. M., and Gale, M., Jr. (2005). Regulating intracellular antiviral defense and permissiveness to hepatitis C virus RNA replication through a cellular RNA helicase, RIG-I. *J Virol* 79, 2689-2699.

Sun, Q., Sun, L., Liu, H. H., Chen, X., Seth, R. B., Forman, J., and Chen, Z. J. (2006). The Specific and Essential Role of MAVS in Antiviral Innate Immune Responses. *Immunity* 24, 633-642.

Sun, Y. W. (1997) RIG-I, a human homolog gene of RNA helicase, is induced by retinoic acid during the differentiation of acute promyelocytic leukemia cell, Thesis, Shanghai Second Medical University.

Taylor, P., Tamura, T., and Ozato, K. (2006). IRF family proteins and type I interferon induction in dendritic cells. *Cell Res* 16, 134-140.

Takahasi, K., Suzuki, N. N., Horiuchi, M., Mori, M., Suhara, W., Okabe, Y., Fukuhara, Y., Terasawa, H., Akira, S., Fujita, T., and Inagaki, F. (2003). X-ray crystal structure of IRF-3 and its functional implications. *Nat Struct Biol* 10, 922-927.

Takaoka, A., Yanai, H., Kondo, S., Duncan, G., Negishi, H., Mizutani, T., Kano, S., Honda, K., Ohba, Y., Mak, T. W., and Taniguchi, T. (2005). Integral role of

IRF-5 in the gene induction programme activated by Toll-like receptors. *Nature* 434, 243-249.

tenOever, B. R., Servant, M. J., Grandvaux, N., Lin, R., and Hiscott, J. (2002). Recognition of the measles virus nucleocapsid as a mechanism of IRF-3 activation. *J Virol* 76, 3659-3669.

tenOever, B. R., Sharma, S., Zou, W., Sun, Q., Grandvaux, N., Julkunen, I., Hemmi, H., Yamamoto, M., Akira, S., Yeh, W. C., *et al.* (2004). Activation of TBK1 and IKKvarepsilon kinases by vesicular stomatitis virus infection and the role of viral ribonucleoprotein in the development of interferon antiviral immunity. *J Virol* 78, 10636-10649.

Thanos, D., and Maniatis, T. (1992). The high mobility group protein HMG I(Y) is required for NF-kappa B-dependent virus induction of the human IFN-beta gene. *Cell* 71, 777-789.

Theofilopoulos, A. N., Baccala, R., Beutler, B., and Kono, D. H. (2005). Type I interferons (alpha/beta) in immunity and autoimmunity. *Annu Rev Immunol* 23, 307-336.

Uematsu, S., Sato, S., Yamamoto, M., Hirotani, T., Kato, H., Takeshita, F., Matsuda, M., Coban, C., Ishii, K. J., Kawai, T., *et al.* (2005). Interleukin-1 receptor-associated kinase-1 plays an essential role for Toll-like receptor (TLR)7- and TLR9-mediated interferon- α induction. *J Exp Med* 201, 915-923.

Visvanathan, K. V., and Goodbourn, S. (1989). Double-stranded RNA activates binding of NF-kappa B to an inducible element in the human beta-interferon promoter. *Embo J* 8, 1129-1138.

Wang, C., Deng, L., Hong, M., Akkaraju, G. R., Inoue, J., and Chen, Z. J. (2001). TAK1 is a ubiquitin-dependent kinase of MKK and IKK. *Nature* 412, 346-351.

Wang, X. (2001). The expanding role of mitochondria in apoptosis. *Genes Dev* 15, 2922-2933.

Wang, Y. Y., Li, L., Han, K. J., Zhai, Z., and Shu, H. B. (2004). A20 is a potent inhibitor of TLR3- and Sendai virus-induced activation of NF-kappaB and ISRE and IFN-beta promoter. *FEBS Lett* 576, 86-90.

Weaver, B. K., Kumar, K. P., and Reich, N. C. (1998). Interferon regulatory factor 3 and CREB-binding protein/p300 are subunits of double-stranded RNA-activated transcription factor DRAFI. *Mol Cell Biol* 18, 1359-1368.

Werts, C., Girardin, S. E., and Philpott, D. J. (2006). TIR, CARD and PYRIN: three domains for an antimicrobial triad. *Cell Death Differ* 13, 798-815.

Xu, L. G., Wang, Y. Y., Han, K. J., Li, L. Y., Zhai, Z., and Shu, H. B. (2005). VISA is an adapter protein required for virus-triggered IFN-beta signaling. *Mol Cell* 19, 727-740.

Yamamoto, M., Sato, S., Mori, K., Hoshino, K., Takeuchi, O., Takeda, K., and Akira, S. (2002). Cutting edge: a novel Toll/IL-1 receptor domain-containing adapter that preferentially activates the IFN-beta promoter in the Toll-like receptor signaling. *J Immunol* 169, 6668-6672.

Yang, K., Puel, A., Zhang, S., Eidenschenk, C., Ku, C. L., Casrouge, A., Picard, C., von Bernuth, H., Senechal, B., Plancoulaine, S., *et al.* (2005). Human TLR-7-, -8-, and -9-mediated induction of IFN-alpha/beta and -lambda is IRAK-4 dependent and redundant for protective immunity to viruses. *Immunity* 23, 465-478.

Yoneyama, M., Kikuchi, M., Matsumoto, K., Imaizumi, T., Miyagishi, M., Taira, K., Foy, E., Loo, Y. M., Gale, M., Jr., Akira, S., *et al.* (2005). Shared and unique functions of the DExD/H-box helicases RIG-I, MDA5, and LGP2 in antiviral innate immunity. *J Immunol* 175, 2851-2858.

Yoneyama, M., Kikuchi, M., Natsukawa, T., Shinobu, N., Imaizumi, T., Miyagishi, M., Taira, K., Akira, S., and Fujita, T. (2004). The RNA helicase RIG-I has an essential function in double-stranded RNA-induced innate antiviral responses. *Nat Immunol* 5, 730-737.

Yoneyama, M., Suhara, W., Fukuhara, Y., Fukuda, M., Nishida, E., and Fujita, T. (1998). Direct triggering of the type I interferon system by virus infection: activation of a transcription factor complex containing IRF-3 and CBP/p300. *Embo J* 17, 1087-1095.

Zhang, X., Wang, C., Schook, L. B., Hawken, R. J., and Rutherford, M. S. (2000). An RNA helicase, RHIV -1, induced by porcine reproductive and respiratory syndrome virus (PRRSV) is mapped on porcine chromosome 10q13. *Microb Pathog* 28, 267-278.

VITAE

Rashu Bhargava was born in Pune, Maharashtra, India, on August 3, 1976, the daughter of Vijay M. Bhargava and Sarita Bhargava. After graduating from Kendriya Vidyalaya, Gwalior, India, she entered the All India Institute of Medical Sciences, New Delhi in 1995. She received the degree of Bachelor of Science in Human Biology with a major in Biochemistry in 1998. In August 1998, she entered the Masters in Biotechnology Program at the All India Institute of Medical Science, New Delhi, where she completed a thesis titled 'Study of apoptosis in immunocompetent cells in human tuberculosis' in the laboratory of Dr. H. K. Prasad. In August 2000, she entered the Graduate Program at Rutgers, N.J. After one year of course work at Rutgers, she transferred to the Graduate School of Biomedical Sciences at UT Southwestern Medical Center, Dallas, where she joined the laboratory of Dr. James Chen in December 2001. In December of 2001, she married her best friend and fellow graduate student, Abhinav Seth.

Permanent Address: 286 East Saddle River Road
Upper Saddle River, NJ 07458